University of Tennessee, Knoxville

TRACE: Tennessee Research and Creative Exchange

Masters Theses

Graduate School

5-2017

Effects of Distance, Antenna, and Channel on an Ultra Wide Band Location System, and Quantifying them to Increase Accuracy

Nicholas Alexander Cavopol
University of Tennessee, Knoxville, ncavopol@vols.utk.edu

Follow this and additional works at: https://trace.tennessee.edu/utk_gradthes

Part of the Other Electrical and Computer Engineering Commons

Recommended Citation

Cavopol, Nicholas Alexander, "Effects of Distance, Antenna, and Channel on an Ultra Wide Band Location System, and Quantifying them to Increase Accuracy. " Master's Thesis, University of Tennessee, 2017.
https://trace.tennessee.edu/utk_gradthes/4705

This Thesis is brought to you for free and open access by the Graduate School at TRACE: Tennessee Research and Creative Exchange. It has been accepted for inclusion in Masters Theses by an authorized administrator of TRACE: Tennessee Research and Creative Exchange. For more information, please contact trace@utk.edu.

To the Graduate Council:

I am submitting herewith a thesis written by Nicholas Alexander Cavopol entitled "Effects of Distance, Antenna, and Channel on an Ultra Wide Band Location System, and Quantifying them to Increase Accuracy." I have examined the final electronic copy of this thesis for form and content and recommend that it be accepted in partial fulfillment of the requirements for the degree of Master of Science, with a major in Electrical Engineering.

Aly E. Fathy, Major Professor

We have read this thesis and recommend its acceptance:

Michael J. Kuhn, Mohamed R. Mahfouz

Accepted for the Council:
Dixie L. Thompson

Vice Provost and Dean of the Graduate School

(Original signatures are on file with official student records.)

Effects of Distance, Antenna, and Channel on an Ultra Wide Band Location System, and Quantifying them to Increase Accuracy

A Thesis Presented for the
Master of Science
Degree
The University of Tennessee, Knoxville

Nicholas Alexander Cavopol
May 2017

Copyright © 2017 by Nicholas A. Cavopol
All rights reserved.

ACKNOWLEDGEMENTS

I would like to first and foremost thank my advisor Dr. Fathy for his support of my academic career and giving me the freedom to find my own areas of interest. I also want to thank Dr. Michael Kuhn for his mentorship, advice, and friendship throughout my graduate career. I would like to thank Dr. Mahfouz for giving me the opportunity to expand my knowledge in the wireless world and thank TechMah LLC for funding my research there.

I would like to thank my friends Jacob and Luke for always being there with a helpful hand or a forceful push to keep me in line and encourage me to continue my education, even if it wasn't the easiest way forward. I especially want to thank my friend Kayla for always being there with a comforting word and completely supporting me when I needed it most. My defense would not have been as well prepared without you.

I would like to thank my father, Alexander, for always pushing me to achieve greater things even though I may not have wanted that path for myself. I would like to thank my mother Allison for always being there for me. Finally I would like to thank my brother Michael for always giving me the ambition to achieve what I set out to do and always giving me competition to keep me motivated.

ABSTRACT

Localization has been evolving rapidly over the last 20 years, especially in the wireless world. From the advent of GPS, as well as the personal smart phone, localization has become accessible to most of the developed world. From the ability to find ones' smartphone using a computer, to being able to locate ones' keys using radio frequencies, there are many ways that localization has entered our lives in the last few years, however most of these either do not have high accuracy, or are only accurate in an outside environment. For indoor tracking, new technologies have been developed to help bridge this gap, Ultra Wide Band (UWB) being one of the front runners.

UWB frequency spectrum has only been approved for public use by the FCC since 2002. The IEEE 802.15.4-2015 standard defines the narrowband ZigBee protocol and also includes a UWB physical layer. The UWB physical layer covers 3-10.6 GHz and includes 15 channels having differing center frequencies with bandwidths of 500 MHz or greater. As such, there is much less research, data, and analysis of these channels compared to other well established bands. When trying to increase the accuracy of a localization system, error sources must be addressed. In the case of UWB, these error sources are somewhat unknown. Through this thesis, we set up experiments to test the effects of range, antenna, and channel on both the shape and strength of the UWB pulse, as well as the effects on accuracy of 2D and 3D localization. Additionally, a software was developed and reviewed to optimize the placement

of wireless receivers to maximize the accuracy of localization across the testing space. This thesis also reviews some of the current technologies associated with localization as well as their claimed accuracies, focusing on wireless technologies.

TABLE OF CONTENTS

Chapter One Introduction....1
Background....1
Introduction to Ultra Wide Band Frequencies....2
Introduction to the Location Algorithms....8
Organization....14
Chapter Two Current Systems and their Accuracies....16
Chapter Three Challenges to achieve High Accuracy....22
Dilution of Precision....22
Antenna Offsets....24
Phase Center Variation....27
Clock Jitter and Drift....29
Chapter Four Experimental Setup....31
Overview of Both the Ranging and Tracking Experiments....31
Chapter Five Ranging Experiment....50
Purpose....50
Experimental Results....50
Chapter Six Tracking Experiment....67
Purpose....67
Error Sources....72
Experimental Results....74
Chapter Seven Dilution of Precision Optimization....89
Purpose....89
Application Overview....89
Chapter Eight Conclusions and Recommendations....103
References....106
Vita....109

LIST OF TABLES

Table 1-1 – UWB channels as defined in [17] 3
Table 1-2 – The UWB Channels used in testing 3
Table 2-1 – Summary of current commercial systems and their specifications. Updated table from [4] 17
Table 4-1 – Information on each of the antennas used for the experiments 33
Table 5-1 – Channel 4 53
Table 5-2 – Channel 5 54
Table 5-3 – Channel 7 60
Table 5-4 – Comparison of all channels and all antennas 61
Table 5-5 – SNR values averaged from separation distances from 2-15 meters 65
Table 5-6 – SNR values averaged from separation distances from 2-28 meters (* channel 5 only had values for 28 meters using the spherical antenna) 65
Table 6-1 – Ranges from each position to every target and anchor 71
Table 6-2 – Error Sources for the tracking experiment and the amount of error that each contributes 73
Table 6-3 – Errors of each channel and antenna configuration. Error is averaged over all positions and is in millimeters 78
Table 6-4 – Error of all channel and antenna configurations in 2D. Error is averaged over all positions 79
Table 6-5 – Averaged errors over all positions. 3D errors are presented next to the 2D data for easier comparison 79
Table 6-6 – Separated accuracy error by position in 3D. Each column is separated by channel and antenna and everything is in millimeters 87
Table 6-7 – Separated accuracy by position in 2D. Each column is separated by channel and antenna and everything is in millimeters 88
Table 7-1 – The correlation of anchors to 95% confidence PDOP values corresponding to Figure 7-3, Figure 7-4, and Figure 7-5 96
Table 7-2 – Summary of the number of anchors versus the PDOP 95% confidence for each zone of the PDOP application corresponding to Figure 7-7, Figure 7-8, and Figure 7-9. 101

LIST OF FIGURES

Figure 1-1 – Example of an Ultra-Wide band signal. First showing the time-domain of a 300 ps wide pulse, and secondly showing an up-converted UWB pulse in the frequency domain compared to a narrowband signal [1]...3
Figure 1-2 – UWB channel 4 transmitter spectrum 4
Figure 1-3 – UWB channel 5 transmitter spectrum 4
Figure 1-4 – UWB channel 7 transmitter spectrum 5
Figure 1-5 – Frame structure of UWB communication as defined in IEEE Std 802.15.4-2015.....7
Figure 1-6 – The structure of a single symbol as defined in [17].....7
Figure 1-7 – The structure of how the preamble part of a UWB frame is made up of multiple symbols 7
Figure 1-8 – How the accumulator signal is generated from the UWB pulse preamble.....9
Figure 1-9 – Visual representaion of the TDOA algoithm to calculate the unknown position of a tag given the known locations of four anchors, or recievers 13
Figure 2-1 – The DecaWave EVK1000 evaluation kit, which uses the DW1000 chip paired with the DecaWave planar monopole antenna.....17
Figure 2-2 – Hardware associated with the Redpoint Positioning system [19]....19
Figure 2-3 – System configuration of the Repoint positioning system [19].....19
Figure 2-4 – Internal UWB module of the Tag and Traq system [21].....20
Figure 2-5 – Ubisense UWB tag [14] 20
Figure 3-1 – Example of how the dilution of precision can increase with the same amount of error for each transmitter and receiver. (A) represents the ideal solution with no error. (B) represents the dilution of precision (POD) in green when error is introduced to the system. (C) represents the increased DOP when one of the anchors is moved. [12] 23
Figure 3-2 – Another example of how anchor placement effects the DOP. From [7].....23
Figure 3-3 – PDOP analysis of the testing space. Graph on left does analysis on entire room, graph on right does analysis of space within the anchors. Red dots represent anchor locations, blue dots represent tag locations. 25
Figure 3-4 – Experiment from [18] that shows in (a) the experimental setup and in (b) the increase in phase center location with the increase of angle.....28
Figure 4-1 – Overview of the testing locations. The master anchor does not move, while the secondary anchor is moved to separation distances of 2 meters, 8 meters, and 15 meters 32
Figure 4-2 – Block diagram of the Ranging Experiment.....33
Figure 4-3 – First experiment with variations of Distance between anchors, antenna, height, and UWB channel. This shows the experiment at 2 meters apart, 1.311 meters off the ground, and using a monopole antenna.....34

Figure 4-4 – Shows the experiment using anchor distance of 15 meters and height 1.311 meters, and using the TechMah Concept antenna.....35
Figure 4-5 – Shows the first experimental setup using the height of 3.20 meters with a distance of 8 meters and using the Decawave antenna. 37
Figure 4-6 – Width comparison of the three antennas used in in the first experiment. From left to right: spherical monopole antenna, Decawave planar monopole antenna, and TechMah planar monopole antenna.....38
Figure 4-7 – Height comparison of all three different antennas used in the first experiment. From top to bottom, spherical monopole antenna, Decawave planar monopole antenna, and TechMah planar monopole antenna.....39
Figure 4-8 – Radiation pattern of the TechMah spherical monopole antenna.....40
Figure 4-9 – Radiation pattern of the TechMah planar monopole antenna 41
Figure 4-10 – Radiation pattern of the DecaWave planar monopole antenna 42
Figure 4-11 – Example of a pulse from channel 4 using the spherical monopole antenna, the receiver and transmitter having a separation distance of 2 meters.....43
Figure 4-12 – Example of a pulse from channel 5 using the spherical monopole antenna, the receiver and transmitter having a separation distance of 2 meters.....44
Figure 4-13 – Example of a pulse from channel 7 using the spherical monopole antenna, the receiver and transmitter having a separation distance of 2 meters.....44
Figure 4-14 – Block diagram of the Tracking Experiment 47
Figure 4-15 – Top down view of the second experiment test space. The red square shwows the origin used for all locations, the red circles denote the locations of each of the anchor positions, and the green circles denote the locations of each of the targets placed on the perimeter of the room. 47
Figure 4-16 – Layout of the test space. Red squares represent anchor locations, green stars represent target locations, cyan circles represent the true tag location, and the magenta circles represent the calculated position 48
Figure 4-17 – Block Diagram of the PDOP optimization application 49
Figure 5-1 – Channel 4 pulse at 2 meters separation distance, height of 1.31 meters, and using the spherical monopole antenna 51
Figure 5-2 – Channel 4 pulse at 15 meters separation distance, height of 1.31 meters, and using the spherical monopole antenna 51
Figure 5-3 – Channel 4 pulse at 28 meters separation distance, height of 1.31 meters, and using the spherical monopole antenna 52
Figure 5-4 – Channel 5 pulse at 2 meters separation distance, height of 1.31 meters, and using the spherical monopole antenna 54
Figure 5-5 – Channel 5 pulse at 15 meters separation distance, height of 1.31 meters, and using the spherical monopole antenna 55
Figure 5-6 – Channel 5 pulse at 28 meters separation distance, height of 1.31 meters, and using the spherical monopole antenna 55

Figure 5-7 – Channel 7 pulse at 2 meters separation distance, height of 1.31 meters, and using the spherical monopole antenna 58
Figure 5-8 – Channel 7 pulse at 15 meters separation distance, height of 1.31 meters, and using the spherical monopole antenna 58
Figure 5-9 – Channel 7 pulse at 28 meters separation distance, height of 1.31 meters, and using the spherical monopole antenna 59
Figure 6-1 – View of the testing space. Decawave anchors at circled in red, the tag is circled in blue, and the targets are circled in green 68
Figure 6-2 – View of testing space from opposite side. Anchors in red circles, tag in blue circle, and targets in green circles. 68
Figure 6-3 – Top down view of the testing space with anchors represented by red circles, targets as green circles, and the origin as the purple square. 69
Figure 6-4 – Top down view of testing space overlaid on structural drawings. Red dots are anchors, green dots are targets, blue dots are tag locations, and the purple square is the origin. 69
Figure 6-5 – Error in millimeters versus channel. Has values for use of TechMah and Decawave antenna using the 2D and 3D algorithm, as well as comparing the use of a Decawave antenna with 2 anchors much lower in the Z dimension. 76
Figure 6-6 – Error in mm versus channel with the use of an offset calculated from an average difference of all ranges compared to the ground true ranges, being applied to every range. 76
Figure 6-7 – Accuracy error compared to channel for each antenna 78
Figure 6-8 – Each channel and antenna configuration compared to each other, with different lines representing which offset is applied as well as whether 2D or 3D positions were calculated. 81
Figure 6-9 – Accuracy of the calculated 3D position as different error sources are mitigated 83
Figure 6-10 – Accuracy of the calculated 2D position as different error sources are mitigated 83
Figure 6-11 – Accuracy in millimeters of location 1 using Offset 2.....84
Figure 6-12 – Accuracy in millimeters of location 2 using Offset 2.....84
Figure 6-13– Accuracy in millimeters of location 3 using Offset 2.....85
Figure 7-1 – Block diagram of the process of optimizing the anchors in the PDOP software 92
Figure 7-2 – Process of the PDOP Application choosing the first 4 anchors. Points are chosen to specify the zone. Distance are calculated between...93
Figure 7-3 – PDOP coverage with the use of 4 anchors 96
Figure 7-4 – PDOP coverage using 6 anchors 97
Figure 7-5 – PDOP coverage with the use of 11 anchors, creating the best PDOP coverage available with this configuration 97
Figure 7-6 – Zone and anchor placements for the floor layout simulation. Each of the 3 zones are outlined with their corresponding anchors marked in a separate color to each other zone's anchors 99

Figure 7-7 – PDOP coverage map using the minimum number of anchors per zone of the floor layout simulation 100
Figure 7-8 – PDOP coverage of the floor layout simulation to get a medium 95% PDOP confidence level 100
Figure 7-9 – PDOP coverage using the maximum number of anchors for each zone 101

LIST OF ABBREVIATIONS

BPM	**Binary Position Modulation**
BPSK	**Binary Phase-Shift Keying**
dBm	**Decibel-Milliwatt**
FCC	**Federal Communications Commission**
FMWC	**Frequency Modulated Continuous Wave**
GPS	**Global Positioning System**
Hz	**Hertz**
LOS	**Line of Sight**
NLOS	**Non Line of Sight**
PDOP	**Position Dilution of Precision**
PHR	**Physical Layer Header**
PHY	**Physical Layer**
RD	**Range Difference**
RMS	**Root Mean Square**
RTLS	**Real-Time Locating System**
SFD	**Start of Frame Delimiter**
SNR	**Signal to Noise Ratio**
TDOA	**Time Difference of Arrival**
TOA	**Time of Arrival**
UWB	**Ultra Wide Band**

CHAPTER ONE
INTRODUCTION

Background

Localization systems have been developed a great extent in the last 20 years. From the GPS that can be found in almost every single cell phone, to different wireless positioning systems used to track assets. Though there are endless applications for positioning systems and software, the accuracy of those systems becomes more and more important for medical applications, as well as asset tracking on expensive equipment. The applications vary from the medical industry, to the construction industry, to practically any industry that wants an indoor localization system. For the medical industry, an accurate indoor tracking system could be used to increase the efficiency of an operating room by placing tags on personnel or equipment and tracking their movement over the course of an operation. By analyzing the data, inefficiencies can be found and help reduce time of operations. Localization systems have extensive uses even without sub-mm accuracy, such as store navigation, airport maps, or even targeted advertising. High accuracy localization systems can be employed with uses such as robotic surgery, precise machining, or even augmented reality.

Introduction to Ultra Wide Band Frequencies

Ultra Wide Band (UWB) signals are defined by the Federal Communications Commission (FCC) as any signal that occupies 500MHz or more bandwidth or any wireless signal which a 20% or higher fractional bandwidth. UWB only recently became available for public use, authorized for unlicensed use in the frequency range of 3.1-10.6 Gigahertz in 2002 by the FCC. However, the FCC limited the power emission for UWB transmitters to -41.3 dBm/MHz [2].

The IEEE 802.15.4-2015 standard defines the narrowband ZigBee protocol and also includes a UWB physical layer [17]. The UWB physical layer covers 3-10.6 GHz and includes 15 channels having differing center frequencies with bandwidths of 500 MHz or greater, as shown in Table 1-1. A UWB pulse has a very wide profile in the frequency domain, which translates a very small width pulse in the time domain, to the order of a few hundred pico-seconds. This is shown in Figure 1-1 which has an example of a UWB pule in the time domain, as well as in the frequency domain juxtaposed with a narrowband pulse.

One of the biggest advantages to using UWB pulses for a localizations system, especially one for indoor use, is that UWB is extremely robust for use in multipath environments as well as having little to no interference with narrowband signals.

For our experiments, we utilize channels 4, 5, and 7. The specifics of these channels are covered in Table 1-2 and samples of each band is shown in Figure 1-2, Figure 1-3, and Figure 1-4. When comparing Table 1-1 and Table 1-2, the bandwidths we used for channels 4 and 7 are limited to 900 MHz

Table 1-1 – UWB channels as defined in [17]

Band group (decimal)	Channel number (decimal)	Center Frequency (MHz)	Band width (MHz)	Mandatory/Optional
0	0	499.2	499.2	Mandatory below 1 GHz
1	1	3494.4	499.2	Optional
	2	3993.6	499.2	Optional
	3	4492.8	499.2	Mandatory in low band
	4	3993.6	1331.2	Optional
2	5	6489.6	499.2	Optional
	6	6988.8	499.2	Optional
	7	6489.6	1081.6	Optional
	8	7488.0	499.2	Optional
	9	7987.2	499.2	Mandatory in high band
	10	8486.4	499.2	Optional
	11	7987.2	1331.2	Optional
	12	8985.6	499.2	Optional
	13	9484.8	499.2	Optional
	14	9984.0	499.2	Optional
	15	9484.8	1354.97	Optional

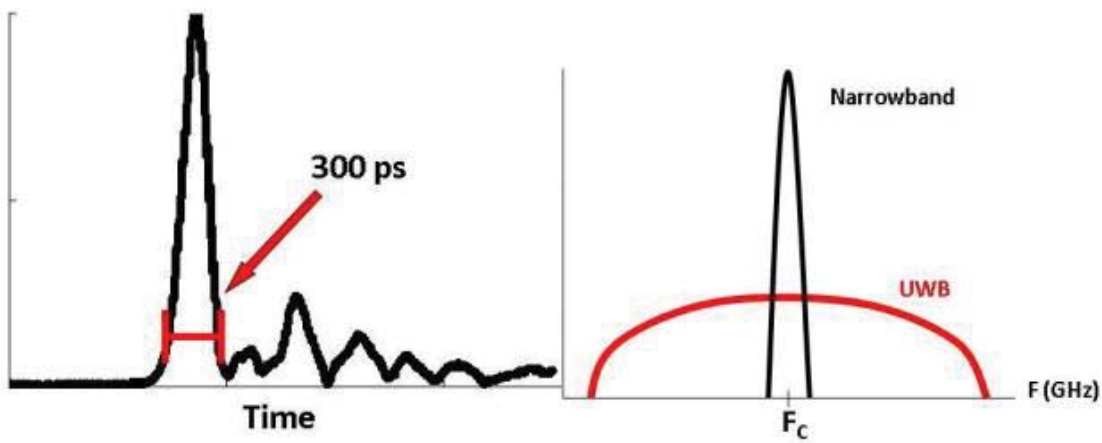

Figure 1-1 – Example of an Ultra-Wide band signal. First showing the time-domain of a 300 ps wide pulse, and secondly showing an up-converted UWB pulse in the frequency domain compared to a narrowband signal [1]

Table 1-2 – The UWB Channels used in testing

Channel Number	Center Frequency (MHz)	Band (MHz)	Bandwidth (MHz)
4	3993.6	3543.6 – 4443.6	900
5	6489.6	6240 – 6739.2	499.2
7	6489.6	6039.6 – 6939.6	900

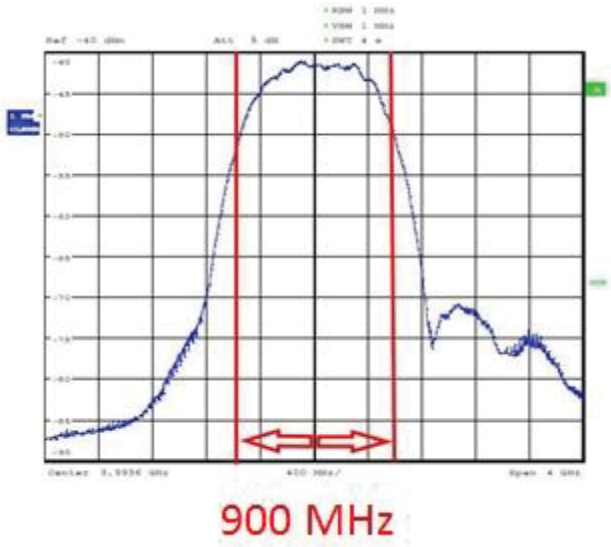

Figure 1-2 – UWB channel 4 transmitter spectrum

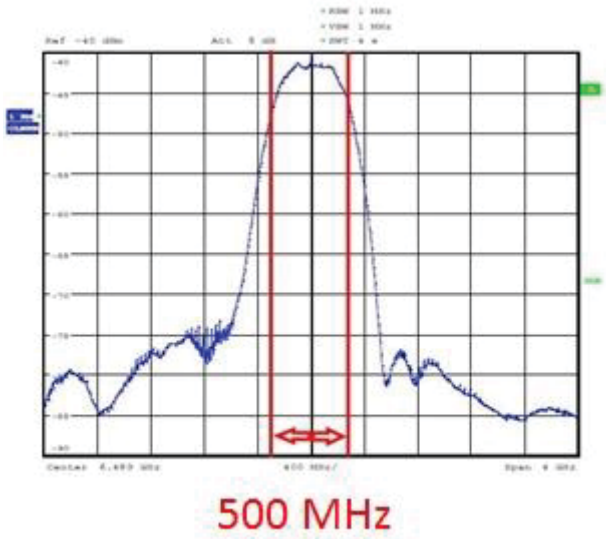

Figure 1-3 – UWB channel 5 transmitter spectrum

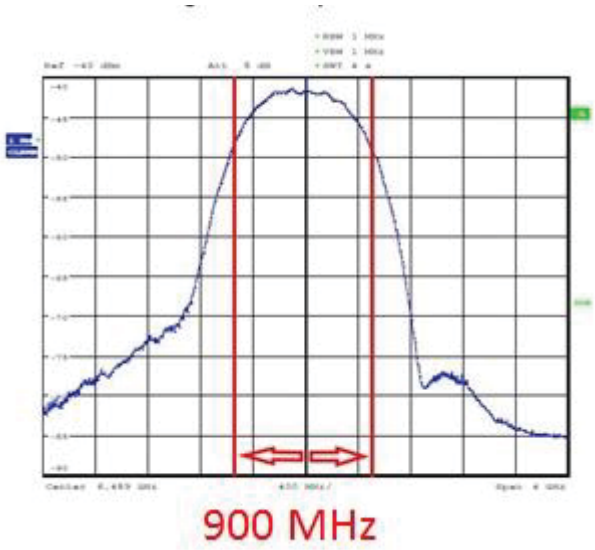

Figure 1-4 – UWB channel 7 transmitter spectrum

due to limitations of the DecaWave DW1000 chip compared to the bandwidth specified by the standard. Even though these do not fill the entire band width as defined in [17], it is still almost double the bandwidth of channel 5. Figure 1-5 shows the structure of the UWB communication standard. Each of the components is made up of symbols, whose makeup is shown in Figure 1-6. As see in Figure 1-6 there are two possible burst locations, each padded by a guard interval. Each symbol is capable of carrying two bits of information, one coming from the position of the burst, referred to as Binary Position Modulation (BPM), and the second coming from the phase, or polarity, of the burst, referred to as Binary Phase-Shift Keying (BPSK). Each frame is made up of 4 separate parts: the preamble, start of frame delimiter (SFD), physical layer (PHY) header (PHR), and the data. The preamble and SFD make up the synchronization header to help identify each frame. The preamble can be set to be 64, 1024, or 4096 symbols long with the SFD being 8 or 64 symbols long. The PHR then defines the length and data rate of the data payload to follow and is 19 bits long. The last part of the frame is the data and can be up to 127 coded octets. Figure 1-7 visually shows how all of these parts fit together. A sample preamble is shown. The spikes, which represent symbols, have two options for polarity, which correlate to the first bit of information. Each of these spikes has two possible locations which it can reside, giving the second bit of information.

The accumulator signal is what we use to measure the strength and shape of the UWB pulse is. This is generated by taking the preamble of

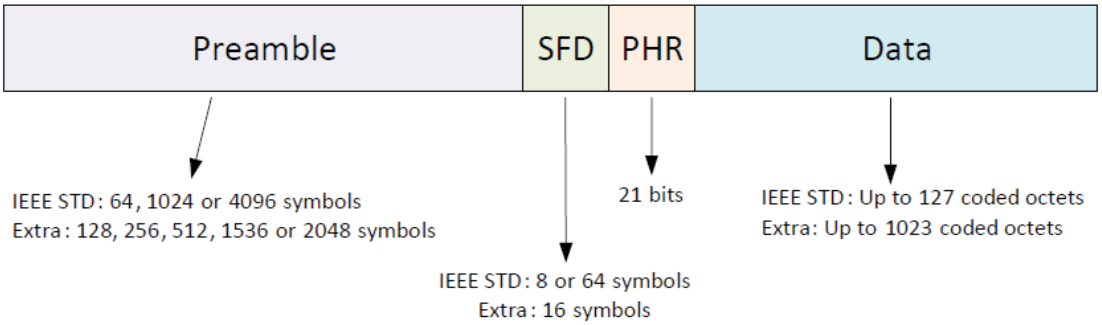

Figure 1-5 – Frame structure of UWB communication as defined in IEEE Std 802.15.4-2015

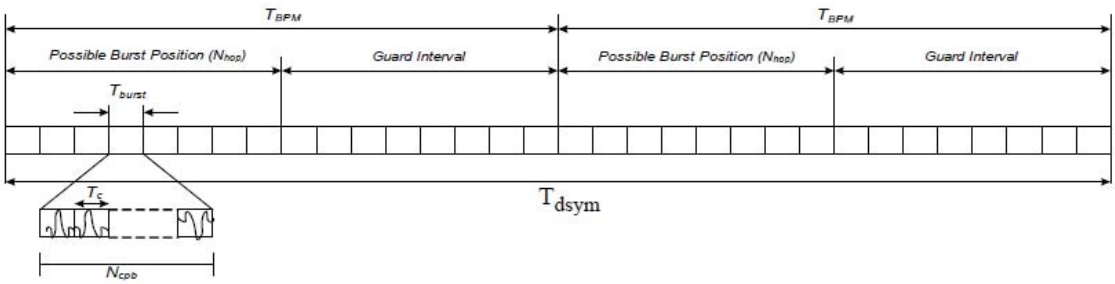

Figure 1-6 – The structure of a single symbol as defined in [17]

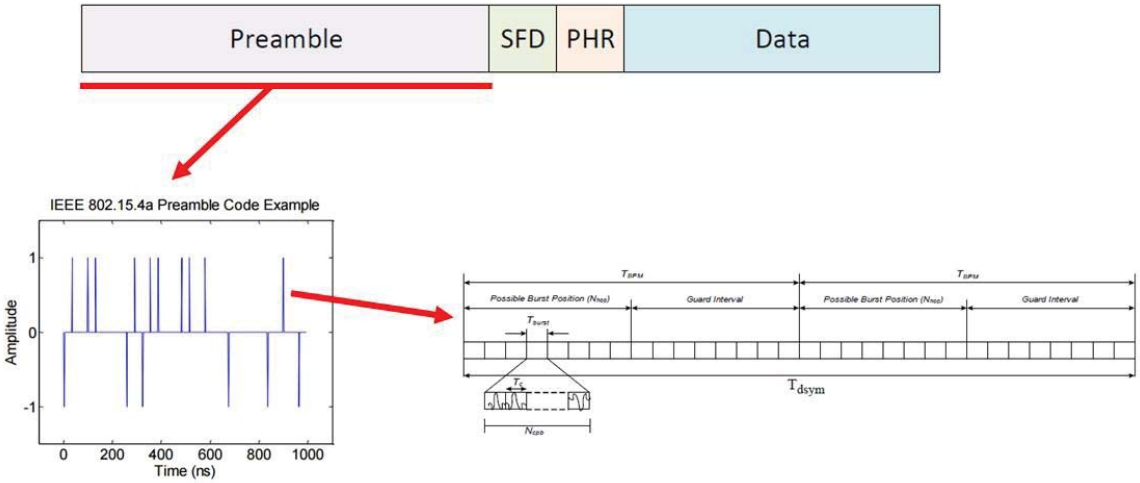

Figure 1-7 – The structure of how the preamble part of a UWB frame is made up of multiple symbols

each frame, autocorrelating it and then summing the whole thing. This process can be seen in Figure 1-8. This is the primary signal that is recorded and analyzed in the ranging experiment covered in Chapter Five.

Introduction to the Location Algorithms

Localization of a target can be accomplished by numerous methods, the most prevalent being GPS which uses ultra-high precision atomic clocks to measures the time-of-flight [1]. However, for indoor localization, this technique is not as applicable but instead a technique of time difference of arrival (TDOA) which uses a set of anchors that have synchronized clocks to find the position of a target that has an unsynchronized clock.

When using TDOA to calculate a transmitter (tag) location, the time of arrival (TOA) of the signal emitted by the transmitter is measured at each receiver (anchor). By knowing the medium it passes through, as well as the speed at which it travels through the medium, a distance can be found, or a range. The range is calculated by finding the differences in time a single signal is received by each of the anchors. These are referred to as the range differences (RD's), each creating a hyperboloid on which the tag should reside. By finding the intersection of all of these hyperboloids, a three dimensional location should be able to be found, given that there are at least 4 anchors. When the error of the system is factored into this calculation, no single point of intersection is usually found. Because of this, a best-fit solution must be used instead. This issue of

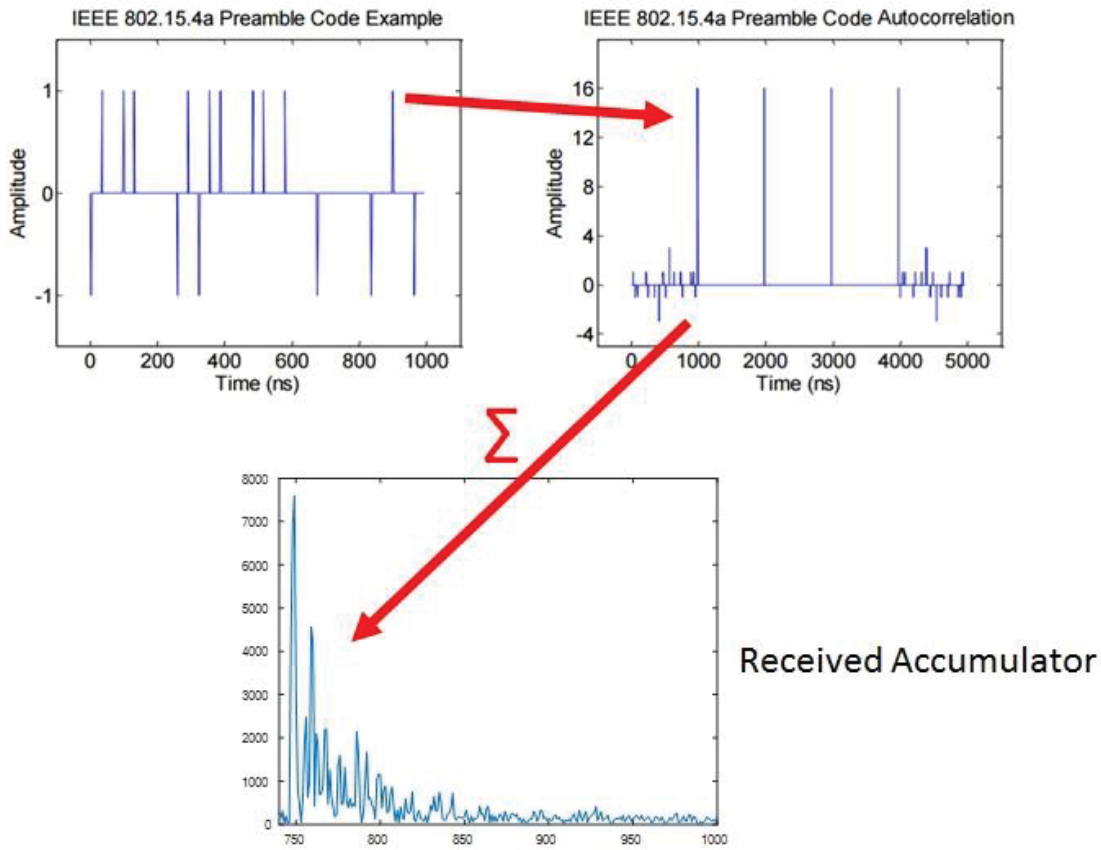

Figure 1-8 – How the accumulator signal is generated from the UWB pulse preamble

multilateration has caused the creation of numerous algorithms to find the best-fit solution. The DecaWave software uses a spherical intersection method to calculate the best fit solution and calculate the final position of the tag being tracked. Another popular algorithm for the best-fit solution is the use of a spherical interpolation algorithm. Both of these algorithms are presented and explained in much detail in [5]. In our positioning system we use the TDOA algorithm to find the unknown location of the tag given known locations of the anchors. Given the known anchor locations, or receivers, as R_{x1} or (x_1, y_1, z_1), R_{x2} or (x_2, y_2, z_2), R_{x3} or (x_3, y_3, z_3), and R_{x4} or (x_4, y_4, z_4), and the unknown location of the tag, or transmitter, defined as (x_u, y_u, z_u). This is visually represented in Figure 1-9. The distance between the each of the four anchors with known locations and the unknown tag location can be defined as ρ_1, ρ_2, ρ_3, and ρ_3 which is given by

Equation 1-1

$$\begin{aligned}\rho_i &= \sqrt{(x_i - x_u)^2 + (y_i - y_u)^2 + (z_i - z_u)^2} + ct_u \\ &= f(x_u, y_u, z_u, t_u)\end{aligned}$$

where i = 1, 2, 3, and 4, c is speed of light, and t_u is the unknown time delay in the hardware. To find the difference between each of the four receiver-to-tag distances, the differential can be written as

Equation 1-2

$$\begin{aligned}\Delta\rho_{1k} &= \rho_1 - \rho_k \\ &= \sqrt{(x_1 - x_u)^2 + (y_1 - y_u)^2 + (z_1 - z_u)^2}\end{aligned}$$

$$-\sqrt{(x_k - x_u)^2 + (y_k - y_u)^2 + (z_k - z_u)^2}$$

where k = 2, 3, and 4. The unknown time delay from Equation 1-1 has been cancelled. Differentiating Equation 1-2 will give

Equation 1-3

$$\begin{aligned} d\Delta\rho_{1k} &= \frac{(x_1 - x_u)dx_u + (y_1 - y_u)dy_u + (z_1 - z_u)dz_u}{\sqrt{(x_1 - x_u)^2 + (y_1 - y_u)^2 + (z_1 - z_u)^2}} \\ &+ \frac{(x_k - x_u)dx_u + (y_k - y_u)dy_u + (z_k - z_u)dz_u}{\sqrt{(x_k - x_u)^2 + (y_k - y_u)^2 + (z_k - z_u)^2}} \\ &= \left(\frac{x_1 - x_u}{\rho_1 - c\tau_u} + \frac{x_k - x_u}{\rho_k - c\tau_u}\right)dx_u \\ &+ \left(\frac{y_1 - y_u}{\rho_1 - c\tau_u} + \frac{y_k - y_u}{\rho_k - c\tau_u}\right)dy_u \\ &+ \left(\frac{z_1 - z_u}{\rho_1 - c\tau_u} + \frac{z_k - z_u}{\rho_k - c\tau_u}\right)dz_u \end{aligned}$$

In Equation 1-3, the only unknown values are considered to be dx_u, dy_u, and dz_u by assuming some initial values for x_u, y_u, and z_u. With these initial values, calculate to find the first set of dx_u, dy_u, and dz_u. Once these values are calculated, they are used to modify the initial tag position to create new values of x_u, y_u, and z_u which again can be considered to be known values. They are then used again in Equation 1-3 to find a new position repeatedly until the absolute values of dx_u, dy_u, and dz_u come below a certain threshold. This threshold is defined as

Equation 1-4

$$\varepsilon = \sqrt{dx_u^2 + dy_u^2 + dz_u^2}$$

The iteration process is concluded once this threshold is reached, and the tag position defined by the x_u, y_u, and z_u is the desired tag location. This is the position which you test against your ground truth, the position known to be correct, to find the total accuracy of your system. The matric form of this iteration process and Equation 1-3 is represented as

Equation 1-5

$$\begin{bmatrix} d\Delta\rho_{12} \\ d\Delta\rho_{13} \\ d\Delta\rho_{14} \end{bmatrix} = \begin{bmatrix} \alpha_{11} & \alpha_{12} & \alpha_{13} \\ \alpha_{21} & \alpha_{22} & \alpha_{23} \\ \alpha_{31} & \alpha_{32} & \alpha_{33} \end{bmatrix} \begin{bmatrix} dx_u \\ dy_u \\ dz_u \end{bmatrix}$$

where

Equation 1-6

$$\alpha_{k-1,1} = \frac{x_1 - x_u}{\rho_1 - c\tau_u} + \frac{x_k - x_u}{\rho_k - c\tau_u}$$
$$\alpha_{k-1,2} = \frac{y_1 - y_u}{\rho_1 - c\tau_u} + \frac{y_k - y_u}{\rho_k - c\tau_u}$$
$$\alpha_{k-1,3} = \frac{z_1 - z_u}{\rho_1 - c\tau_u} + \frac{z_k - z_u}{\rho_k - c\tau_u}$$

The solution to Equation 1-6 is given by

Equation 1-7

$$\begin{bmatrix} dx_u \\ dy_u \\ dz_u \end{bmatrix} = \begin{bmatrix} \alpha_{11} & \alpha_{12} & \alpha_{13} \\ \alpha_{21} & \alpha_{22} & \alpha_{23} \\ \alpha_{31} & \alpha_{32} & \alpha_{33} \end{bmatrix}^{-1} \begin{bmatrix} d\Delta\rho_{12} \\ d\Delta\rho_{13} \\ d\Delta\rho_{14} \end{bmatrix}$$

where $[\ ]^{-1}$ represents the inverse of a matrix. In this case it represents the inverse of the α matrix. In the case that there are more than four anchors, or

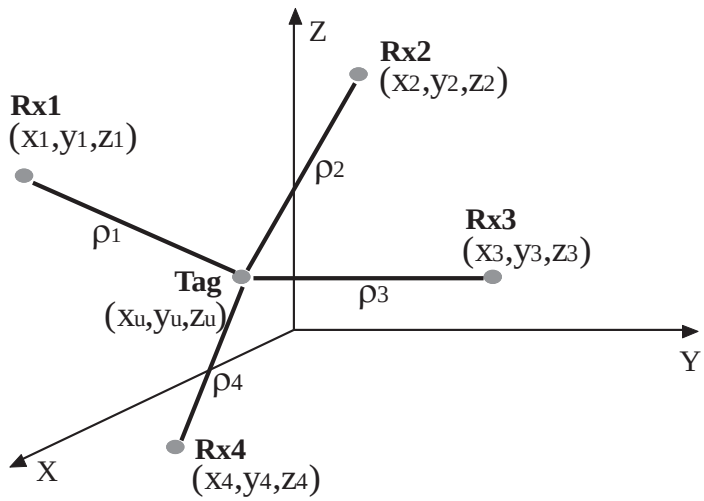

Figure 1-9 – Visual representaion of the TDOA algoithm to calculate the unknown position of a tag given the known locations of four anchors, or recievers

receivers, the least squares approach can be applied to find the solution for the location of the tag.

Organization

Chapter 2 overviews the current Real-Time Locating Systems as well as their accuracies. It focuses on the commercially available. The specifications of each system are discussed and compared to each other, with emphasis on the factors important to asset tracking applications.

Chapter 3 covers the challenges faced for achieving high precision and accuracy systems. It is broken up into the four main sources of error: the dilution of precision, the antenna offset, the phase center variation, and the clock jitter and drift. Each of these are discussed exploring the sources of each of these errors, and the ways to mitigate these errors to help achieve better accuracy and precision in our application.

Chapter 4 covers the experimental setup of the two physical experiments that were conducted as well as a quick summary of the dilution of precision optimization software that was developed to optimize the number of anchors and placement to achieve a specified level of dilution.

Chapter 5 focuses on the results of the ranging experiment. It covers the results from channels 4, 5, and 7. Using each channel, the distance is varied between the two anchors, and the data analyzed. Additionally, the antenna effects are shown between the three available antennas: the TechMah planar monopole

antenna, the DecaWave planar monopole antenna, and the spherical monopole antenna.

Chapter 6 covers the results of the tracking experiment as well as how each of the error sources were mitigated and the resulting accuracy achieved. It covers each of the specific sources of error and how once mitigated, a sub millimeter accuracy for static positions can result. Additionally, it shows the dilution of precision over the testing space and correlates it to the need for anchor placement optimization.

Chapter 7 covers the dilution of precision optimization software. The software's capabilities are shown and discussed as well as the results. Graphical representations of the software are shown to help illustrate how the dilution of precision varies across your whole testing space.

Chapter 8 concludes the paper and gives recommendations from all of the data collected to help create a system which maximizes the accuracy of an indoor asset tracking system. It discusses the ways to optimize your system configuration as well as calibration techniques to maximize your accuracy.

CHAPTER TWO
CURRENT SYSTEMS AND THEIR ACCURACIES

There are various tracking systems that have already come to market, as well as systems that are in the research phase. This section will summarize what technologies and systems are commercially available as well as stating their accuracies and other factors. When considering localization systems, there are two main categories: indoor and outdoor. While GPS is the main system used in localization for outdoor tracking, its indoor accuracy is very poor. GPS uses time-of-flight measurement for calculating position, but for indoor applications Time Difference of Arrival (TDOA) is the standard. Other indoor location systems employ Wi-Fi, RFID, Bluetooth low energy, and ultrasound for positioning purposes but none is as accurate as UWB. A TDOA system utilizes base stations, or receivers, which all have a synchronized clock and measure the difference in time between all of the receivers from an unsynchronized tag. The two main ways to achieve this are to use a frequency modulated continuous wave (FMCW), or UWB. FMCW has been used extensively with differing levels of accuracy, from 10cm in an outdoor environment, 20 cm for an indoor environment, and even 1 cm in a Line of Sight (LOS), multipath free environment. The biggest advantage to the use of UWB for this process is that it is much more robust in a multipath environment, making it much more effective for a variety of environments. Table 2-1 shows a comparison of all the currently available commercial systems as well as some of their specifications. Figure 2-1 shows

Table 2-1 – Summary of current commercial systems and their specifications. Updated table from [4]

Company	**PulsON [10]**	**DART [13]**	**Ubisense [14]**	**Symeo [15]**	**ScenSor [11] (DecaWave)**	**Tag and Traq [21]**	**Redpoint [9]**
Frequency (GHz)	3.1-5.3	6.35-6.75	6.0-8.0	5.725-5.875	3.5-6.5	3.5-4	3.5-6.5
Range (m)	300-1100	50	>160	400	300	38	30-50
Tag Weight	58 g	20 g	580 g	1.4 kg	NA	NA	Not Listed
No. of Tags	1	3500/s	1000	NA	11,000	Multiple	1000s
Refresh Rate (Hz)	8-154	0.01-200	20	25	64 M	1	2
Localization	TW-ToF	TDoA	TDoA/AoA	RToF	Tof/TDoA	TWR	TWR
Accuracy (cm)	2.1	<30	15	10	10	30-60	20
Technology	UWB	UWB	UWB	FMCW	UWB	UWB	UWB

Figure 2-1 – The DecaWave EVK1000 evaluation kit, which uses the DW1000 chip paired with the DecaWave planar monopole antenna

the DecaWave evaluation kit which employs most of the same hardware as the system used for our testing and experiments. As can be seen in the comparison table, most of the systems have accuracies that are in the range of 10-30 cm, the exception being the PulsON system that has an accuracy of around 2.1 cm. However, unlike the other systems which can handle multiple tags, even up to 10,000 in the case of the DecaWave, the PulsON system can only track a single tag at a time. The next notable feature of these systems is their range, which varies from around 50m with the Red Point and Dart system all the way to 1000 m with the PulsON system. Range is extremely important for an asset tracking system simply for the range of use in the facility. The larger range a system offers, the better coverage of the facility can use for tracking all of the equipment as well as personnel.

ABG Tag and Traq, as well as the Red Point positioning use the DW1000 chip in their hardware. This shows that it is tried and true to work for commercial applications, as well as having the ability to have the highest accuracy within the available commercial products. Figure 2-2 and Figure 2-3 show the physical Red Point positioning product and their system configuration respectively. Figure 2-4 shows the physical UWB module which is used for UWB communication in the Tag and Traq system. Shown in Figure 2-4 is the UWB chip antenna and is listed as “T03” on the circuit board. Additionally, Figure 2-5 shows a physical tag of the Ubisense Dimension 4 system.

Figure 2-2 – Hardware associated with the Redpoint Positioning system [19]

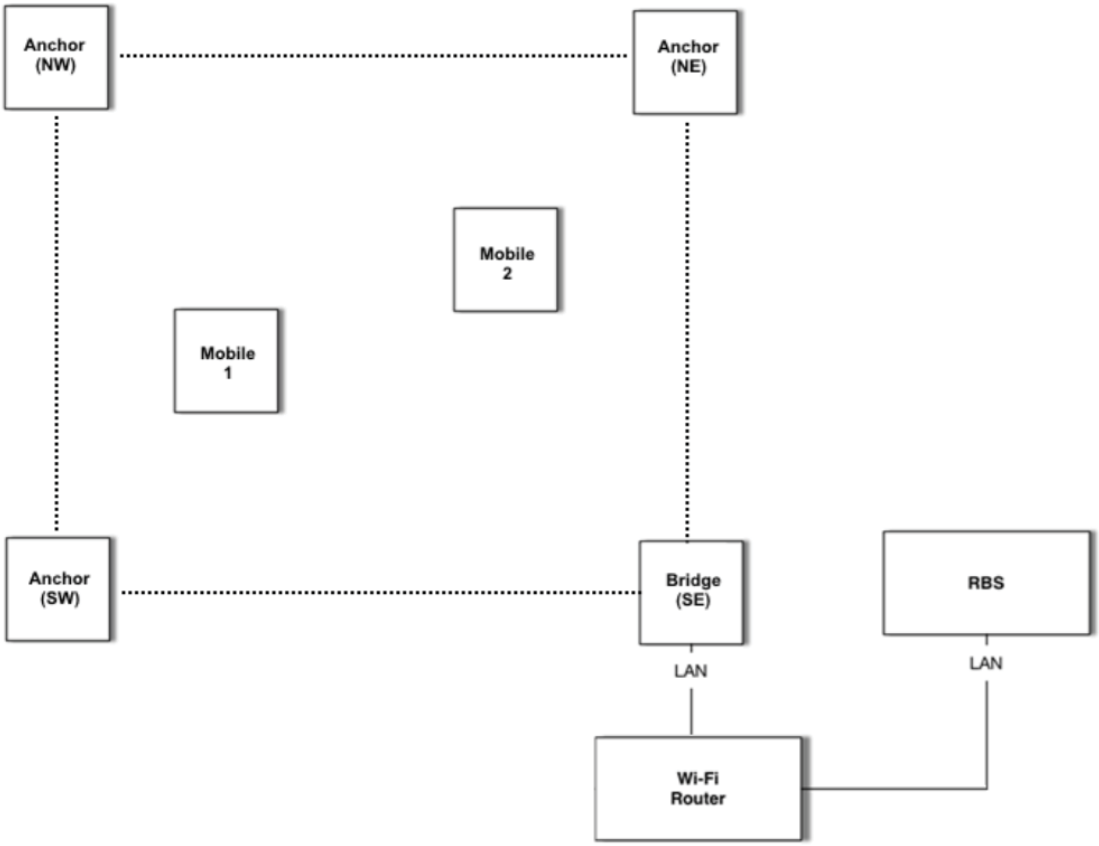

Figure 2-3 – System configuration of the Repoint positioning system [19]

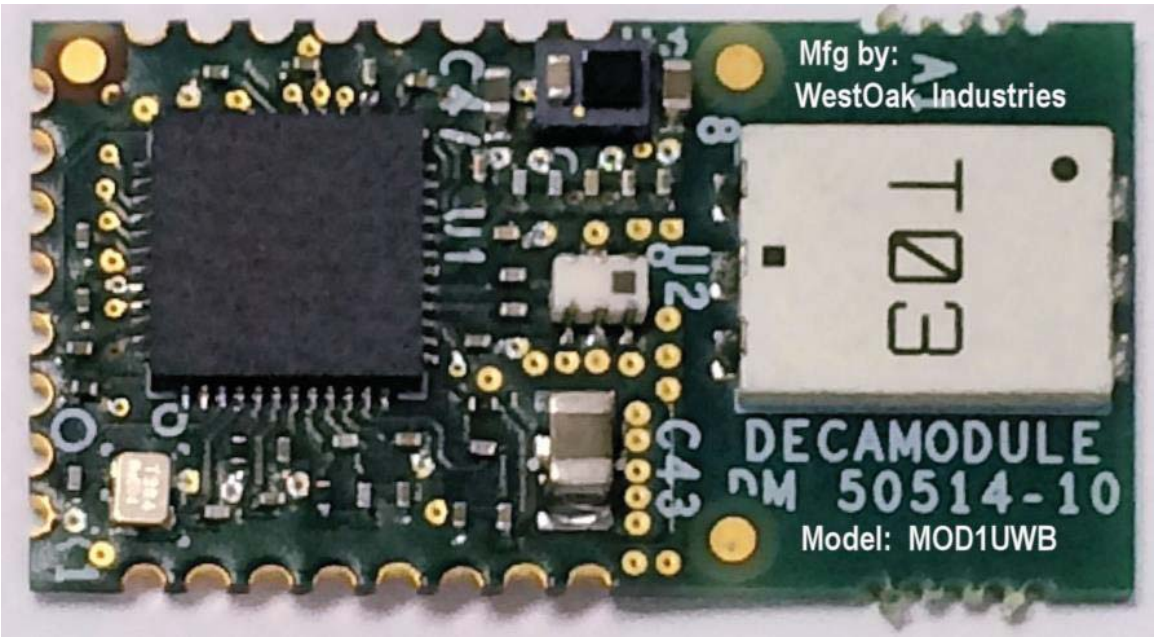

Figure 2-4 – Internal UWB module of the Tag and Traq system [21]

Figure 2-5 – Ubisense UWB tag [14]

DecaWave's DW1000 chip is comparable to all of the other UWB systems and was available for use. It had the ability to track multiple tags as well as support multiple anchors for use. The code was also available for use making it the best option as a beginning system and to use to perform testing and experiments. However, it had issues which needed to be addressed. First of all, accuracy was listed as 10 cm, which compared to other systems was quite good, but for our purposes, was an area to be improved. Additionally, the DecaWave positioning system used a clock which was prone to jitter and drift, which made high accuracy hard to achieve. There was also a substantial lack of information regarding Ultra Wide Band systems and how different factors would affect them. This lack of information led to our first experiment which varied multiple variables such as type of antenna used or channel. This experiment helped increase our knowledge of not only the software, but the hardware as well. Once this data had been collected and analyzed, a second experiment was carried out to find the accuracy of the system, as well as the ability to post process the data to help increase the accuracy of the system. Once this data was analyzed, one of the sources of error seemed to come from the anchor placement due to different tag locations resulting in different accuracies. This again had little information, especially for varying testing spaces. This led to the final section of this thesis which deals with the optimization software for anchor placement,

CHAPTER THREE
CHALLENGES TO ACHIEVE HIGH ACCURACY

To achieve high accuracy in any localization system, the sources of error must be identified, and mitigated. This section will go into some of the sources of error that we identified for our experiments, as well as ways we handled them to increase our overall tracking accuracy. The main sources of error that we will discuss are dilution of precision, antenna offsets, phase center variation, and clock jitter and drift.

Dilution of Precision

Geometric dilution of precision is created from the placement of all of the anchors and how they are spread out across the testing space. Figure 3-1 and Figure 3-2 help show how this can change the accuracy of the system with only the change of anchor locations. The entire testing area can be populated with Position (3D) Dilution of Precision (PDOP) values, showing which positions around the room will experience lower accuracy due to anchor placement. This can be accomplished because there is an algorithm that can be run to analyze the PDOP, given the locations of all of the anchors and the location in at which it will be calculated. There is a separate factor for each dimension, the X, Y, and Z. Each of these factors act as a multiplier to the error. Thus, if there is a lot of variation in the Y dimension anchor locations but not in the Z, the PDOP-y

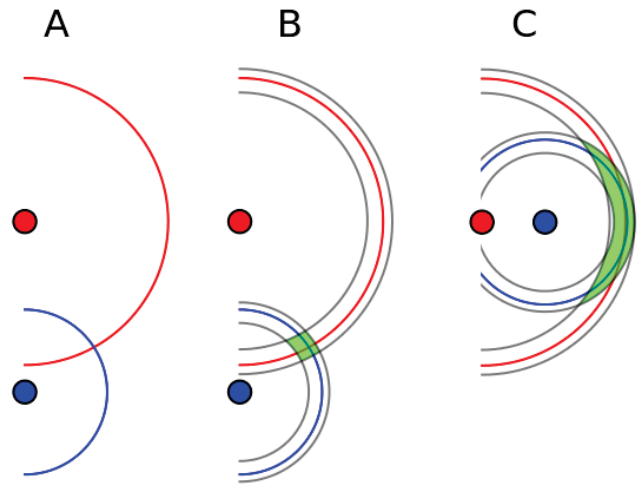

Figure 3-1 – Example of how the dilution of precision can increase with the same amount of error for each transmitter and receiver. (A) represents the ideal solution with no error. (B) represents the dilution of precision (POD) in green when error is introduced to the system. (C) represents the increased DOP when one of the anchors is moved. [12]

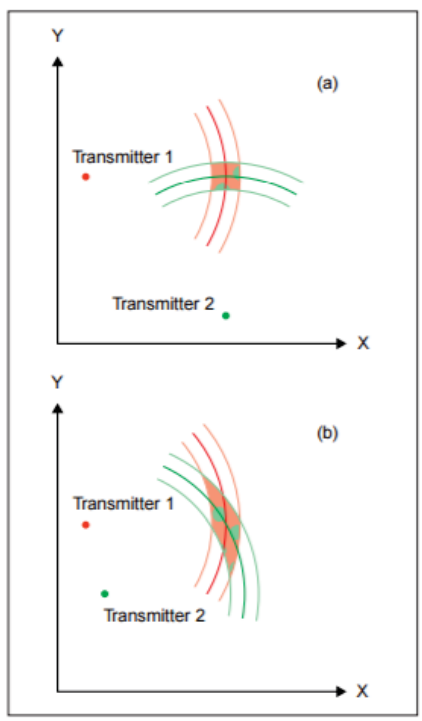

Figure 3-2 – Another example of how anchor placement effects the DOP. From [7]

would be quite low, possibly below 1, whereas the PDOP-z will be a much higher value, possibly around 3 or 4. The total PDOP of that location is a combination of all of the separate PDOP values in each dimension. To help characterize this over the whole experiment and testing space, a program was developed which calculated the PDOP value at each value across the testing space. Figure 3-3 shows the results of this program's analysis. The first graph on the left of the figure shows the analysis of the entire room in which testing was conducted. As can be seen by the colorbar, the values increase all the way to over 35, showing that at that location the error would be horrible. However, the second graph shown on the right of the figure shows the analysis of only the area within the perimeter of the anchors. Here, the values vary from below 1 to slightly above 3.5. This shows that's within the testing area it is quite a bit more accurate, but there are still positions that the accuracy will just be less accurate than others. When looking at the tag testing locations for the tracking experiment, represented by cyan dots, it can be seen that positions 1 and 2 have a higher PDOP value than those of positions 3 and 4. Due to this we should expect the accuracy of the tracking system to be higher for position 3 than either 1 or 2.

Antenna Offsets

By using UWB antennas with a TDOA algorithm, the arrival times of each of the pulses are extremely important to the final accuracy of the system. Slight differences in these values can create a large amount of error. One of the ways

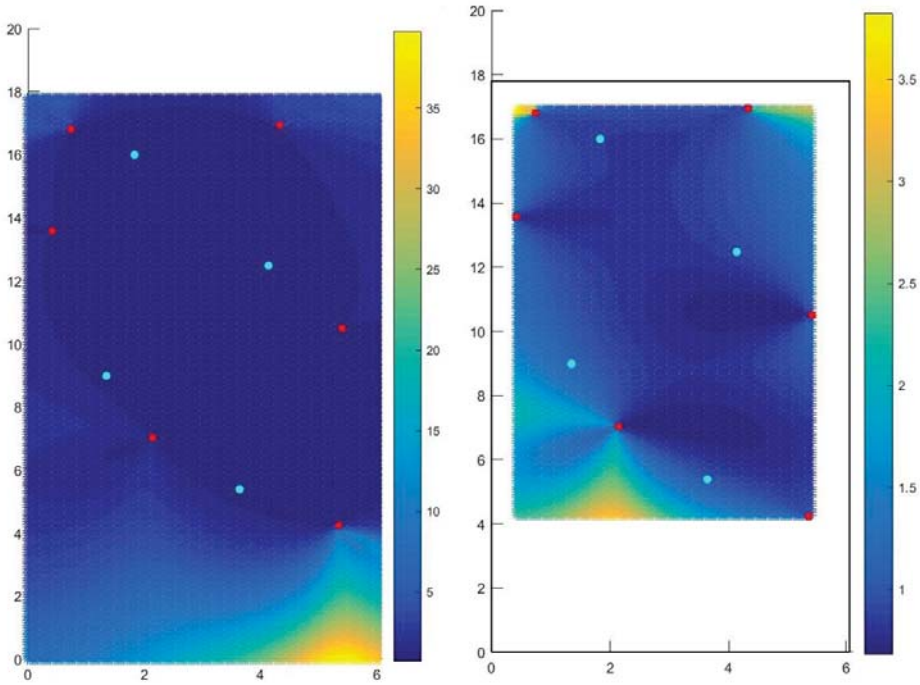

Figure 3-3 – PDOP analysis of the testing space. Graph on left does analysis on entire room, graph on right does analysis of space within the anchors. Red dots represent anchor locations, blue dots represent tag locations.

that this time of arrival can be effected is by the internal resistance and path length inside the electronics and antenna when the signal is received. The DecaWave system has a factor which can be changed to help mitigate this error, however, in our testing, the value was very difficult to accurately assign so that it did not affect the position accuracy. However, in post processing of the data, there are multiple ways in which this error can be mitigated and accounted for, helping reduce the error created from this source. By physically measuring the range between all the anchors, as well as the tag to the anchor and comparing it to the received range data, a difference can be found. By averaging all of these difference values, an offset can be created that can later be used to alter all of the range values being received before the data is input into the location algorithm. By doing this, it helps eliminate this antenna offset during a calibration step where the ranges could be physically measured, and in our case, we were able to eliminate approximate 590 mm of error. Additionally, data could be collected at a specified set of points all across the entire testing space. To guarantee a good representation of the whole testing space in this offset being calculated, a variety of points from the perimeter of the testing volume throughout the inside of the volume must be taken. Without this calibration to help eliminate this error source, there will be a constant value in all of the range samples which will offset the calculated position once it is input to the location algorithm.

Phase Center Variation

Phase center variation of the antenna becomes a larger error source once testing is conducted in larger 3 dimensional spaces. It is generated from a change in the measured phase center of the antenna when there is a difference of angle between the receiving and transmitting antennas. Most of the antennas used are planar and cannot be perfectly positioned in accordance with each other, there will be some angle difference from each connection between anchors as well as tags. As Figure 3-4 shows, as an antenna is rotated from -45 to +45 degrees, the relative phase center changes, creating a displacement that can increase to 10mm. When correlating this to a 3D localization scenario, this error source will vary at every point across the volume because of the different angles associated with the connection channels from the tag transmitter to each of the anchor receivers. Additionally, the rotation of the tag can vary even at one stationary point. This type of error can be helped with the use of a spherical monopole antenna or any antenna that is less prone to this phase center variation.

However, for our experiment, each tag transmitter had a set DecaWave antenna that was integrated into the design, as well as insufficient numbers of monopole antennas to attach to all anchors being used for the tracking experiment.

For our experiment, instead of trying to eliminate this error with the antenna type, we went about mitigating it during the post processing of the data. The true range from each location of the tag to each of the anchors can be measured,

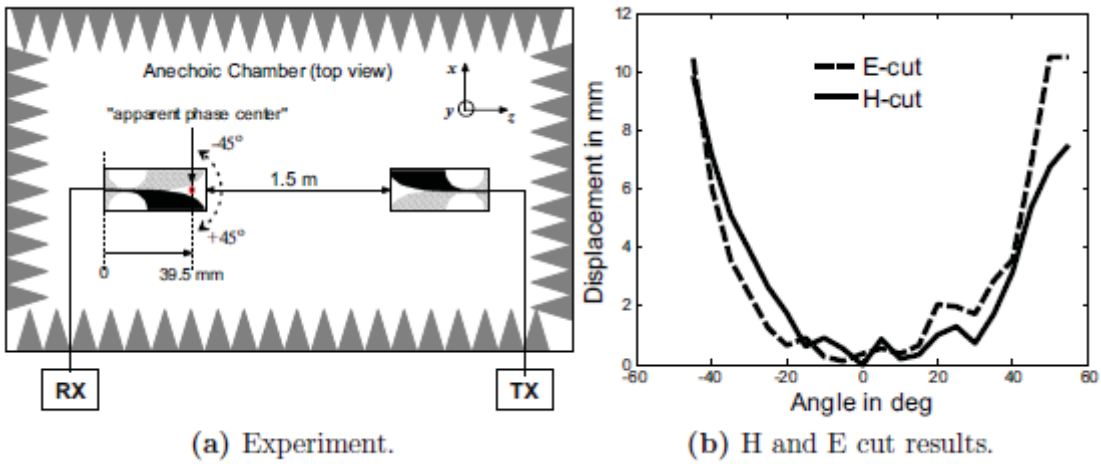

(a) Experiment. (b) H and E cut results.

Figure 3-4 – Experiment from [18] that shows in (a) the experimental setup and in (b) the increase in phase center location with the increase of angle

and then the measured values can be compared and an offset found. With this offset found for each communication channel between the tag and each anchor and at each specific location, the offset can then be applied to the data to correct for the variance in the antenna phase center location. In our experiment, this correction was able to eliminate approximately 58 mm of error from the total accuracy error of our tracking experiment.

Clock Jitter and Drift

With the use of a system that uses TDOA to calculate the position of a tag, the clock can become a large source of error if it is not as high quality as some other clocks. With a clock that is not of highest quality, there will be variances in its stability. This can result in the drifting of the clock which in turn will translate to a position solution which drifts along with the clock. If the system was wired together this would be less of an issue because of the ability to fully sync all of the clock together constantly. However, with a wireless system the clocks can be synced, but once this has been done each separate clock can drift at its own rate. Additionally, each clock is prone to jitter, basically an inconsistent clock reading that is accepted at a certain tolerance. Whereas jitter is relatively easy to mitigate with the use of an averaging filter used to normalize values of a certain window size, the drift of the clocks can become a much larger issue to address. The easiest way to mitigate for this in post processing is again the use of

averaging. However, unlike the window size necessary for jitter mitigation, to be able to mitigate the effects of clocks drift must be significantly larger because of the time constant associated with the drift. For our tracking experiment, we were able to eliminate approximately 13 mm and 11 mm of error from clock jitter and drift respectively. This was achieved with a 100 sample window size for the jitter and a 6500 sample window size for drift.

CHAPTER FOUR
EXPERIMENTAL SETUP

Overview of Both the Ranging and Tracking Experiments

The main focus of this paper is the development of the PDOP optimization software that can be used as a design tool for a UWB tracking system that uses a TDOA algorithm for localization. However, it will also cover two prior experiments which help identify how the UWB system functions and give a baseline for its accuracy. The focus of these is to research the differences of distance, antenna, height, and multipath effects on a UWB positioning system. Furthermore, these results will be analyzed to create a system in which the strength and quality of the pulse can be determined and given weight, thus increasing the accuracy of the calculated position. It can also be used to help determine the number of anchors necessary for a desired accuracy in a specified space.

All of the data used in this section is gathered systematically with multiple variables for the experiment. The first experiment consisted of 2 anchors, set on rigid tripods that had variable height. Each data collection set had 200 accumulator pulse samples taken. The distance between anchors is varied from 2.0 meters to 15 meters with Line Of Sight (LOS) maintained as shown in Figure 4-1, with another measurement of ~28.2 meters with Non Line Of Sight (NLOS) between anchors. Figure 4-3 and Figure 4-4 show the experiment set up at 2

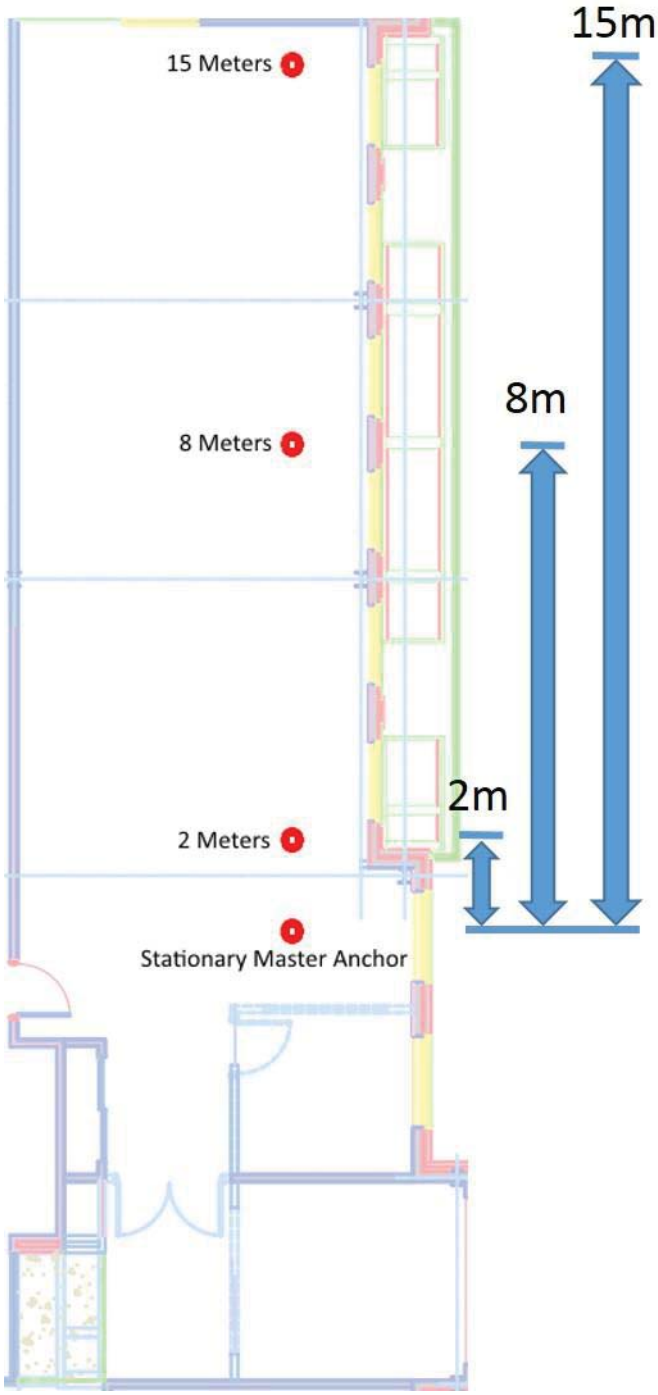

Figure 4-1 – Overview of the testing locations. The master anchor does not move, while the secondary anchor is moved to separation distances of 2 meters, 8 meters, and 15 meters

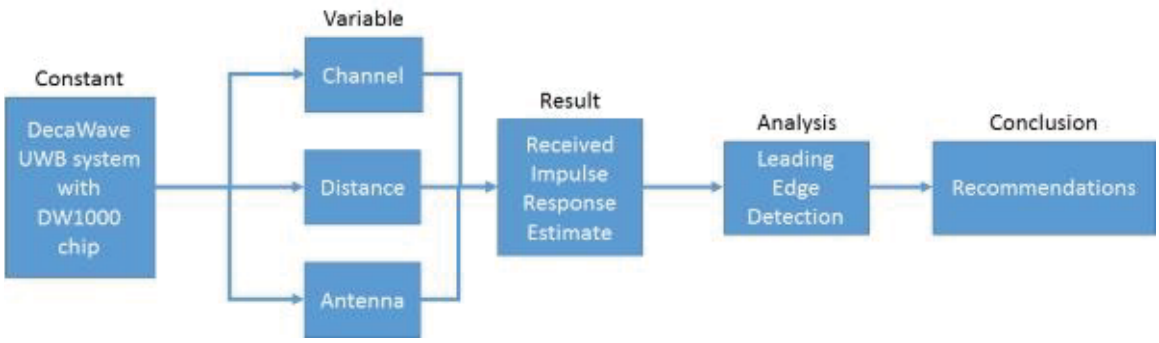

Figure 4-2 – Block diagram of the Ranging Experiment

Table 4-1 – Information on each of the antennas used for the experiments

	DecaWave Planar Monopole	**Spherical Monopole**	**TechMah Planar Monopole**
Gain	2.2 dBi at 4 GHz 3.3 dBi at 6.5 GHz	2.1 dBi at 4 GHz 2.9 dBi at 6 GHz	-2.4 dBi at 3.5 GHz -0.4 dBi at 6.5 GHz
Operating Frequency	3 GHz - 6 GHz	3 GHz - 10 GHz	3.6 GHz - 10 GHz
Radiation pattern	Omni-directional	Omni-directional	Omni-directional

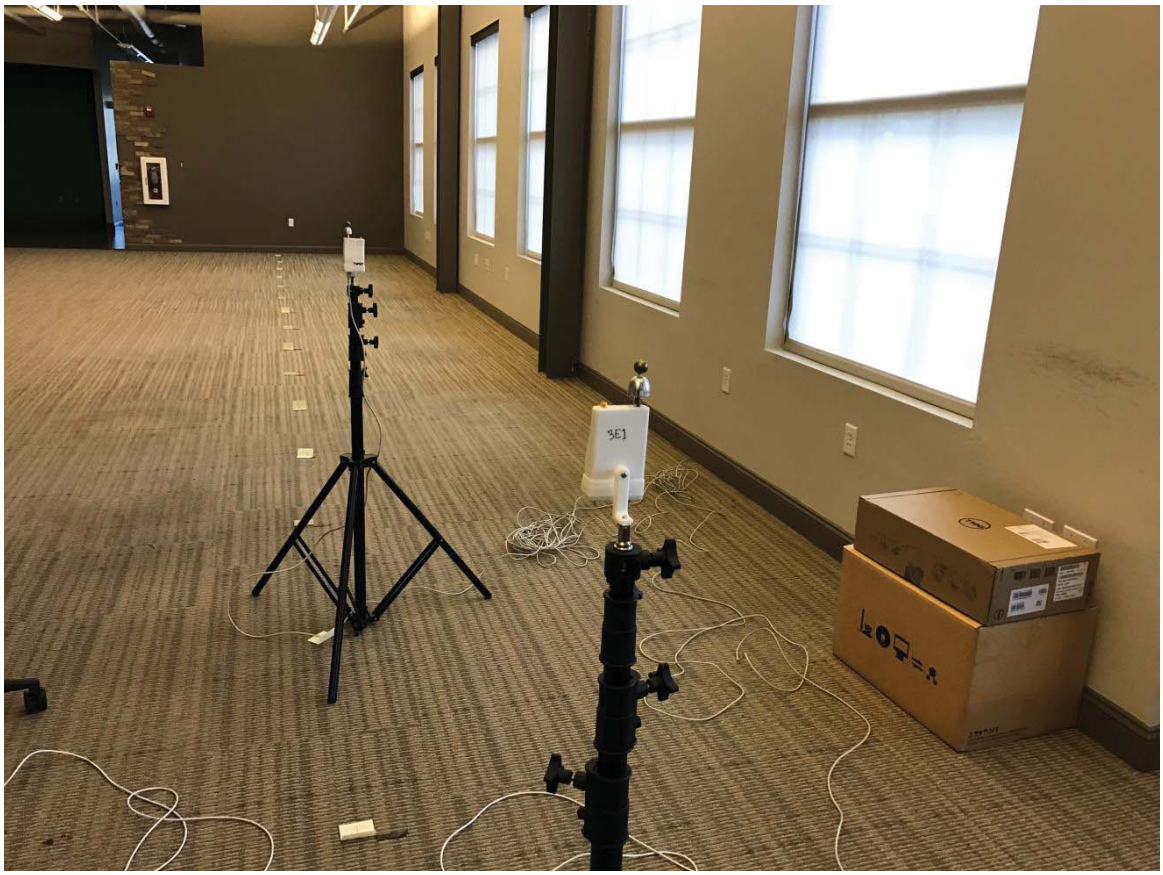

Figure 4-3 – First experiment with variations of Distance between anchors, antenna, height, and UWB channel. This shows the experiment at 2 meters apart, 1.311 meters off the ground, and using a monopole antenna.

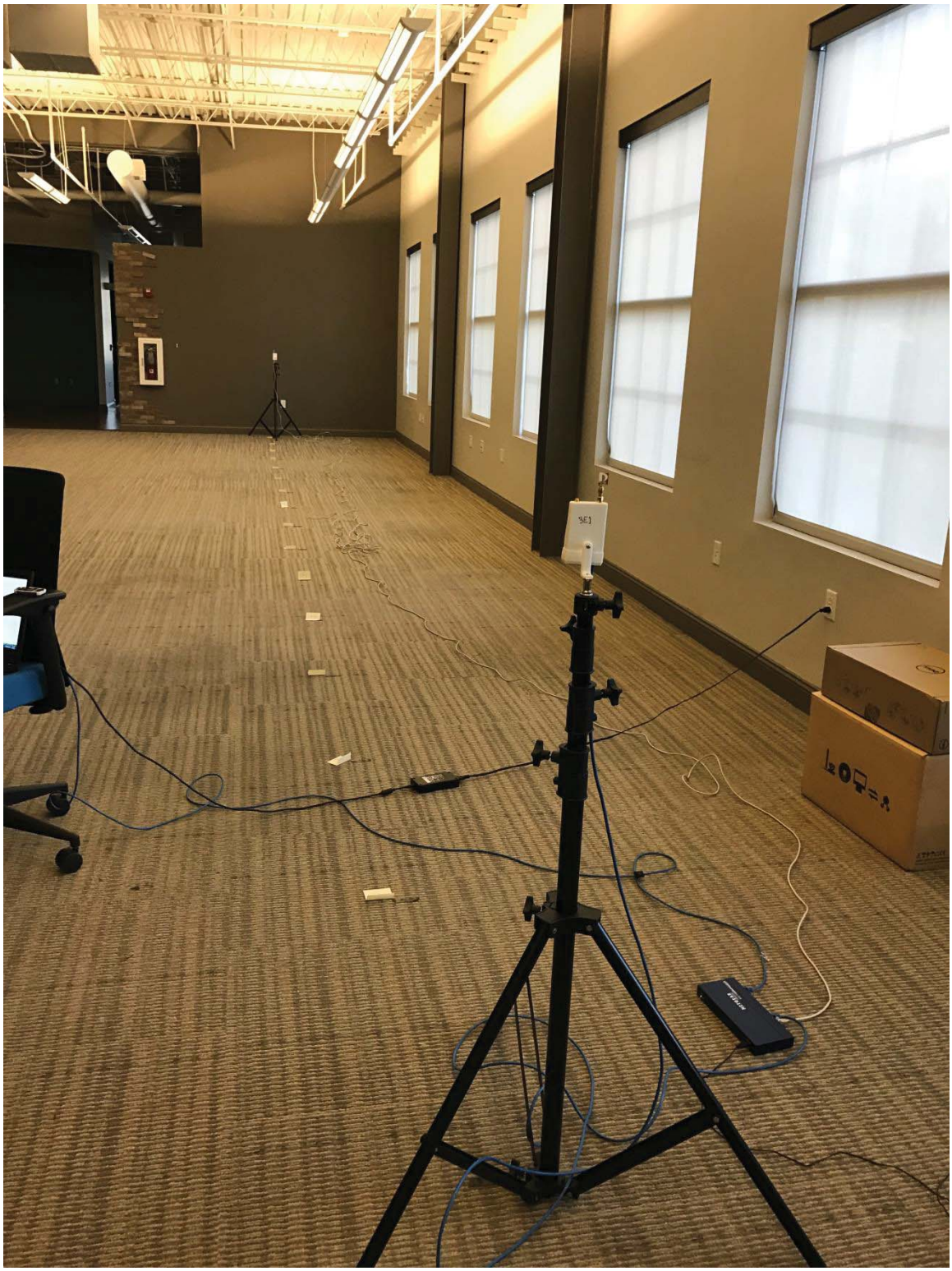

Figure 4-4 – Shows the experiment using anchor distance of 15 meters and height 1.311 meters, and using the TechMah Concept antenna.

meters and 15 meters respectively. The height of the anchors was varied from 1.311 meters off the ground to 3.201 meters. Figure 4-3 shows the height of 1.311 meters while Figure 4-5 shows the height of 3.201. The antenna was changed between 3 different types of UWB antennas. The first is the antenna supplied with the Decawave positioning system and will be referred to as the Decawave antenna. The second is a spherical monopole antenna that was fabricated at TechMah and will be referred to as the spherical monopole antenna. The final antenna is another UWB antenna that was created to decrease the form factor of the original Decawave antenna, and will be referred to as the TechMah concept antenna. Figure 4-6 and Figure 4-7 show all of the different antennas together with a ruler so that differences in size can easily be shown. The radiation patterns for the TechMah spherical monopole antenna are shown in Figure 4-8, Figure 4-9 for the TechMah planar monopole antenna, and Figure 4-10 for the DecaWave planar monopole antenna. Finally, the different channels for the UWB signal were varied, using channels 4, 5 and 7. Figure 4-11, Figure 4-12, and Figure 4-13 show an example of a pulse of each channel.

The second experiment, referred to as the tracking experiment, was a test of the entire positioning system while also collecting accumulator data. This was done to show that by calculating parameters associated to the accumulator pulse and its strength, the overall calculated position of the tag can be calculated with better accuracy than the original system. This experiment consisted of six UWB anchors spread around an open, indoor space at varying heights and distances

Figure 4-5 – Shows the first experimental setup using the height of 3.20 meters with a distance of 8 meters and using the Decawave antenna.

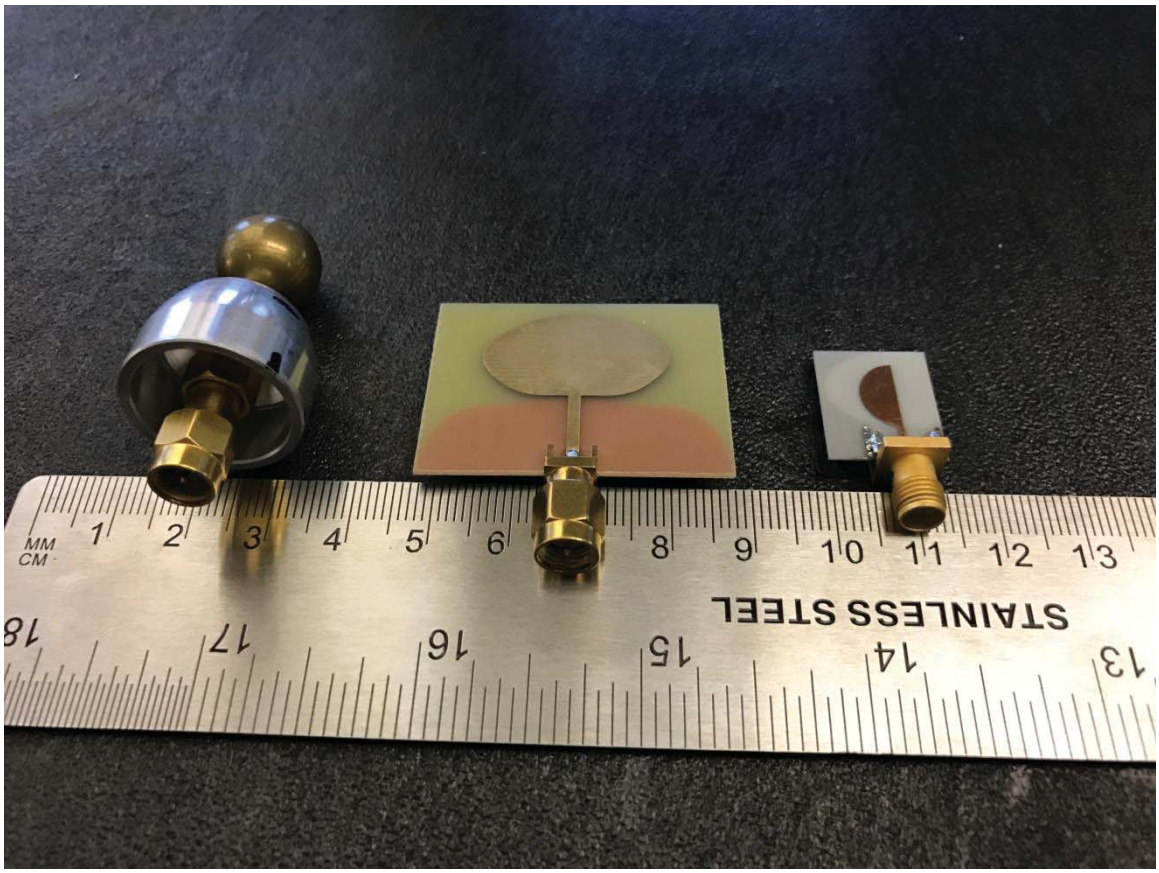

Figure 4-6 – Width comparison of the three antennas used in in the first experiment. From left to right: spherical monopole antenna, Decawave planar monopole antenna, and TechMah planar monopole antenna

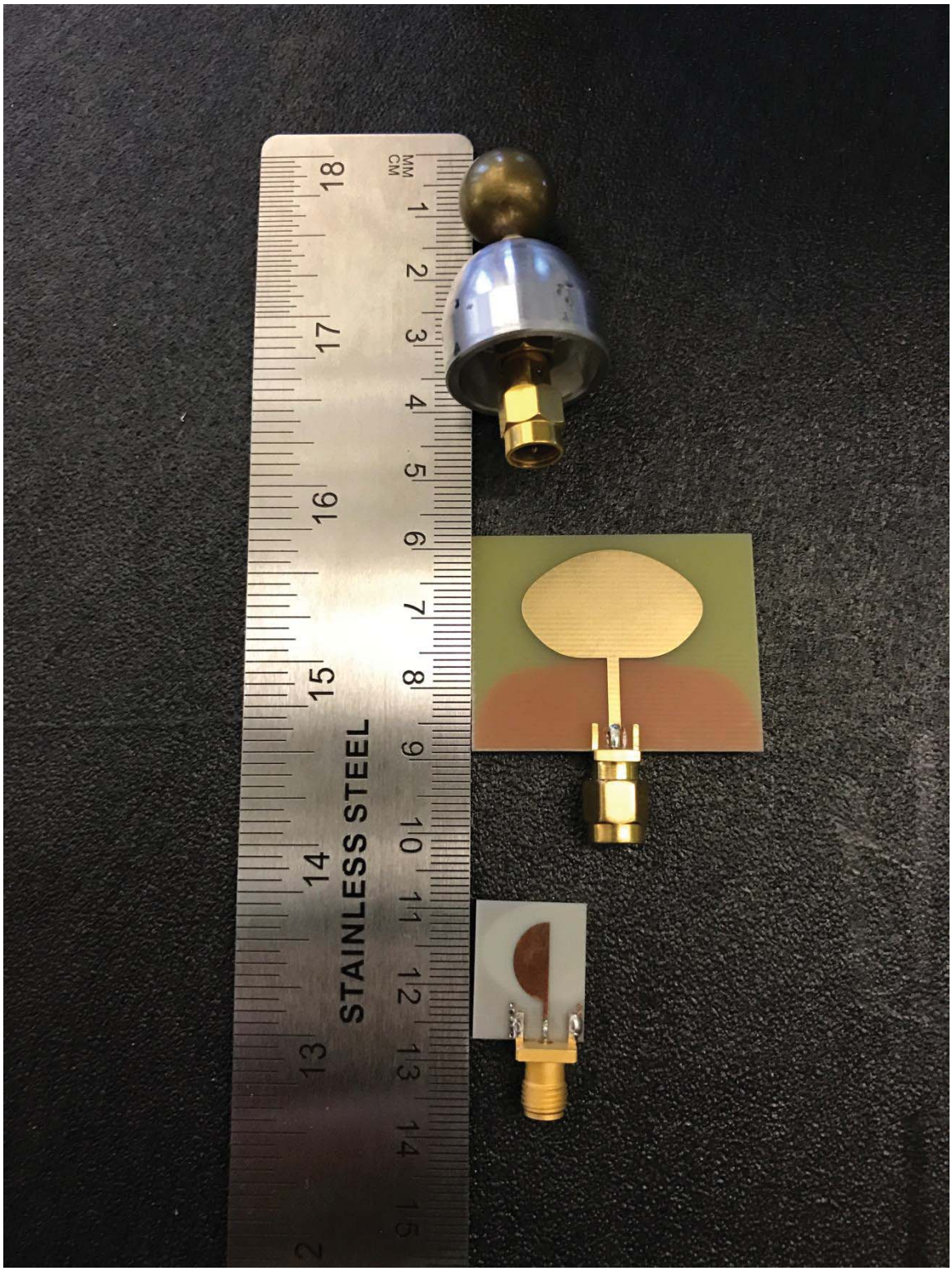

Figure 4-7 – Height comparison of all three different antennas used in the first experiment. From top to bottom, spherical monopole antenna, Decawave planar monopole antenna, and TechMah planar monopole antenna

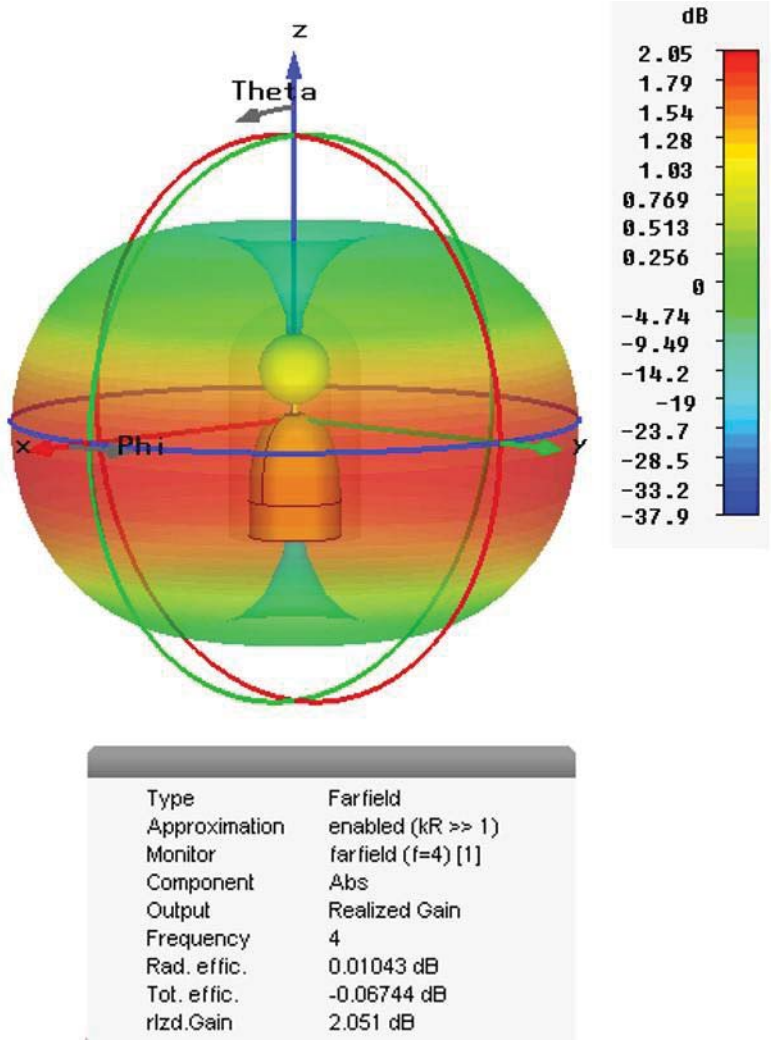

Figure 4-8 – Radiation pattern of the TechMah spherical monopole antenna

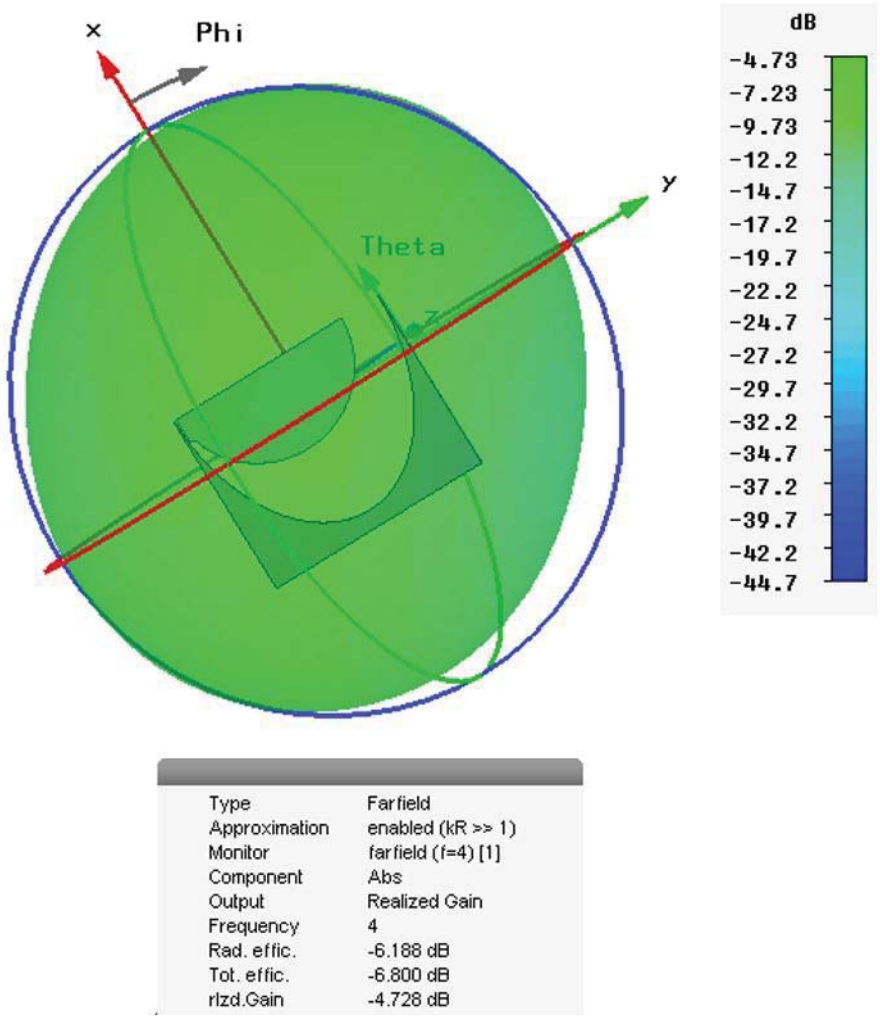

Figure 4-9 – Radiation pattern of the TechMah planar monopole antenna

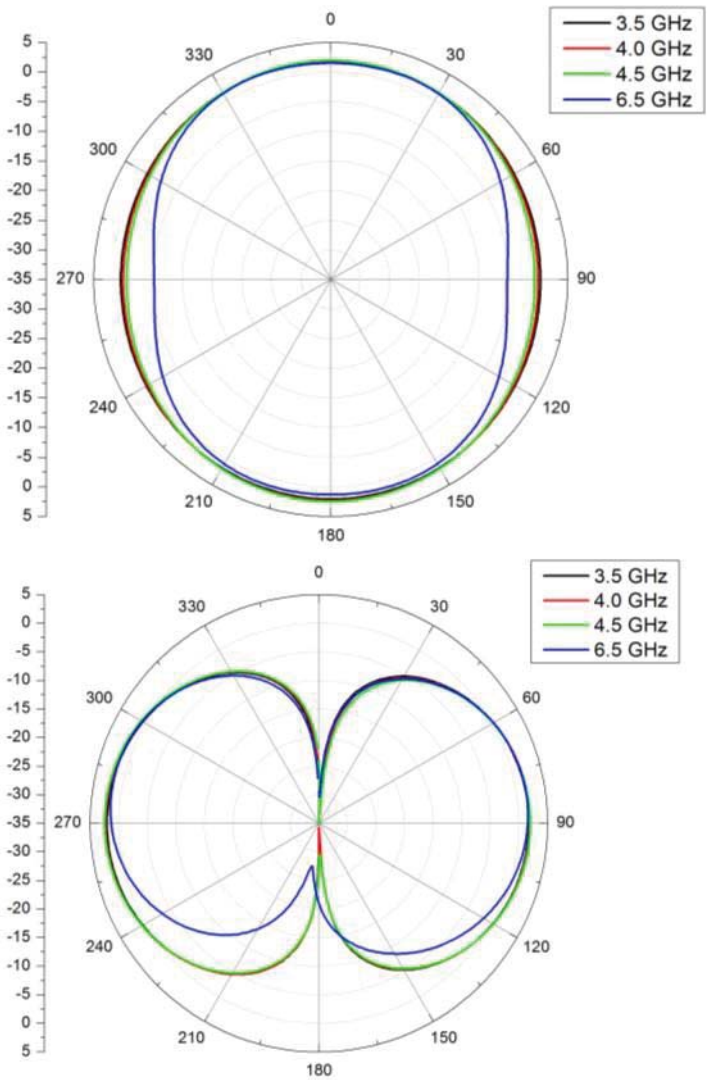

Figure 4-10 – Radiation pattern of the DecaWave planar monopole antenna

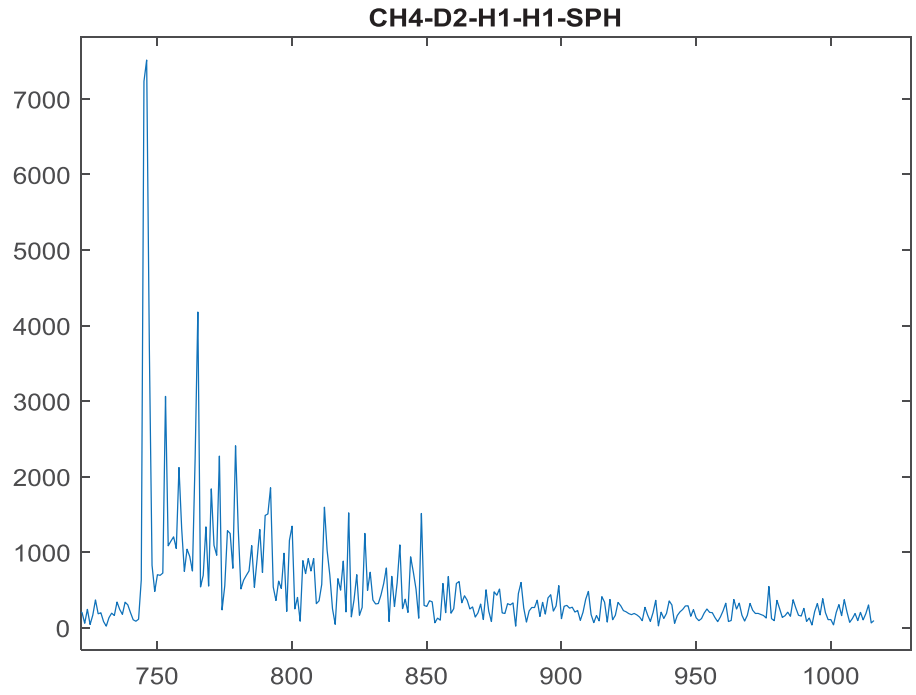

Figure 4-11 – Example of a pulse from channel 4 using the spherical monopole antenna, the receiver and transmitter having a separation distance of 2 meters

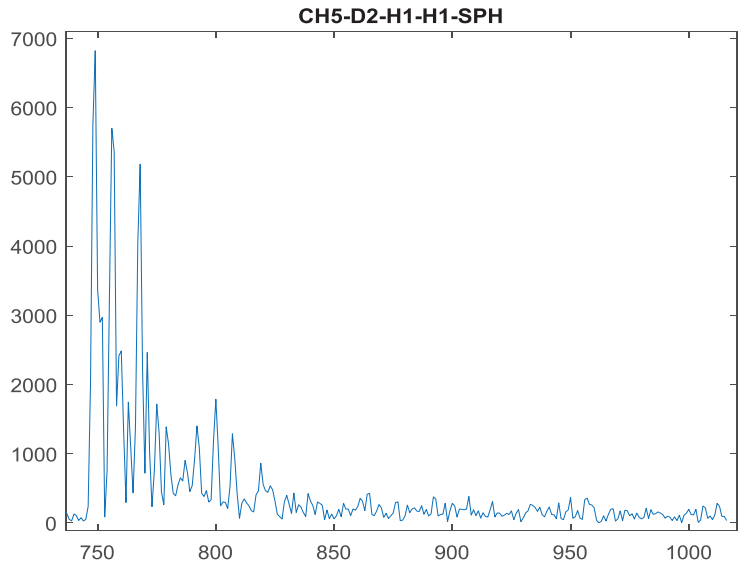

Figure 4-12 – Example of a pulse from channel 5 using the spherical monopole antenna, the receiver and transmitter having a separation distance of 2 meters

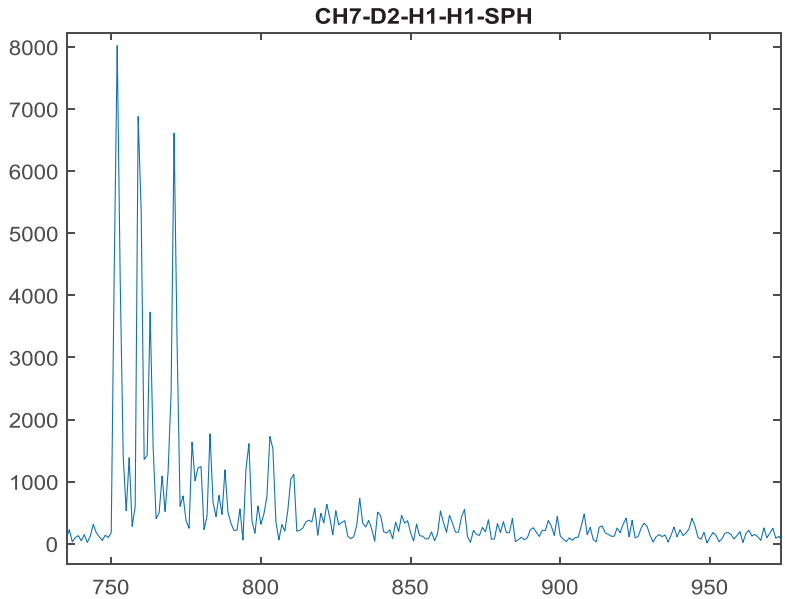

Figure 4-13 – Example of a pulse from channel 7 using the spherical monopole antenna, the receiver and transmitter having a separation distance of 2 meters

from each other. One tag was tracked and had its position calculated. The tag was positioned at four different locations across the space containing the anchors. At each location, a set of 20,000 accumulator pulses was collected, taking approximately 10 minutes. Each of the four locations for the tag had a data set collected at each of the three UWB channels.

One of the most important factors in any experiment when attempting to measure the accuracy is the ability to have the base truth, in this case of position. The size of the space makes it impractical to use optical tracking systems to gain a ground truth location, so instead, the use of a laser range-finder was used. In addition to measuring the distances to each anchor from the tag location, there were eight targets placed on the surrounding perimeter of the space. At each of the four tag locations, the distance to each target and anchor was measured multiple times and averaged. Once these distances were measured, multiple location algorithms were used to find the location. These were described further in Chapter 2. Figure 4-15 shows a top down view of the space with the locations of the anchors and targets marked, while Figure 4-16 shows a three dimensional view created using Matlab to help show the variation in height.

The accuracy of the system and algorithm used are dependent on the variation of all of the anchors in each direction. In the data, it can be seen that in the Y direction the location was most accurate, while in the Z it was least. This can be explained because in the Y location there was a very large variation all of the

locations of the tags, while the Z is much harder to vary because of the room constraints.

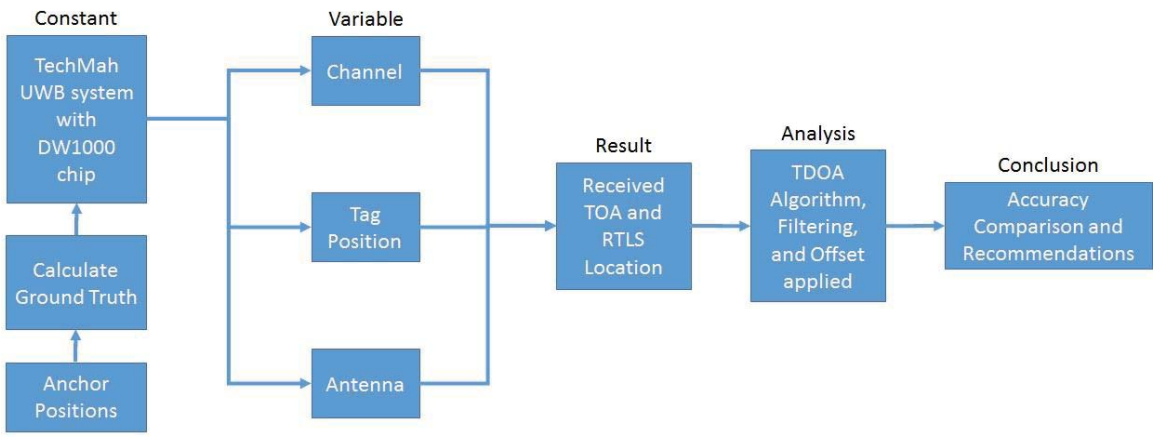

Figure 4-14 – Block diagram of the Tracking Experiment

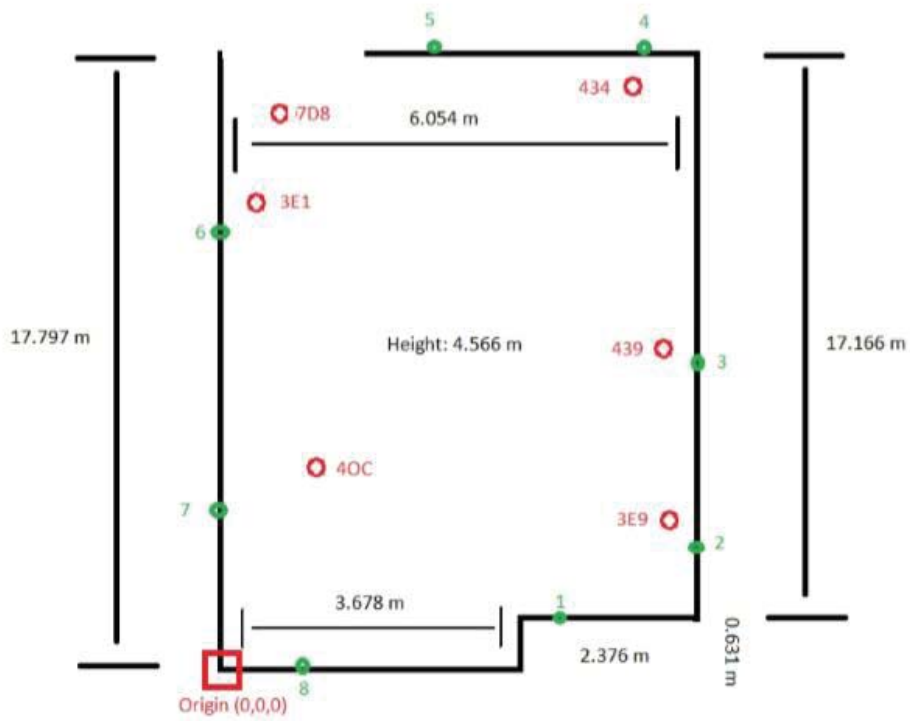

Figure 4-15 – Top down view of the second experiment test space. The red square shwows the origin used for all locations, the red circles denote the locations of each of the anchor positions, and the green circles denote the locations of each of the targets placed on the perimeter of the room.

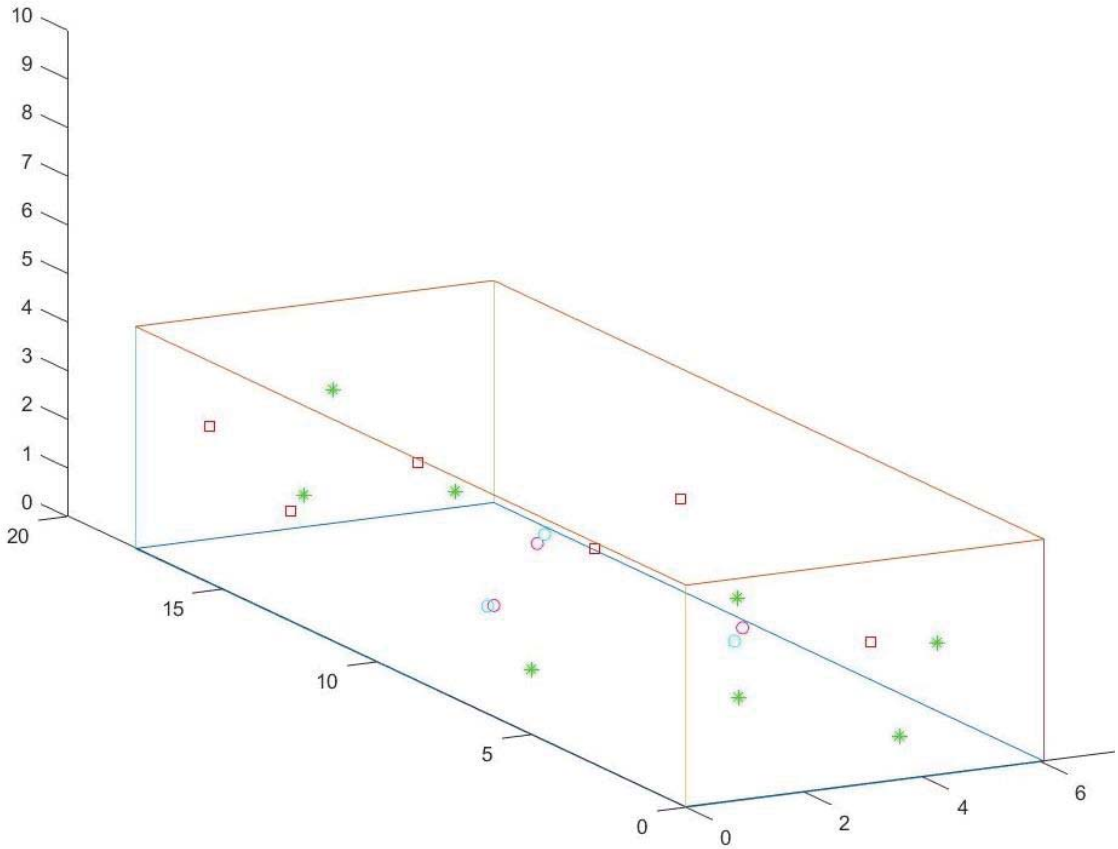

Figure 4-16 – Layout of the test space. Red squares represent anchor locations, green stars represent target locations, cyan circles represent the true tag location, and the magenta circles represent the calculated position

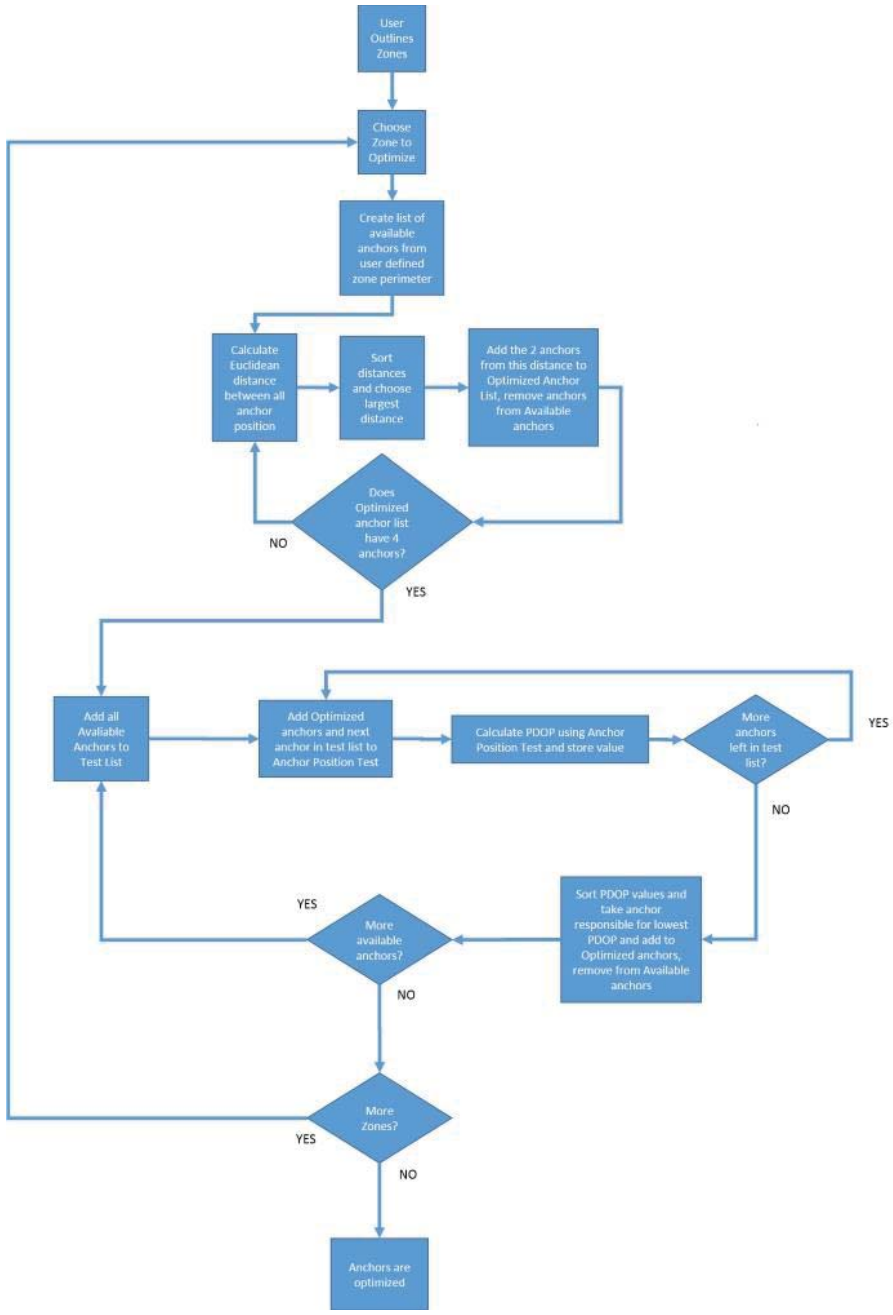

Figure 4-17 – Block Diagram of the PDOP optimization application

CHAPTER FIVE
RANGING EXPERIMENT

Purpose

The purpose of this experiment was to characterize the differences in the accumulator signal due to changing the distance, channel, and antenna. The experiment uses two way ranging and the accumulator mode of the system. The data is imported, graphed, and run through a leading edge detection algorithm to help understand the differences between the data collected. The experiment also serves as a test to see the differences between bandwidth of 500MHz versus that of 900MHz, and if there are measurable differences.

Experimental Results

Following are Figure 5-1 through Figure 5-9 as well as Table 5-1 through Table 5-6 which show the results from the ranging test. For each channel, info is divided by antenna and then compared by distance. Figure 5-1, Figure 5-2, and Figure 5-3 show a single pulse to illustrate a typical signal at each distance. All of these are taken at the lowest height and they all use the spherical antenna. After these graphs, Table 5-1 displays the DW1000 leading edge detection algorithm's results for the spherical monopole antenna, Decawave planar monopole antenna, and TechMah planar monopole antenna operating on channel 4 over a 100 sample accumulator size. Each antenna was evaluated at

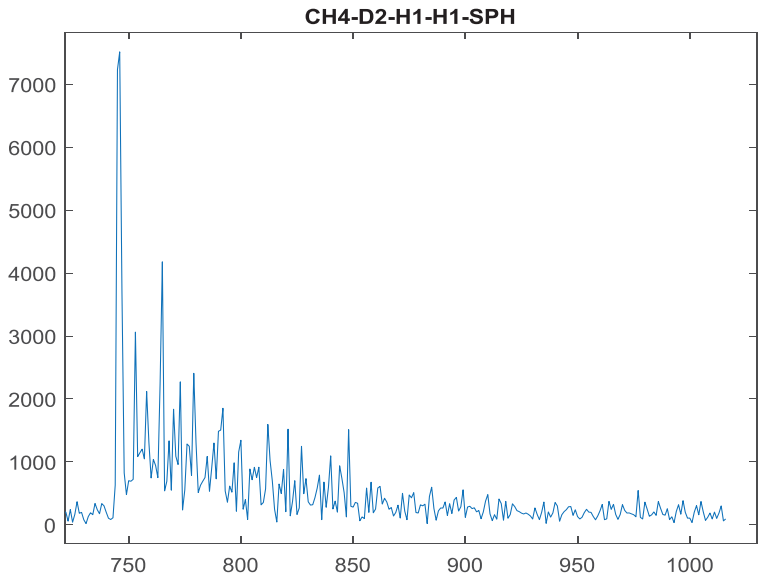

Figure 5-1 – Channel 4 pulse at 2 meters separation distance, height of 1.31 meters, and using the spherical monopole antenna

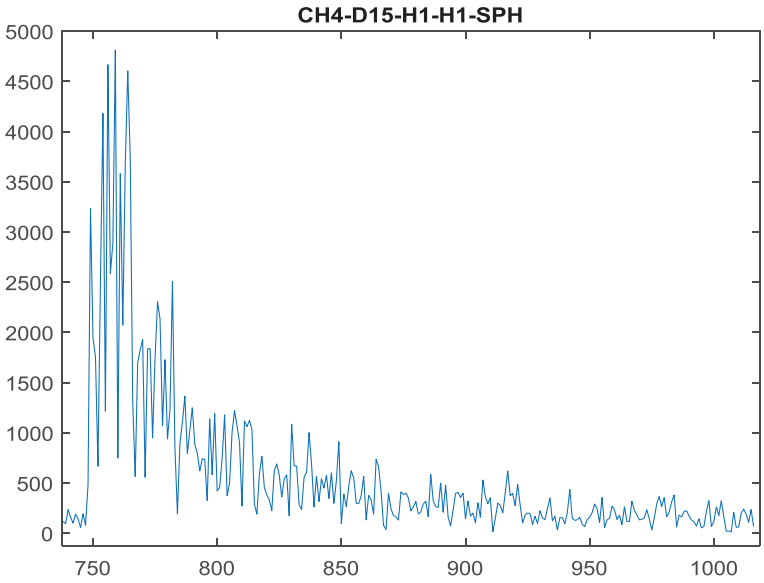

Figure 5-2 – Channel 4 pulse at 15 meters separation distance, height of 1.31 meters, and using the spherical monopole antenna

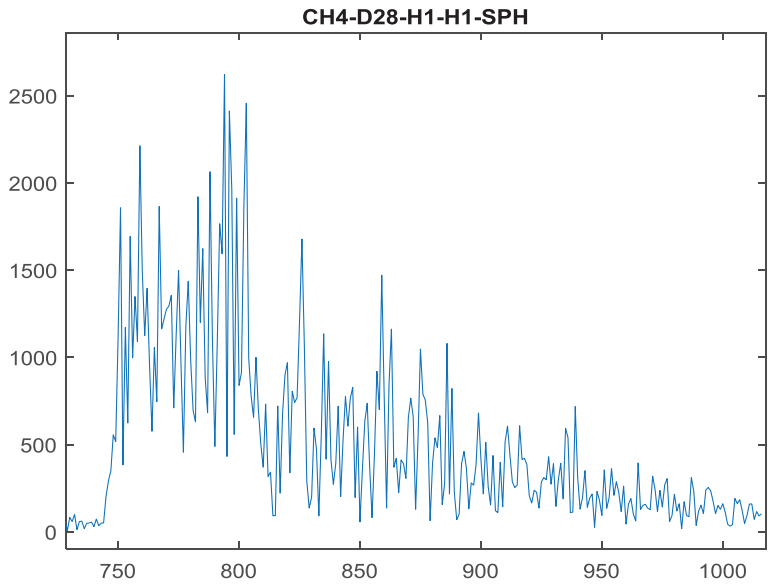

Figure 5-3 – Channel 4 pulse at 28 meters separation distance, height of 1.31 meters, and using the spherical monopole antenna

Table 5-1 – Channel 4

SPHERICAL	IND_MEAN	IND_STD	VAL_MEAN	VAL_STD	NOISE_MEAN	NOISE_STD	PEAK_MEAN	PEAK_STD	SNR_MEAN	SNR_STD
2.0 METERS	745.0606	2.4221	864.4584	883.5292	740.6659	97.8004	7.66E+03	425.2508	20.3576	1.2302
8.0 METERS	744.9733	2.9133	844.4941	852.7496	656.6777	100.4804	6.42E+03	409.269	19.8902	1.4434
15.0 METERS	745.434	2.97E+00	958.6168	614.1914	590.9396	8.47E+01	4.84E+03	209.531	18.3539	1.4863
28.2 METERS	743.4154	8.3033	776.0037	234.6196	428.663	63.5313	2.67E+03	152.1884	15.9816	1.4416
DECAWAVE	Ind_Mean	Ind_Std	Val_Mean	Val_Std	Noise_Mean	Noise_Std	Peak_Mean	Peak_Std	SNR_Mean	SNR_Std
2.0 METERS	744.9805	3.6213	948.0654	955.7414	720.9324	287.3991	7.58E+03	618.8377	20.6928	1.9672
8.0 METERS	745.4695	2.7205	935.6016	655.0301	597.8133	112.6852	5.21E+03	435.4119	18.9213	1.5386
15.0 METERS	747.3151	3.61E+00	1.66E+03	901.5529	480.8993	5.12E+01	5.88E+03	365.779	21.7763	1.0005
28.2 METERS	742.8378	8.6363	583.7057	122.3931	300.8796	44.0203	1.83E+03	90.8616	15.766	1.2756
TECHMAH	Ind_Mean	Ind_Std	Val_Mean	Val_Std	Noise_Mean	Noise_Std	Peak_Mean	Peak_Std	SNR_Mean	SNR_Std
8.0 METERS	745.45	2.3817	1.18E+03	1.00E+03	627.1053	104.467	6.81E+03	418.5195	20.8143	1.3518
15.0 METERS	745.4989	2.45E+00	1.46E+03	870.1993	421.8056	6.02E+01	6.28E+03	370.7024	23.5331	1.2936
28.2 METERS	742.1195	4.9405	587.2859	96.9028	253.9594	37.3741	1.54E+03	109.066	15.7485	1.3521

Table 5-2 – Channel 5

SPHERICAL	IND_MEAN	IND_STD	VAL_MEAN	VAL_STD	NOISE_MEAN	NOISE_STD	PEAK_MEAN	PEAK_STD	SNR_MEAN	SNR_STD
2.0 METERS	745.5228	4.2076	1.75E+03	905.3945	625.9787	57.8278	6.91E+03	211.967	20.8961	0.87
8.0 METERS	745.4109	2.2681	1.40E+03	564.1679	280.326	36.348	5.26E+03	187.6304	25.5277	1.1329
15.0 METERS	745.3132	2.66E+00	1.19E+03	506.8371	218.9073	3.33E+01	4.50E+03	133.696	26.3463	1.2927
28.2 METERS	720.3495	7.6314	317.0055	97.578	206.4414	39.9971	8.38E+02	191.6638	12.0362	1.817
DECAWAVE	Ind_Mean	Ind_Std	Val_Mean	Val_Std	Noise_Mean	Noise_Std	Peak_Mean	Peak_Std	SNR_Mean	SNR_Std
2.0 METERS	745.5658	2.4009	1.46E+03	920.3758	569.7851	48.8794	7.72E+03	354.8933	22.6652	0.794
8.0 METERS	745.7739	2.367	1.81E+03	669.5759	413.8826	46.6098	6.31E+03	203.3888	23.7146	0.9236
15.0 METERS	745.4561	2.43E+00	1.52E+03	672.2241	235.9918	4.31E+01	5.84E+03	164.9912	28.0101	1.4814
28.2 METERS										
TECHMAH	Ind_Mean	Ind_Std	Val_Mean	Val_Std	Noise_Mean	Noise_Std	Peak_Mean	Peak_Std	SNR_Mean	SNR_Std
8.0 METERS	745.2414	3.195	2.12E+03	270.2054	208.4961	33.8198	5.09E+03	176.8383	27.8581	1.325
15.0 METERS	745.1384	2.44E+00	1.06E+03	288.7037	209.5659	2.88E+01	3.12E+03	107.7735	23.5167	1.1673

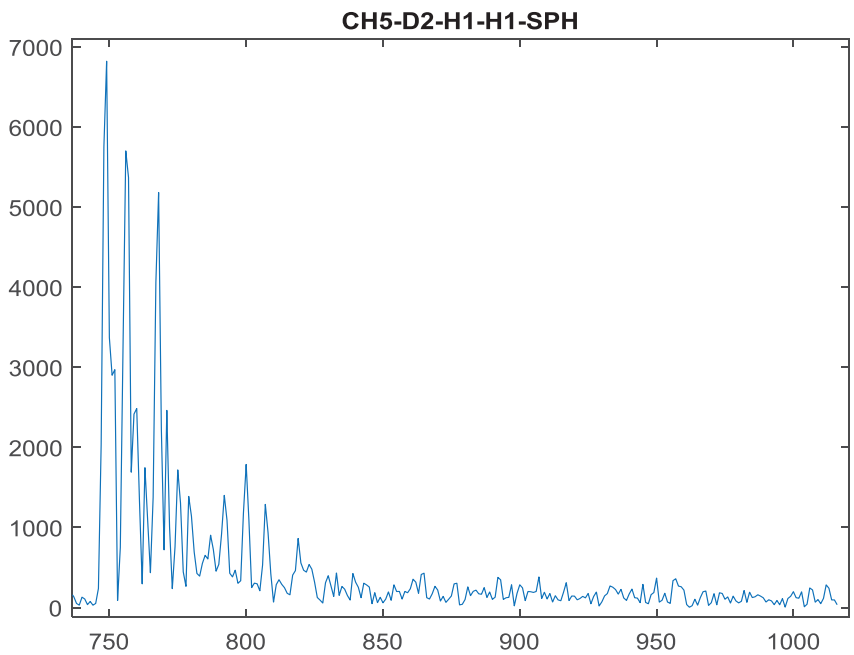

Figure 5-4 – Channel 5 pulse at 2 meters separation distance, height of 1.31 meters, and using the spherical monopole antenna

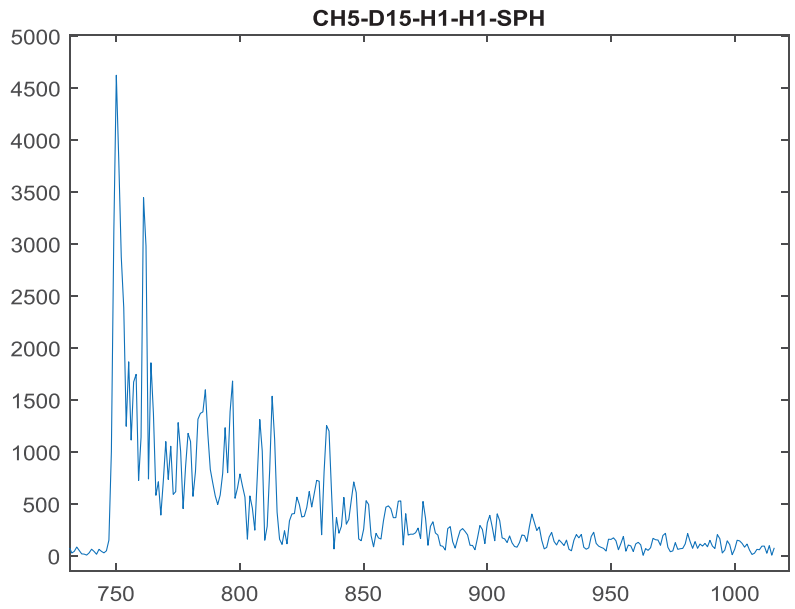

Figure 5-5 – Channel 5 pulse at 15 meters separation distance, height of 1.31 meters, and using the spherical monopole antenna

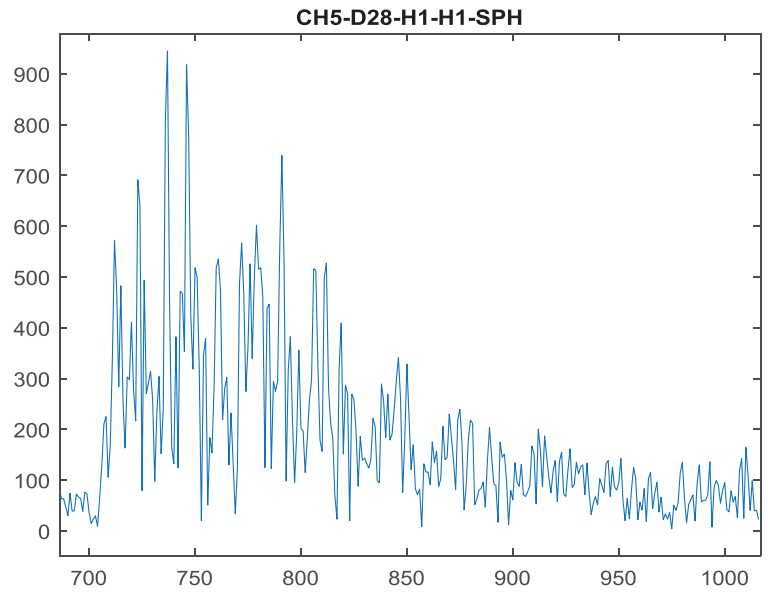

Figure 5-6 – Channel 5 pulse at 28 meters separation distance, height of 1.31 meters, and using the spherical monopole antenna

distances of 2, 8, 15, and 28 meters. Figure 5-1, Figure 5-2, and Figure 5-3 illustrate a typical accumulator received UWB signal at distances of 2, 8, and 28 meters for channel 4, respectively.

Table 5-2 displays the DW1000 leading edge detection algorithm's results for the spherical monopole antenna, Decawave planar monopole antenna, and TechMah planar monopole antenna over a 100 sample accumulator size. Each antenna has the values for the distances of 2, 8, 15, and 28 meters. Figure 5-4, Figure 5-5, and Figure 5-6 represent a typical accumulator pulse at distances of 2, 8, and 28 meters respectively using channel 5.

Table 5-3 displays the DW1000 leading edge detection algorithm's results for the spherical antenna, Decawave planar monopole antenna, and TechMah planar monopole antenna over 100 sample accumulator size. Each antenna has the values for the distances of 2, 8, 15, and 28 meters. Figure 5-7, Figure 5-8, and Figure 5-9 represent a typical accumulator pulse at distances of 2, 8, and 28 meters respectively, operating on channel 7.

Table 5-4 combines all of the values from each antenna into a single table for easier comparison. When comparing the signal to noise ratio (SNR) values of each of the antennas on channel 4, they are all relatively close to each other, around 20 dB. However, the spherical antenna has its SNR values decrease as distance increases, but both the Decawave and TechMah planar monopole antennas have their best SNR value at 15 meters. Looking at the standard deviation of their SNR values, the spherical and TechMah antenna have the most

consistent standard deviations, at around 1.4 and 1.3 dB respectively. The Decawave planar monopole antenna varies from a maximum of 1.9 dB at the closest 2 m, to its minimum value of 1.0 dB at 15 meters.

Figure 5-1, Figure 5-4, and Figure 5-7 show the cleanest example of a pulse for channels 4, 5 and 7 respectively. Some multipath effects can be seen, specifically the peaks that have a larger amplitude than the first arrival peaks. The Ultra Wide Band pulse is characterized by a beginning pulse at a high amplitude, which quickly decays exponentially. Because of this characteristic, if there is no reflection, a sample pulse will have an almost immediate peak, which quickly decays without any increase in amplitude after the initial peak. However, Figure 5-1 clearly shows two to three instances where the amplitude increases after the initial peak. This can be explained by the initial pulse being reflected off of a separate surface before arriving at the receiver which creates multiple paths in which the signal can be received, referred to as multipath. With an experiment using Line of Sight (LOS), this is not as important to factor into error correction because the pulse that travels directly from the emitter to the receiver is the closest distance and thus will arrive before any other multipath pulses. The direct pulse will not have lost energy during reflection and because of this will have the highest energy level of all of the pulses received.

When moving to an experiment with Non Line of Sight (NLOS), this becomes a much bigger problem because there will be multiple paths which can be received at the same time. Additionally, energy levels will vary on how many

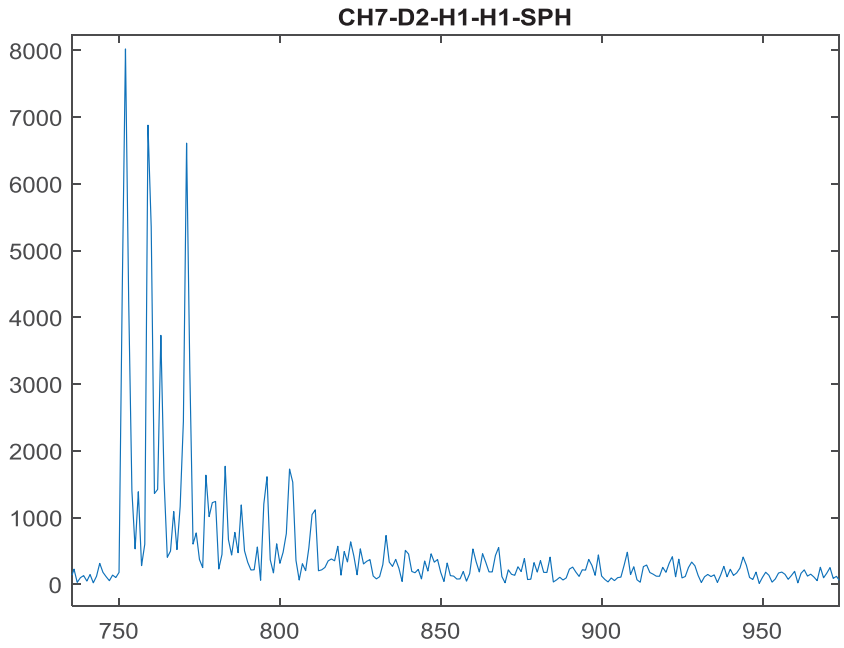

Figure 5-7 – Channel 7 pulse at 2 meters separation distance, height of 1.31 meters, and using the spherical monopole antenna

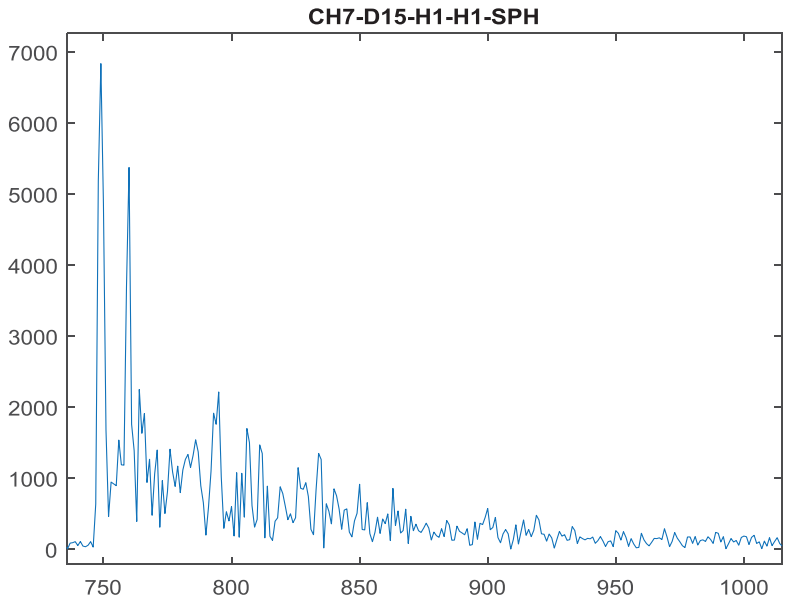

Figure 5-8 – Channel 7 pulse at 15 meters separation distance, height of 1.31 meters, and using the spherical monopole antenna

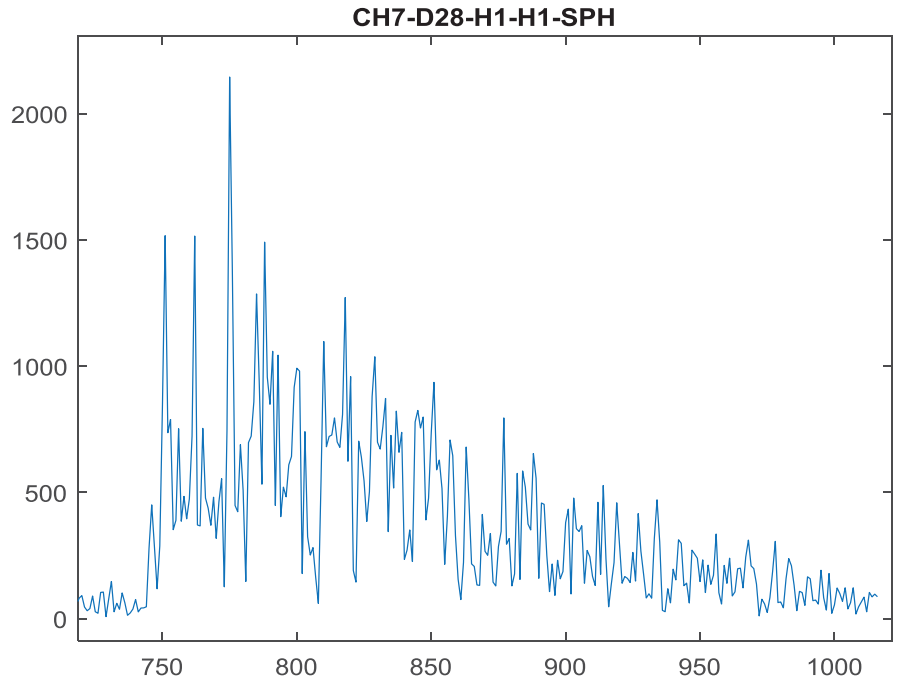

Figure 5-9 – Channel 7 pulse at 28 meters separation distance, height of 1.31 meters, and using the spherical monopole antenna

Table 5-3 – Channel 7

SPHERICAL	IND_MEAN	IND_STD	VAL_MEAN	VAL_STD	NOISE_MEAN	NOISE_STD	PEAK_MEAN	PEAK_STD	SNR_MEAN	SNR_STD
2.0 METERS	745.4016	2.7119	827.374	935.5007	678.7554	72.3399	7.30E+03	385.7301	20.6631	0.9469
8.0 METERS	746.0667	2.3063	1.54E+03	753.3432	434.3773	59.9212	6.93E+03	245.4504	24.1359	1.1829
15.0 METERS	745.3663	2.42E+00	1.31E+03	982.6357	327.7101	4.75E+01	6.61E+03	361.56	26.172	1.1844
28.2 METERS	742.9771	5.6411	631.0198	190.5918	260.5838	43.4654	1.91E+03	137.566	17.3919	1.5259
DECAWAVE	Ind_Mean	Ind_Std	Val_Mean	Val_Std	Noise_Mean	Noise_Std	Peak_Mean	Peak_Std	SNR_Mean	SNR_Std
2.0 METERS	745.1551	2.4	745.231	931.0668	712.274	146.1059	7.68E+03	271.2693	20.8372	1.8057
8.0 METERS	745.4018	2.3625	1.01E+03	911.7503	455.4167	60.9959	7.18E+03	342.6212	24.0212	1.2274
15.0 METERS	745.6622	2.24E+00	1.02E+03	809.4227	436.6772	6.10E+01	7.00E+03	326.0517	24.1816	1.1993
28.2 METERS	744.7826	3.5694	666.8791	141.7373	330.6322	59.0755	1.78E+03	170.6895	14.7183	1.6478
TECHMAH	Ind_Mean	Ind_Std	Val_Mean	Val_Std	Noise_Mean	Noise_Std	Peak_Mean	Peak_Std	SNR_Mean	SNR_Std
8.0 METERS	749.024	4.1144	2.67E+03	644.1529	310.5382	50.5378	6.30E+03	481.2416	26.2227	1.4181
15.0 METERS	745.2493	2.42E+00	1.28E+03	614.3393	212.3534	3.24E+01	5.22E+03	325.1733	27.8837	1.3916
28.2 METERS	726.4398	8.3586	359.9597	76.1806	213.1289	29.7541	8.89E+02	120.962	12.3963	1.4447

Table 5-4 – Comparison of all channels and all antennas

	IND_MEAN	IND_STD	VAL_MEAN	VAL_STD	NOISE_MEAN	NOISE_STD	PEAK_MEAN	PEAK_STD	SNR_MEAN	SNR_STD
SPHERICAL					**Channel 4**					
2.0 METERS	745.0606	2.4221	864.4584	883.5292	740.6659	97.8004	7.66E+03	425.2508	20.3576	1.2302
8.0 METERS	744.9733	2.9133	844.4941	852.7496	656.6777	100.4804	6.42E+03	409.269	19.8902	1.4434
15.0 METERS	745.434	2.97E+00	958.6168	614.1914	590.9396	8.47E+01	4.84E+03	209.531	18.3539	1.4863
28.2 METERS	743.4154	8.3033	776.0037	234.6196	428.663	63.5313	2.67E+03	152.1884	15.9816	1.4416
DECAWAVE										
2.0 METERS	744.9805	3.6213	948.0654	955.7414	720.9324	287.3991	7.58E+03	618.8377	20.6928	1.9672
8.0 METERS	745.4695	2.7205	935.6016	655.0301	597.8133	112.6852	5.21E+03	435.4119	18.9213	1.5386
15.0 METERS	747.3151	3.61E+00	1.66E+03	901.5529	480.8993	5.12E+01	5.88E+03	365.779	21.7763	1.0005
28.2 METERS	742.8378	8.6363	583.7057	122.3931	300.8796	44.0203	1.83E+03	90.8616	15.766	1.2756
TECHMAH										
8.0 METERS	745.45	2.3817	1.18E+03	1.00E+03	627.1053	104.467	6.81E+03	418.5195	20.8143	1.3518
15.0 METERS	745.4989	2.45E+00	1.46E+03	870.1993	421.8056	6.02E+01	6.28E+03	370.7024	23.5331	1.2936
28.2 METERS	742.1195	4.9405	587.2859	96.9028	253.9594	37.3741	1.54E+03	109.066	15.7485	1.3521
SPHERICAL					**Channel 5**					
2.0 METERS	745.5228	4.2076	1.75E+03	905.3945	625.9787	57.8278	6.91E+03	211.967	20.8961	0.87
8.0 METERS	745.4109	2.2681	1.40E+03	564.1679	280.326	36.348	5.26E+03	187.6304	25.5277	1.1329
15.0 METERS	745.3132	2.66E+00	1.19E+03	506.8371	218.9073	3.33E+01	4.50E+03	133.696	26.3463	1.2927
28.2 METERS	720.3495	7.6314	317.0055	97.578	206.4414	39.9971	8.38E+02	191.6638	12.0362	1.817
DECAWAVE										
2.0 METERS	745.5658	2.4009	1.46E+03	920.3758	569.7851	48.8794	7.72E+03	354.8933	22.6652	0.794
8.0 METERS	745.7739	2.367	1.81E+03	669.5759	413.8826	46.6098	6.31E+03	203.3888	23.7146	0.9236
15.0 METERS	745.4561	2.43E+00	1.52E+03	672.2241	235.9918	4.31E+01	5.84E+03	164.9912	28.0101	1.4814

Table 5-4 Continued

	IND_MEAN	IND_STD	VAL_MEAN	VAL_STD	NOISE_MEAN	NOISE_STD	PEAK_MEAN	PEAK_STD	SNR_MEAN	SNR_STD
TECHMAH										
8.0 METERS	745.2414	3.195	2.12E+03	270.2054	208.4961	33.8198	5.09E+03	176.8383	27.8581	1.325
15.0 METERS	745.1384	2.44E+00	1.06E+03	288.7037	209.5659	2.88E+01	3.12E+03	107.7735	23.5167	1.1673
SPHERICAL					**Channel 7**					
2.0 METERS	745.4016	2.7119	827.374	935.5007	678.7554	72.3399	7.30E+03	385.7301	20.6631	0.9469
8.0 METERS	746.0667	2.3063	1.54E+03	753.3432	434.3773	59.9212	6.93E+03	245.4504	24.1359	1.1829
15.0 METERS	745.3663	2.42E+00	1.31E+03	982.6357	327.7101	4.75E+01	6.61E+03	361.56	26.172	1.1844
28.2 METERS	742.9771	5.6411	631.0198	190.5918	260.5838	43.4654	1.91E+03	137.566	17.3919	1.5259
DECAWAVE										
2.0 METERS	745.1551	2.4	745.231	931.0668	712.274	146.1059	7.68E+03	271.2693	20.8372	1.8057
8.0 METERS	745.4018	2.3625	1.01E+03	911.7503	455.4167	60.9959	7.18E+03	342.6212	24.0212	1.2274
15.0 METERS	745.6622	2.24E+00	1.02E+03	809.4227	436.6772	6.10E+01	7.00E+03	326.0517	24.1816	1.1993
28.2 METERS	744.7826	3.5694	666.8791	141.7373	330.6322	59.0755	1.78E+03	170.6895	14.7183	1.6478
TECHMAH										
8.0 METERS	749.024	4.1144	2.67E+03	644.1529	310.5382	50.5378	6.30E+03	481.2416	26.2227	1.4181
15.0 METERS	745.2493	2.42E+00	1.28E+03	614.3393	212.3534	3.24E+01	5.22E+03	325.1733	27.8837	1.3916
28.2 METERS	726.4398	8.3586	359.9597	76.1806	213.1289	29.7541	8.89E+02	120.962	12.3963	1.4447

times the pulse has been reflected before it reaches the receiver. This is especially evident in Figure 5-3 which represents a NLOS experiment at a separation distance of about 28 meters. Instead of the strong initial spike of the pulse followed by exponential decay as is expected from LOS experiments, Figure 5-3 shows a multitude of spikes of very similar energy being received across a period of time, creating somewhat of a table or plateau of received pulses. These are followed by another plateau of values all sharing similar energy levels, lower than that of the initial pulses.

Similar effects can be seen for channels 5 and 7. Figure 5-4 shows the strongest pulse of channel 5, but clearly shows that multipath is also a major factor at spacing as close as 2 meters. Figure 5-7 also shows this is the case with channel 7 as well. Instead of one large peak with exponential decay following the peak, each of these channels has two more peaks that are very similar in amplitude to the initial pulse. However, at a separation distance of 8 meters, the initial multipath effects seem to become less prevalent. There are not as many multipath spikes as before and do not last for as long in the tail of the signal.

The effects of separation distance between the emitter and the receiver, as expected the energy level which correlates to the amplitude of the initial peak decreases as the distance increases. Comparing the peak amplitude at a separation distance of 15 meters to two meters, a percentage of retained power can be calculated for the increase of approximately 7.5 times. channel 4 had the largest decrease in received power, maintaining only about 60% of its initial

power at 2 meters separation distance. channel 5 has a slight increase, maintaining 67% of its original power from a two meter separation distance. channel 7 preforms the best at maintaining its power over distance, maintaining 87% of its original power at two meters separation distance compared to that of 15 meters. However, when the separation distance is increased all the way to 28 meters, channel 5 has the lowest power retention, only being able to deliver 14% of its original power at a separation distance of 2 meters. Channel 4 and 7 preform similarly with power deliveries of 33% and 28% respectfully. This drastic decrease in power delivered using channel 5 became apparent when multiple tests could not be completed using the channel because of the lack of power being delivered. Channels 4 and 7 were not as susceptible to this, showing that if a very large separation distance must be used, channel 5 should be avoided. Table 5-4 is a compilation of Table 5-1, Table 5-2, and Table 5-3, making it easy for comparison between all of the antenna, distance and channel variations. The first factor that is extremely important for the use of the UWB pulse is the signal to noise ratio (SNR). The algorithm outputs this value for each pulse, and these values are averaged over all of the samples taken. The highest SNR value achieved is slightly over 28, using channel 5 and the Decawave antenna with a separation distance of 15 meters. Table 5-5 and Table 5-6 show the averaged SNR values, separated by channel and antenna. Table 5-5 averages the values

Table 5-5 – SNR values averaged from separation distances from 2-15 meters

	Channel 4	Channel 5	Channel 7
Spherical	19.5	24.3	23.7
Decawave	20.5	24.8	23.0
TechMah	22.2	25.7	27.1

Table 5-6 – SNR values averaged from separation distances from 2-28 meters (* channel 5 only had values for 28 meters using the spherical antenna)

	Channel 4	Channel 5	Channel 7
Spherical	18.6	21.2	22.1
Decawave	19.3	24.8*	20.9
TechMah	20.0	25.7*	22.2

from the separation distances from 2-15 meters, whereas Table 5-6 averages the values from 2-28 meters. One important thing to note about these tables is that channel 5 was unable to function using the Decawave or TechMah antenna at a spacing of 28 meters, so its values are the same in Table 5-5 and Table 5-6, making comparisons to other channels in Table 5-6 irrelevant.

As Table 5-5 shows, channel 5 has the highest SNR values, regardless of which antenna is used. The only exception to this is channel 7 with the use of the TechMah antenna. Each channel is pretty consistent with the SNR values, showing that it is not very antenna dependent. The only outlier in this is the use of the TechMah antenna and channel 7, which clearly improves the SNR quite substantially. This is averaged over all of the data taken from numerous separation distances, it is not unreasonable to say that the highest SNR values can be achieved by using channel 7 paired with the TechMah antenna. It can be seen that the TechMah antenna produces the highest SNR values compared to the other antennas, regardless of which channel is being used.

CHAPTER SIX
TRACKING EXPERIMENT

Purpose

This experiment's purpose is to help understand the effects that different channels, antennas, and locations have on an Ultra Wide Band (UWB) positioning system. To conduct this experiment, six anchors were placed around our testing space and their positions measured by rangefinder. All three dimensions were varied to help get as much variation as possible, however, because of the physical dimensions of the testing space as well as the tripods on which the anchors were mounted, the Y dimension was able to be varied the most, followed by the X and finally the Z having the least amount of variation. After the main testing was completed, a way to mount two anchors at a lower Z location was made, and an additional test was made. These second set of results are compared to the normal results to help show how the variation in each dimension assists with the accuracy in that dimension. Figure 6-1 and Figure 6-2 show pictures of the testing space form two separate angles. The anchors, targets, and tag locations are circled in red, green, and cyan respectively. Figure 6-3 and Figure 6-4 display top down views of the testing area. Figure 6-3 illustrates a drawn diagram including some dimensions as well as anchor identifiers. Figure 6-4 has the locations mapped to the building blueprints. Figure 4-6 and Figure 4-7 show the different antennas used in this experiment,

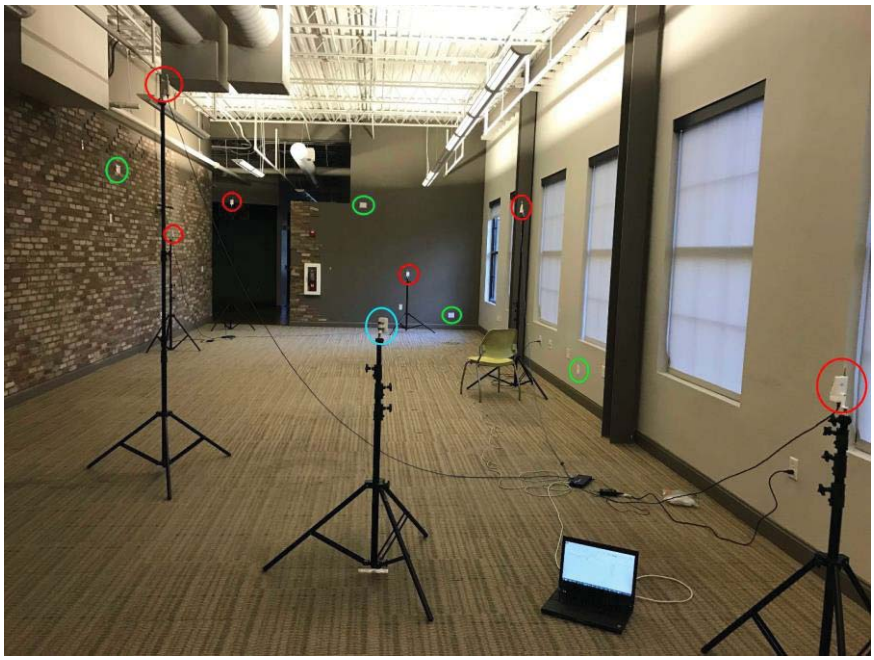

Figure 6-1 – View of the testing space. Decawave anchors at circled in red, the tag is circled in blue, and the targets are circled in green

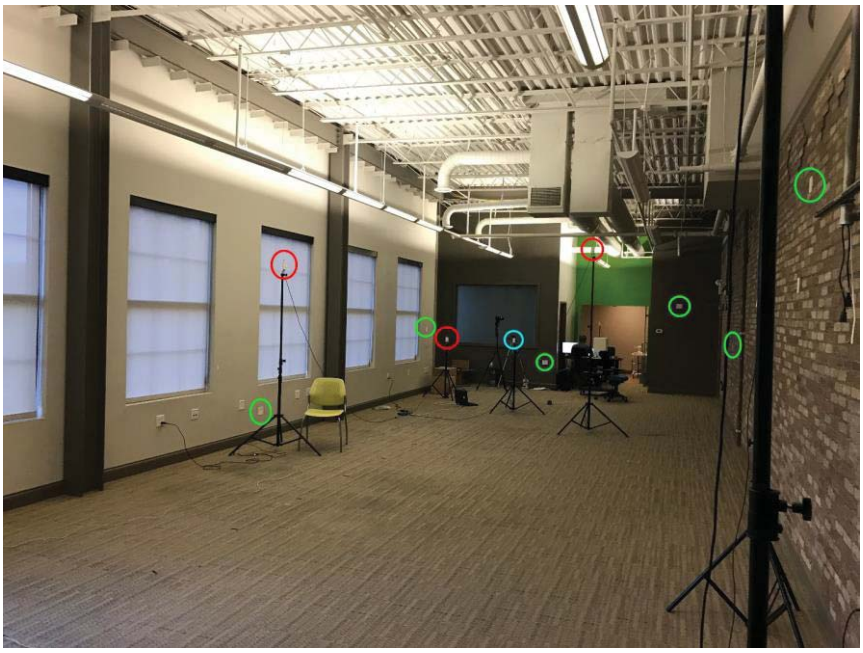

Figure 6-2 – View of testing space from opposite side. Anchors in red circles, tag in blue circle, and targets in green circles.

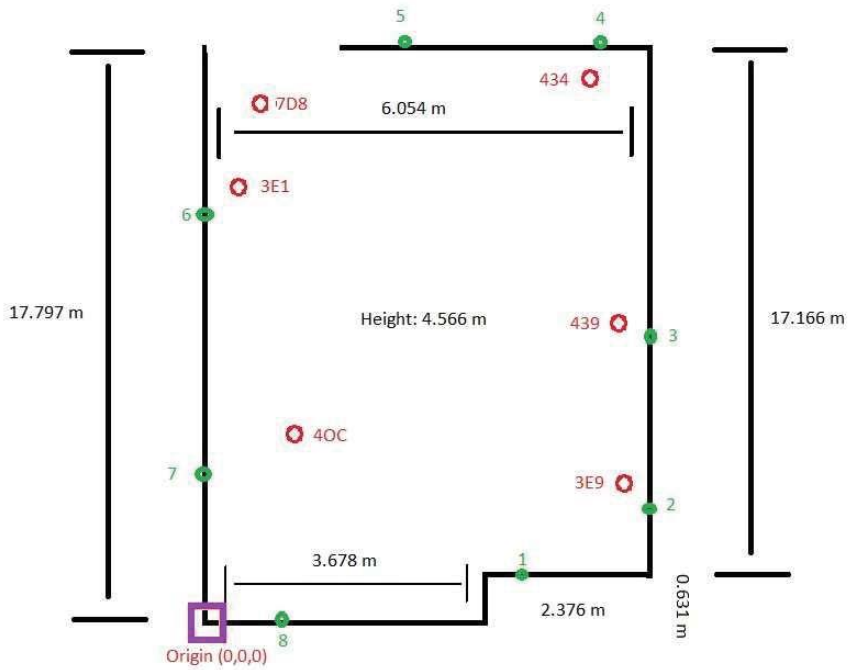

Figure 6-3 – Top down view of the testing space with anchors represented by red circles, targets as green circles, and the origin as the purple square.

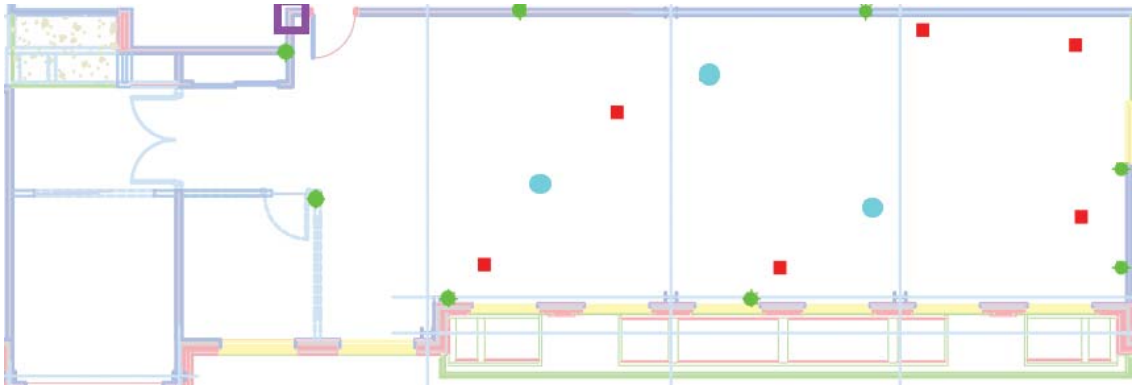

Figure 6-4 – Top down view of testing space overlaid on structural drawings. Red dots are anchors, green dots are targets, blue dots are tag locations, and the purple square is the origin.

mainly the TechMah and Decawave antenna. They are displayed next to a ruler so that their dimensions can be seen and compared to each other.

The tracking experiment consisted of moving a tag to 4 separate locations, running the system, and determining the location. For a ground truth, a range finder was used to find the true ranges to all of the anchors, as well as the true ranges to all of the targets set up around the room, which are shown in Table 6-1. These ranges were then input into the same spherical intersection algorithm that is used in the Decawave software to calculate a true position. However, because the tags were all mounted on the same tripod that had a constant height, the height measurement was taken by rangefinder. To create the ground truth location for each of the 4 locations, the Z coordinate is calculated by range finder, with the X and Y is calculated by using the spherical intersection algorithm. The algorithm is fed by 6 ranges found by rangefinder to the 6 anchors, and an additional 8 ranges to each of the 8 targets spread around the perimeter of the testing space. Each of the anchor positions and target locations are found using the rangefinder, measuring to walls, ceiling, and floor, calculating them using the known room's dimensions. These locations are also fed into the spherical intersection algorithm.

Once an established ground truth has been made, the location calculated by the system is compared to it. The raw data of range differences from the system are extracted so that they can be used in post processing to help identify sources of error and ways to mitigate them to increase accuracy. Once the error has been

Table 6-1 – Ranges from each position to every target and anchor

	Position 1	Position 2	Position 3	Position 4
Target 1	4.798	8.771	11.864	15.553
Target 2	3.094	7.28	9.25	13.18
Target 3	5.167	4.88	3.3	7.5
Target 4	12.577	9.733	5.528	4.125
Target 5	12.5	9.147	5.578	2.801
Target 6	7.977	3.919	4.4	4.339
Target 7	3.668	4.207	8.54	11.19
Target 8	6.094	9.029	12.915	16.061
Anchor 1 (3E9)	2.062	6.205	8.321	12.319
Anchor 2 (439)	5.482	4.448	2.566	6.697
Anchor 3 (434)	11.576	8.485	4.459	2.715
Anchor 4 (7D8)	11.87	7.974	5.667	1.903
Anchor 5 (3E1)	11.87	4.712	3.931	2.862
Anchor 6 (40C)	2.781	2.601	5.967	9.123

accounted for, the increases in accuracy are plotted and explained to show the progression of accuracy for the system using different techniques.

Error Sources

The main sources of error come from antenna delay, phase center variation, clock jitter, clock drift, and geometric dilution of precision. Each of these result in separate amounts of error within the accuracy of the location calculation, shown in Table 6-2 and can be calculated by taking the difference between the ground truth and the calculated position. A single error value per position and antenna can be calculated by taking the root mean square (RMS) of each of the 3 dimensions, creating one value to describe that particular configurations accuracy.

Jitter is the most common source of error, but can be easily mitigated by taking a moving average of all of the values to smooth out all of the data. The window size of this moving average can be varied, the larger it is, the smoother the result will be. However, this will also result in an increase of response time for the system. A small window size will maintain a quick responsive, but will be more vulnerable to large amounts of jitter.

The second source of error that can be found is clock drift. Due to the nature of the DecaWave system, it uses the time of arrival (TOA) of the signals to calculate the position. The need to have synchronized clocks between all of the anchors is extremely important to the functionality of the system, however, quality of these

Table 6-2 – Error Sources for the tracking experiment and the amount of error that each contributes

Error Source	Approximate Amount of Error Measured (mm)
Antenna Delay	590
Phase Center Variation	58
Clock Jitter	13
Clock Drift	11

clocks can be sacrificed for cheaper options to keep unit costs low. Lower quality clocks can exhibit drift in accuracy, which is characterized as clock drift as illustrated in Figure 6-11. Looking at the calculated position of a stationary tag, the coordinates will slowly drift with time. The only true way to mitigate this error is the use of a higher quality clock that is more stable and less prone to drift. However, with the use of averaging, the effects can be minimized. To successfully accomplish this, the averaging window size needs to be quite substantial. The large window size will take a large amount of drift over time and average it together to find the position at which it is drifting around. This will drastically reduce the responsiveness of the system for dynamic measurements, but for static measurements it is less of an issue.

For this experiment, the jitter was accounted for by taking an average of the range data before it is fed into the spherical intersection algorithm. By taking this average on the raw data, it helps minimize the error down the line, where as if this average was taken after the calculation had been made, the effect would be less significant.

Experimental Results

Figure 6-5 shows the Root Mean Squares (RMS) of the error for all dimension for the raw data without error correction. As can be seen, it is in the range of upwards of 80 cm for three dimensional position calculations, and upwards of 20 cm for two dimensional position calculation. The first major contributor to the sizeable amount of error in regards to accuracy is the antenna delay. This is

characterized by the amount of resistance within the electronics and the subsequent time delay created from the time at which the signal is actually received at the antenna to the time it is registered at the chip. The Decawave software has a variable which can be changed to help mitigate this error, however it is not very effective. To mitigate this source of error, we compared the raw range data received from each anchor to the range data that was measured with the rangefinder. In a perfectly accurate system, these values should be the same. However, by taking the difference of these values for every range at every position and averaging them, an offset could be calculated. This offset was then subtracted from each of the raw ranges and then used for position calculations. Figure 6-6 shows the subsequent errors after this offset was applied. As Figure 6-6 shows, the error decreased dramatically for both 3D and 2D position calculations. The RMS error has decreased to below 25 cm for all antennas and all channels. The lowest error is around 8 cm using this offset. The next source of error that can be identified and accounted for is that of phase center variation for the antennas. The orientation of each of the anchor's antennas to each other anchor antenna varies for each tag position because the antennas being used are planar and are in a three dimensional space. Each connection to an anchor varies from one anchor to another. This difference will produce variations in each range measured. It will change from position to position as well as anchor to anchor. The easiest way to mitigate this error is similar to the first offset taken. The calculated ranges are again compared to the

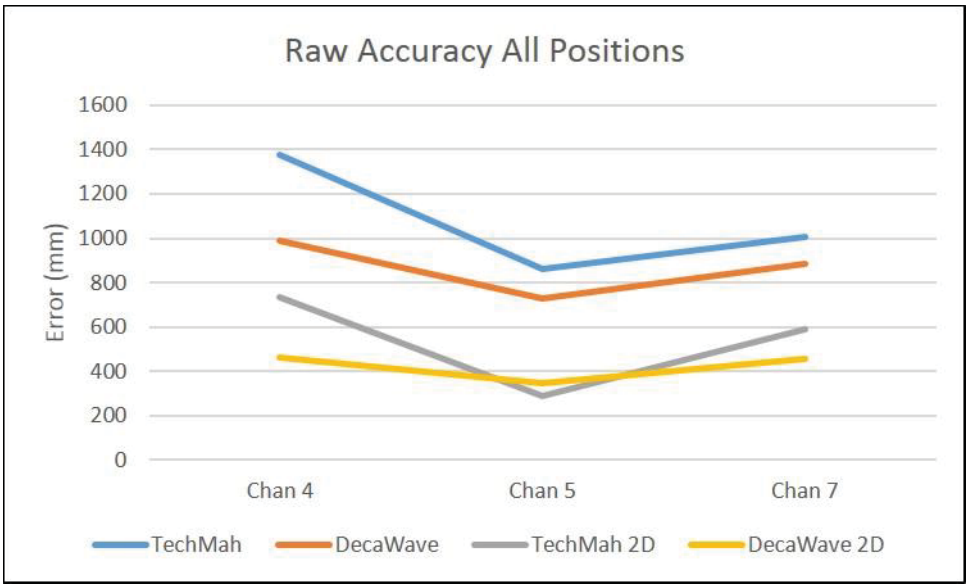

Figure 6-5 – Error in millimeters versus channel. Has values for use of TechMah and Decawave antenna using the 2D and 3D algorithm, as well as comparing the use of a Decawave antenna with 2 anchors much lower in the Z dimension.

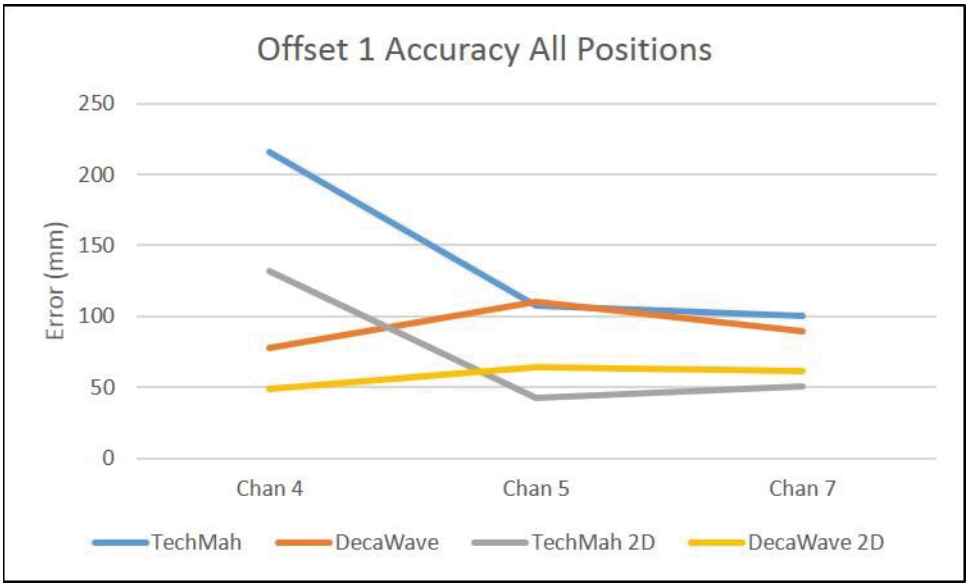

Figure 6-6 – Error in mm versus channel with the use of an offset calculated from an average difference of all ranges compared to the ground true ranges, being applied to every range.

true ranges, but unlike the previous method of an average being taken across all the ranges to each anchor, instead each anchor connection has its range compared to the true range, and the difference subtracted out of each anchor connection measured range separately before position calculation. By doing this, it ensures that each range is as close to correct to the true range as is possible with the system, disregarding the other sources of error such as drift and jitter. Once each of these unique offsets is calculated, they are subtracted from the measured ranges before the position calculation is made. Referred to as offset 2, Figure 6-7 shows the subsequent error of the system with these offsets applied.

Table 6-3, Table 6-4, and Table 6-5 show the changes in accuracy of all of these variations and the differences between the raw position calculation, the use of offset 1, and the use of offset 2 to mitigate the antenna delay and phase center variation respectively. Table 6-3 and Table 6-4 show the error averaged over all of the positions, respective to 3D and 2D calculations. Table 6-5 takes the data from Table 6-3 and Table 6-4 and compares them side to side, showing the differences between 2D and 3D accuracy error in position calculation. As is expected, the 2D position calculation is almost always more accurate than that of the 3D. However it can also be seen that the data from the low anchor setup is also measurably better than the other 3D position calculations. The one instance where this is not the case is using the first offset to mitigate the antenna delay on channel 4. The DecaWave antenna seems to perform better under these

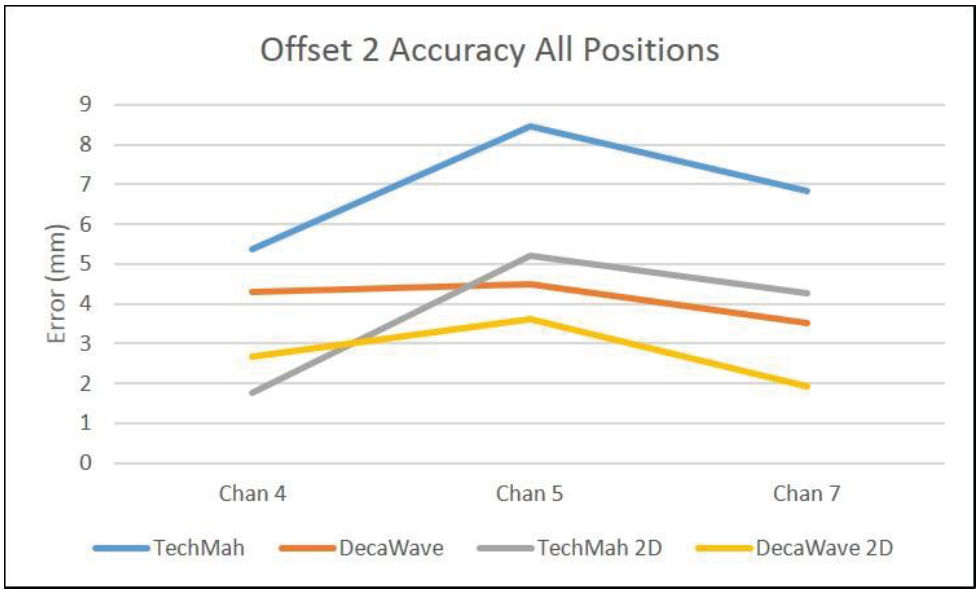

Figure 6-7 – Accuracy error compared to channel for each antenna

Table 6-3 – Errors of each channel and antenna configuration. Error is averaged over all positions and is in millimeters

	Raw Error All Positions	Error using Offset 1	Error using Offset 2
CH4T	1376.566667	215.6329	5.357866667
CH5T	861.6333333	107.5644	8.464566667
CH7T	1008.666667	100.3294333	6.834966667
CH4D	988.3333333	77.5257	4.301733333
CH5D	727.0666667	110.2173333	4.483866667
CH7D	885.9333333	89.6785	3.4983
CH4D_LOW	830.9	144.79935	6.98295
CH5D_LOW	383.15	98.66145	5.42715
CH7D_LOW	833.15	73.62	2.47755

Table 6-4 – Error of all channel and antenna configurations in 2D. Error is averaged over all positions

	Raw Error All Positions 2D	2D Error using Offset 1	2D Error using Offset 2
CH4T	731.4	132.0557667	1.7721
CH5T	289.3333333	42.07306667	5.207166667
CH7T	591.3	50.255	4.263666667
CH4D	461.5	48.70696667	2.677533333
CH5D	344.9333333	63.91046667	3.619333333
CH7D	454	61.3087	1.913166667
CH4D_LOW	528.75	77.927	2.6991
CH5D_LOW	196.45	81.14135	4.00815
CH7D_LOW	489.4	57.3915	2.03545

Table 6-5 – Averaged errors over all positions. 3D errors are presented next to the 2D data for easier comparison

	Raw Error All Positions	Raw Error All Positions 2D	Error using Offset 1	2D Error using Offset 1	Error using Offset 2	2D Error using Offset 2
CH4T	1376.566667	731.4	215.6329	132.0557667	5.357866667	1.7721
CH5T	861.6333333	289.3333333	107.5644	42.07306667	8.464566667	5.207166667
CH7T	1008.666667	591.3	100.3294333	50.255	6.834966667	4.263666667
CH4D	988.3333333	461.5	77.5257	48.70696667	4.301733333	2.677533333
CH5D	727.0666667	344.9333333	110.2173333	63.91046667	4.483866667	3.619333333
CH7D	885.9333333	454	89.6785	61.3087	3.4983	1.913166667
CH4D_LOW	830.9	528.75	144.79935	77.927	6.98295	2.6991
CH5D_LOW	383.15	196.45	98.66145	81.14135	5.42715	4.00815
CH7D_LOW	833.15	489.4	73.62	57.3915	2.47755	2.03545

circumstances. However, because the rest of the cases show that the lower anchor positions seem to assist accuracy, there is strong evidence that the more physical variation there is in each dimension, the better the results will be achieved. This is shown in Figure 6-7 where the low anchor data seems closer in accuracy to that of the 2D position calculations than the other 3D position calculations.

As Figure 6-7 shows, the error is greatly reduced with the application of this second offset. The highest error for the system has decreased to less than 2 mm, with the lowest error being close to 1.7 mm. This is the instance where most of the error has been mitigated. The jitter and clock drift have been decreased using averaging of the data. However, because the sampling window size was not big enough to completely remove the clock drift, the ability to achieve sub millimeter accuracy is still out of reach. The antenna delay as well as the phase center variation have been eliminated by calculating the differences in range data from the expected to the received. By mitigating all of these error sources, it shows that the system is capable of an accuracy up to 1-2 mm for static tag tracking.

Figure 6-8 shows the average error for each antenna and channel combination with each of the different offsets applied. When looking at the raw data as well as some of the data using the first offset, channel 5 tends to be better or just as good as other channels. Once the phase center variation has been accounted for, channel 5 can be seen to have the lowest SNR values. In every instance, be

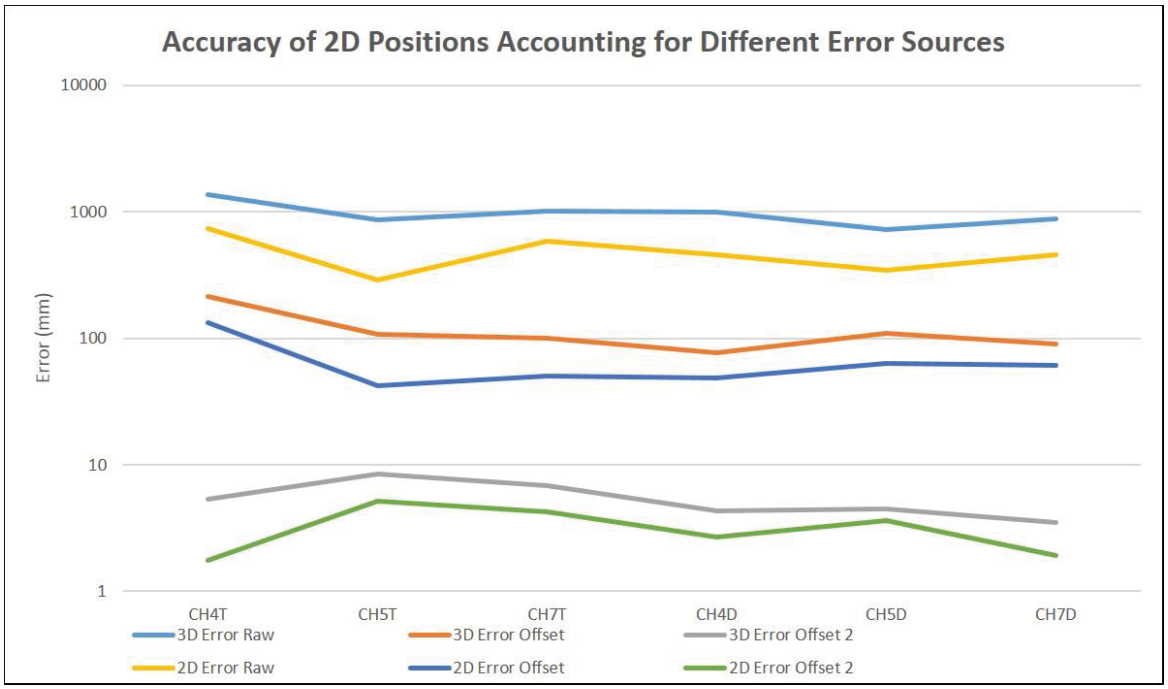

Figure 6-8 – Each channel and antenna configuration compared to each other, with different lines representing which offset is applied as well as whether 2D or 3D positions were calculated.

it different antennas or the use of the lower anchor positions, channel 5 has a lower accuracy than both channel 4 and channel 7.

Figure 6-9 and Figure 6-10 show the progression of accuracy as each source of error is addressed. The error is shown on a logarithmic scale, which represents the decrease of error for the 2D and 3D position calculations. Figure 6-11, Figure 6-12, and Figure 6-13 show the accuracy over time for positions 1, 2, and 3 respectively. The graphs show that there is still some clock drift present, but overall the data is pretty stable. As the data suggests, it is clear that the accuracy in the Y dimension is significantly more stable than the other dimensions, with Z showing the least stability. This can be explained with the variation of the anchors in each of the dimensions. The more physical variation in anchor placement, the better accuracy will be achieved in that dimension. Position 1 has more error than positions 2 and 3. This can be explained by the geometric dilution of precision. Given on the placement of the anchors, a factor can be calculated to determine a factor of this dilution of precision, referred to as PDOP. To calculate this factor, only the locations of the anchors being used and the position at which the tag is located are needed. A simulation was created to map out the whole test space to show how this dilution of precision varies over the whole test space. This is shown in Figure 3-3, with the simulation on the left showing the whole testing room mapped using the PDOP analysis, and the graph on the right showing the PDOP analysis of the area inside of the anchors perimeter. As the color bar on the right indicates, the values for the whole space

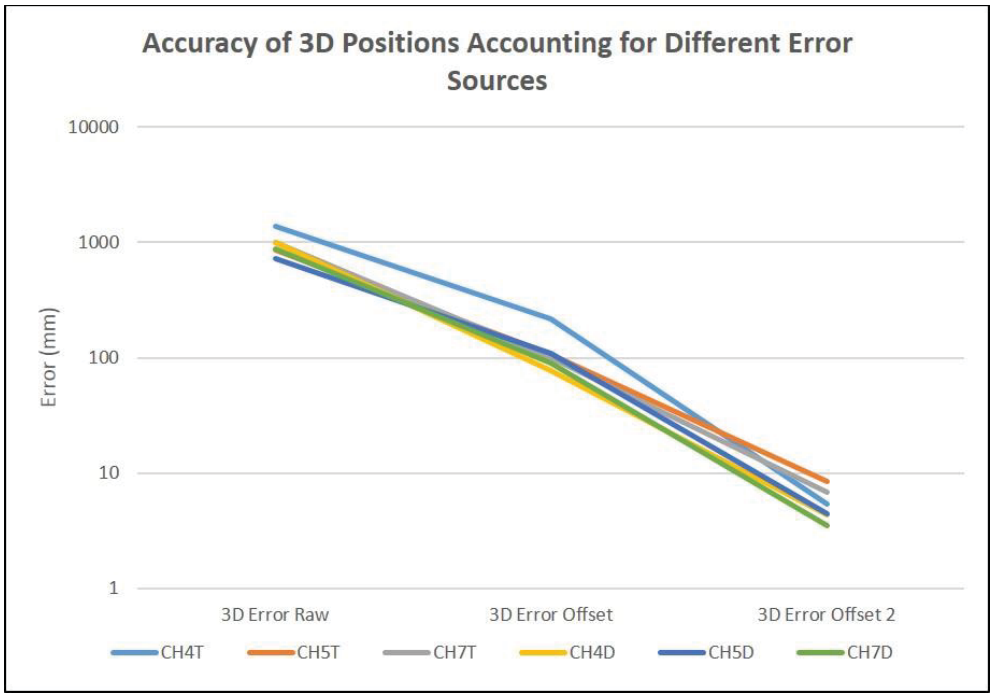

Figure 6-9 – Accuracy of the calculated 3D position as different error sources are mitigated

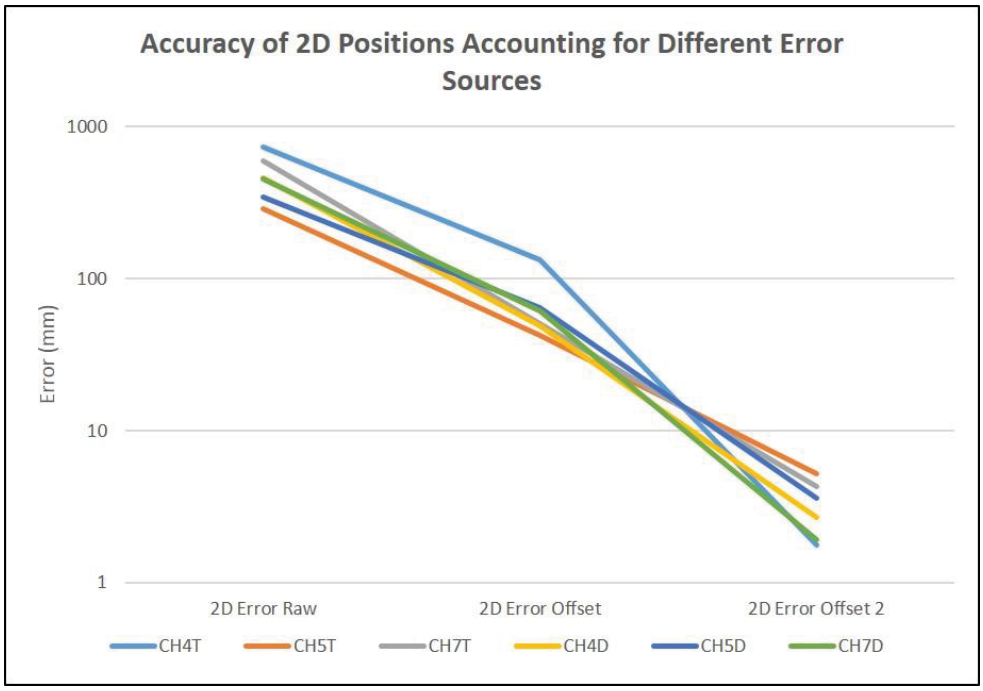

.

Figure 6-10 – Accuracy of the calculated 2D position as different error sources are mitigated

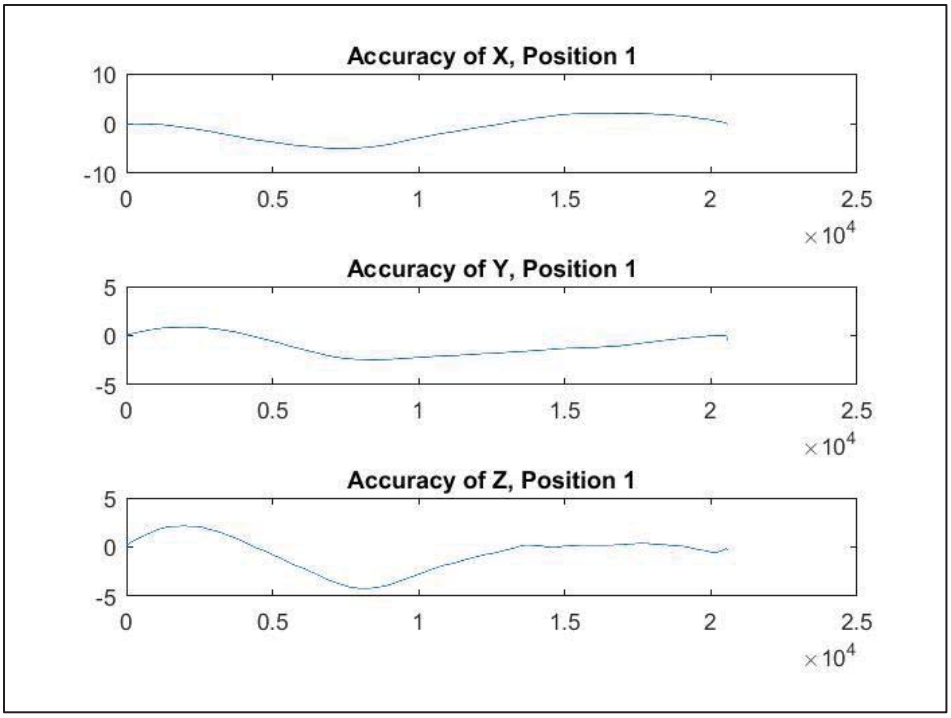

Figure 6-11 – Accuracy in millimeters of location 1 using Offset 2

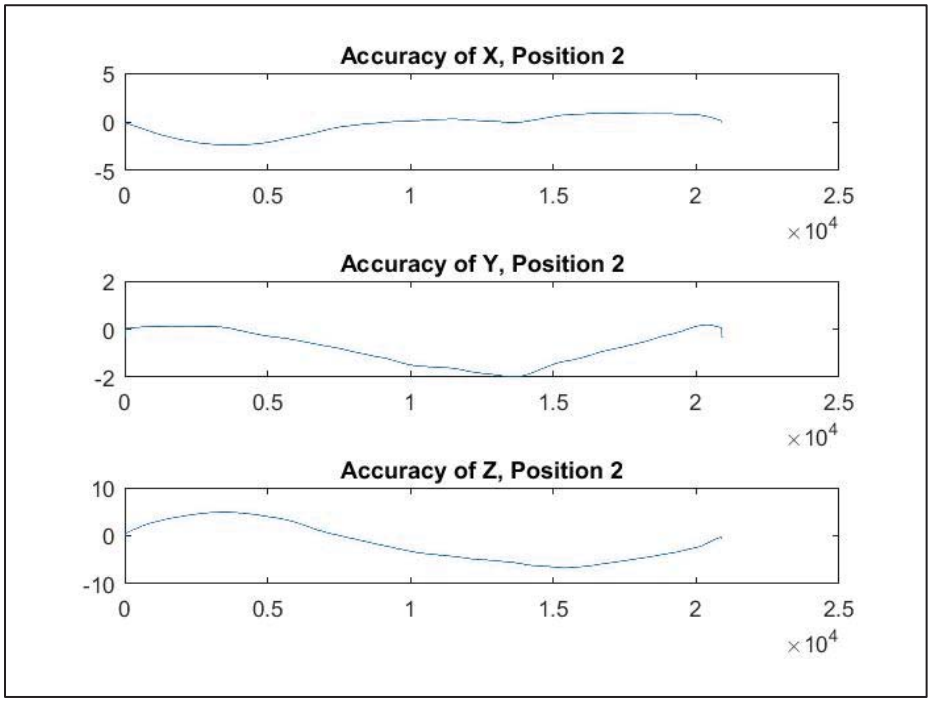

Figure 6-12 – Accuracy in millimeters of location 2 using Offset 2

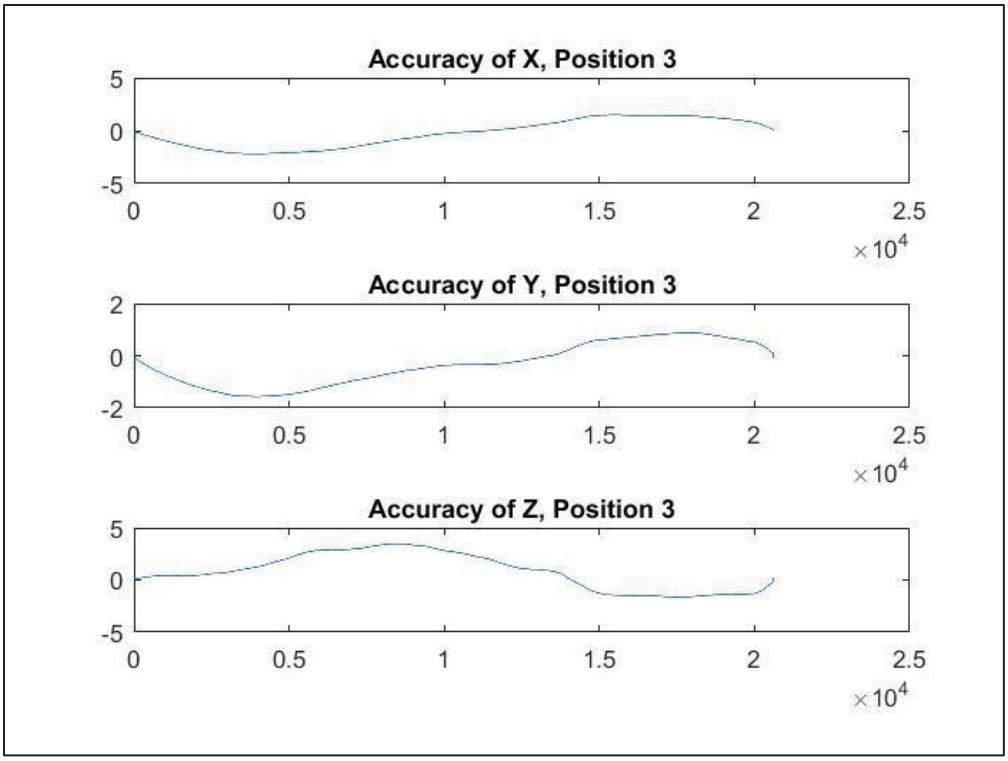

Figure 6-13– Accuracy in millimeters of location 3 using Offset 2

vary to a maximum value of 35, whereas the testing space varies to a maximum around 4. As this analysis shows, positions 1 and 2 have a higher DPOP value than that of positions 3 and 4. If all other factors kept constant, the accuracy for positions 3 and 4 should always be higher than those of 1 and 2. This can obviously be changed by the locations of the anchors. This type of analysis should be conducted prior to final anchor placement so that the area which requires the highest accuracy can be optimized using the PDOP values in that area.

To help ease the comparison of accuracy across all of the positions, the data has been collected into Table 6-6 for 3D accuracy, and Table 6-7 for 2D accuracy. It is separated by position as well as the different methods of mitigating the large sources of error.

Table 6-6 – Separated accuracy error by position in 3D. Each column is separated by channel and antenna and everything is in millimeters

	CH4T	**CH5T**	**CH7T**	**CH4D**	**CH5D**	**CH7D**	**CH4D_LOW**	**CH5D_LOW**	**CH7D_LOW**
raw_means	RMS	RMS	RMS	RMS	RMS	RMS	RMS	RMS	RMS
Position 1	845.2	604.3	695.2667	548.5667	532.9333	557.5667			
Position 2	524.1	273.6	548.6667	526.1667	343.5333	499.3667	530.5333	255.6667	482.5667
Position 3	774.9	438.1	419	555.2667	258.0667	404.6	373.8	120.2333	414.8667
offset_acc_means									
Position 1	142.5021	40.5813	32.67077	42.47683	45.02347	56.6656			
Position 2	66.523	86.93083	47.37363	41.54593	55.05747	31.84557	52.6516	45.42197	34.00927
Position 3	100.7377	21.80317	55.51223	31.22987	58.8162	48.564	86.9203	56.43767	46.10757
offset2_acc_means									
Position 1	4.333467	4.442767	4.0654	2.813433	2.6977	1.9847			
Position 2	2.060467	5.058667	3.023367	1.8196	0.911	2.124533	3.750967	2.9837	1.354567
Position 3	1.416333	3.006867	2.189	1.2534	3.521967	1.368633	2.240733	2.790967	1.3449

Table 6-7 – Separated accuracy by position in 2D. Each column is separated by channel and antenna and everything is in millimeters

	CH4T	**CH5T**	**CH7T**	**CH4D**	**CH5D**	**CH7D**	**CH4D_LOW**	**CH5D_LOW**	**CH7D_LOW**
raw_2D_means	RMS	RMS	RMS	RMS	RMS	RMS	RMS	RMS	RMS
Position 1	480.25	230.6	415.05	226.55	332	227.25			
Position 2	387.3	185.8	351.55	348.85	216.6	313.25	349.25	168	292.4
Position 3	510.6	149	411.6	321.7	130.05	318.7	327.9	100.95	321.55
offset_2D_acc_means									
Position 1	96.6546	34.35315	50.6275	18.92625	33.00465	51.03195			
Position 2	93.21695	30.3415	11.4177	43.06795	72.00325	36.04955	53.14885	59.55425	40.75115
Position 3	64.57235	12.45615	23.36305	28.22525	18.08395	36.7405	56.7249	46.4335	38.6898
offset2_2D_acc_means									
Position 1	2.08935	4.68125	4.97645	3.18015	2.8845	1.1515			
Position 2	0.9338	3.2181	2.57905	1.3185	0.436	1.57075	2.1294	2.4215	1.39435
Position 3	0.5071	2.8315	0.981	0.95335	3.9361	1.1149	1.3482	2.6494	1.16635

CHAPTER SEVEN
DILUTION OF PRECISION OPTIMIZATION

Purpose

The purpose of this software is to create a design tool for setting up a UWB positioning system which uses a TDOA localization algorithm. It optimizes the anchor positions of the system to minimize the number of anchors needed as well as the errors created from the dilution of precision. The PDOP value determines how much geometric error will be introduced due to the placement of the anchors across the testing space. By minimizing this PDOP value over the whole testing space, the overall accuracy of your system will be increased compared to a testing setup that has poorly placed anchors.

Application Overview

The tracking experiment of Chapter 6 shows that one of the factors that can contribute to the location error is the positioning of the anchors themselves, characterized by PDOP. This dilution of precision was discussed in Chapter 3. In an effort to find the locations which minimize this factor, an application was made with the ability to outline your testing space, divided into separate zones. Each zone refers to a set testing area with which a specific set of anchors will be used. By the use of separate zones, you can optimize a large testing area but only use the anchors specified in each zone.

The PDOP software application is made to be user friendly with the ability to optimize anchor placement over any space as long as you have a layout or blueprint of the space. When initiated, the software asks for the location of the layout that you want to simulate anchor placement and PDOP coverage. Once the image is selected, you are asked for a reference measurement to correlate the number of pixels of the image to the actual dimensions of the space. When completed, you are prompted to outline each zone you wish to optimize. You can outline a single zone or numerous zones. Currently, the application treats each zone separately with no duplicate zone use per anchor.

After the zones for the space have been identified, the layout of the space with the outlined zones is shown to the user. The application then asks the user to define the desired level of PDOP 95% confidence as well as the resolution. The resolution is defined as the number of intervals that each dimension (2D) of the layout will be divided into. The dimensions of your zone in the X and Y direction are found by taking the difference between the maximum and minimum values of all of the points which identify the outline of your zone. As an example, if your zone is identified by the points (1,1), (1,6), (11,6), and (11,1), your zone dimensions would be 10 in the X and 5 in the Y. If your resolution was then defined as 100, each dimension is split into 100 intervals, 0.1 units wide in the X dimension, and 0.05 units wide in the Y dimension. At each point, the PDOP is calculated with the given anchor positions. This creates a map across the testing

space of the PDOP values. By increasing the resolution, you will have smaller gaps in between calculated PDOP points.

When all of these points have been calculated, they are averaged together to create a mean PDOP value as well as the standard deviation for the PDOP. From these, the PDOP 95% confidence interval is made by taking the mean PDOP value and adding two standard deviations. This creates a single value that can be used to determine the overall PDOP. This is the main metric that is used to evaluate the overall PDOP coverage. With this value, you can claim that 95% of your testing space will be that level of PDOP or lower.

The PDOP algorithm requires the location to be tested, as well as the locations of all of the anchors. One of the main purposes of the PDOP software is to create the lowest 95% PDOP confidence interval with the fewest number of anchors while still being able to deliver a PDOP confidence interval lower than that specified by the user. To achieve this, the software has an optimization sequence to achieve PDOP coverage with the fewest number of anchors and lowest PDOP values. The sequence is set up in two steps which are outlined in the block diagram of Figure 7-1.

The first sequence of choosing the first 4 anchors in the optimization list is visually presented in Figure 7-2. The software uses every point that the user defines during the drawing of the zone as a possible anchor location. Once it has all of these points, it calculates the Euclidean 2D distance between all of these points and sorts them in descending order. The two anchors that are

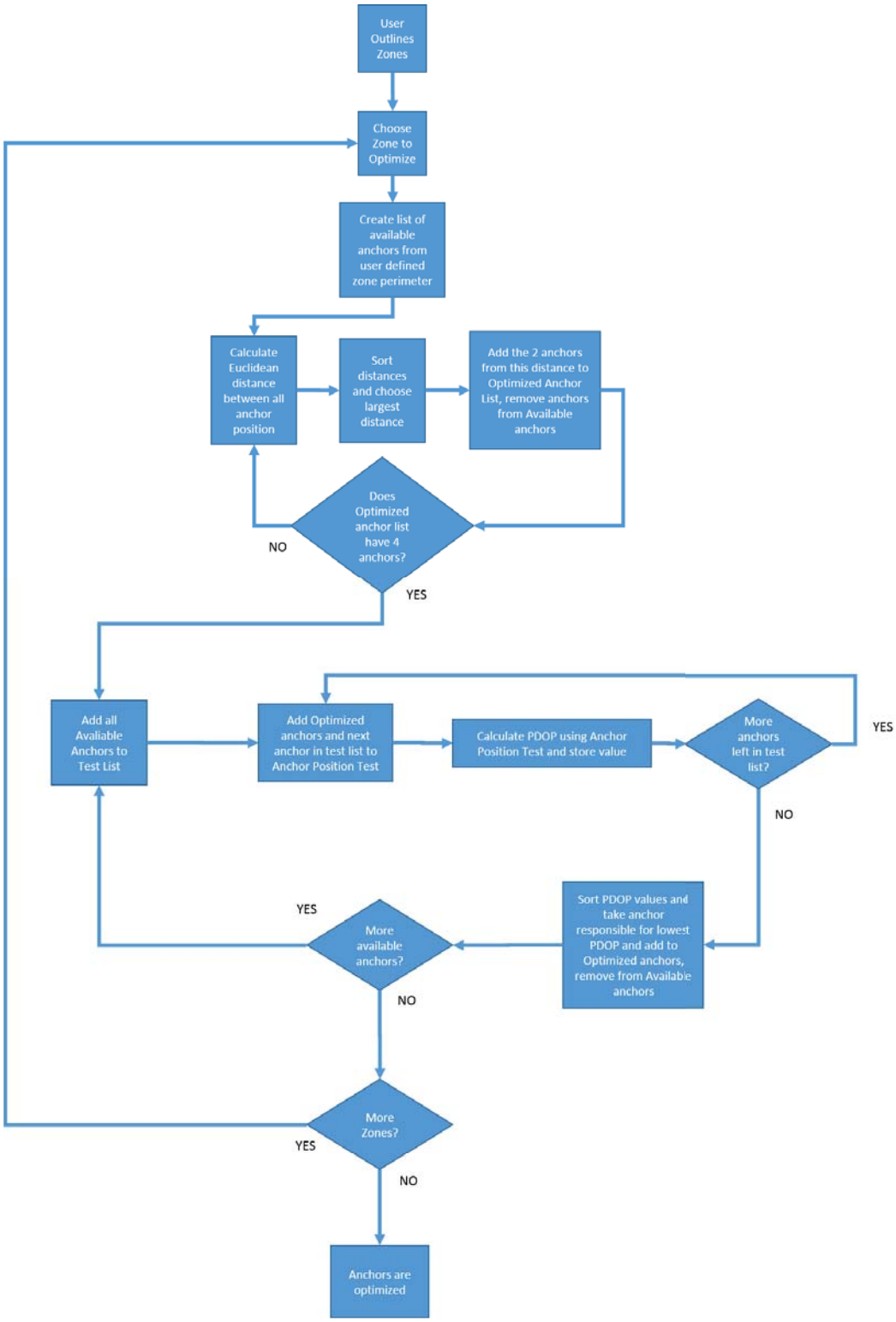

Figure 7-1 – Block diagram of the process of optimizing the anchors in the PDOP software

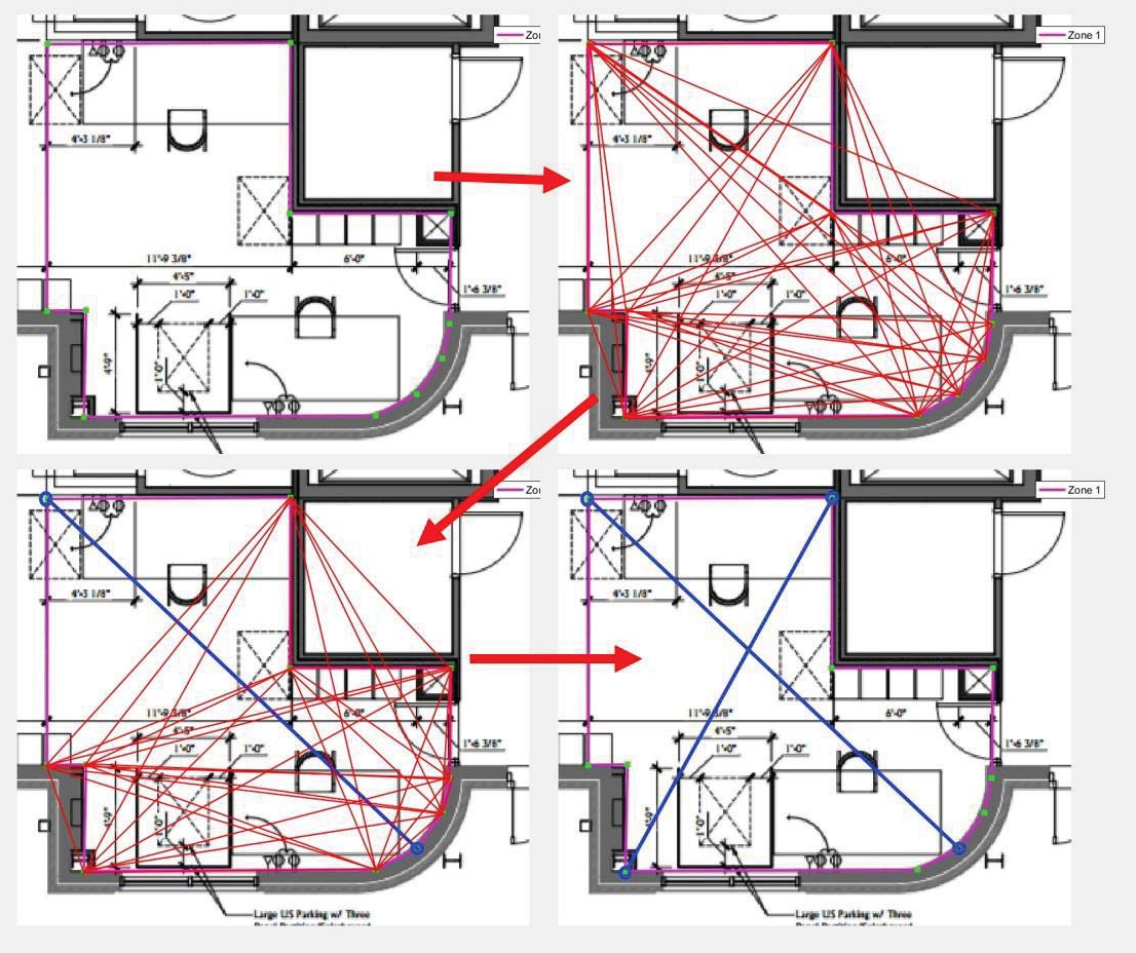

Figure 7-2 – Process of the PDOP Application choosing the first 4 anchors. Points are chosen to specify the zone. Distance are calculated between

furthest apart are taken out of the available anchors and put into an optimized anchor list. Once again, all of the distances are calculated for the remaining locations and sorted in descending order. As before, the two anchors that share the largest distance between each other are placed into the optimized anchors list. Once these first four anchors are identified, the PDOP algorithm can be used, which makes up the second step of the anchor optimization process.

The process of optimization at first just took the four anchors which had the largest distances from the initial sorting. This led to the problem of having multiple anchors close to each other, each sharing similar distances to a lone anchor. This can be seen in Figure 7-2 with the top left most anchor and the anchors which make up the curve in the bottom right. Previously, the top left most anchor would be chosen along with three anchors on the curve. This is because each anchor on the bottom right curve share the largest distances. If these four anchors were chosen, the coverage would result in a higher PDOP average than alternative anchor placements. Due to this issue, the anchors which make up the largest distance are removed from the second round of distance calculations.

The second step of creating the anchor optimization list has the four initial anchor positions and adds an additional anchor from the list to be tested. The PDOP algorithm is ran and the value saved using every available location for the 5th anchor. At the end the values are compared, and the anchor that produced the lowest PDOP value is added to the anchor optimization list. The process is then

repeated, this time with five base anchors and the sixth being tested. This is done until all of the available anchors are within the anchor optimization list. By using this method, when trying to achieve a specific PDOP average, each added anchor will have the highest effect on the PDOP average.

To illustrate how the 95% PDOP confidence level decreases, Table 7-1 displays the values and associated number of anchors for one zone as shown by Figure 7-3, Figure 7-4, and Figure 7-5. Each of these show the PDOP coverage with four anchors, six anchors, and 11 anchors respectively. As these figures illustrate, the PDOP coverage has a distinct decrease in effectiveness in the overall PDOP coverage value as the total number of anchors increases. Just the increase from four anchors to six anchors produces close to a 34.8% decrease in overall PDOP confidence. However, the increase from six anchors to 11 anchors only has an 8.70% decrease in overall PDOP confidence. This is characterized even more in our main simulation which covers a whole office space and consists of three separate zones.

Figure 7-6 shows the outline of each of these zones as well as the location of all possible anchor locations to be used. The software was then ran for different levels of desired 95% PDOP confidence. Figure 7-7, Figure 7-8, and Figure 7-9 show the PDOP map of the test space for these different levels of PDOP confidence. Table 7-2 gives the number of anchors and the corresponding PDOP confidence level for each zone. As was the case in the single zone example, the introduction of the fifth, sixth, and in the case of Zone 1, seventh

Table 7-1 – The correlation of anchors to 95% confidence PDOP values corresponding to Figure 7-3, Figure 7-4, and Figure 7-5

	Low PDOP	**Medium PDOP**	**High PDOP**
Number of Anchors	11	6	4
95% confidence PDOP	0.84	0.92	1.41

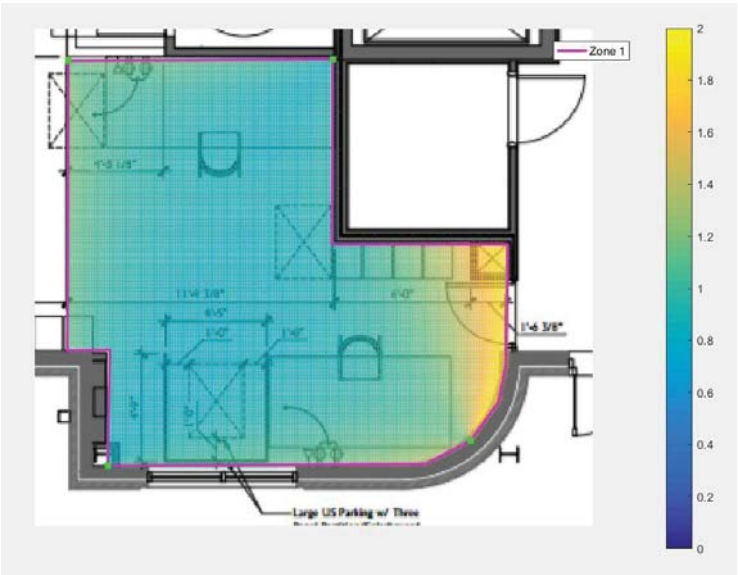

Figure 7-3 – PDOP coverage with the use of 4 anchors

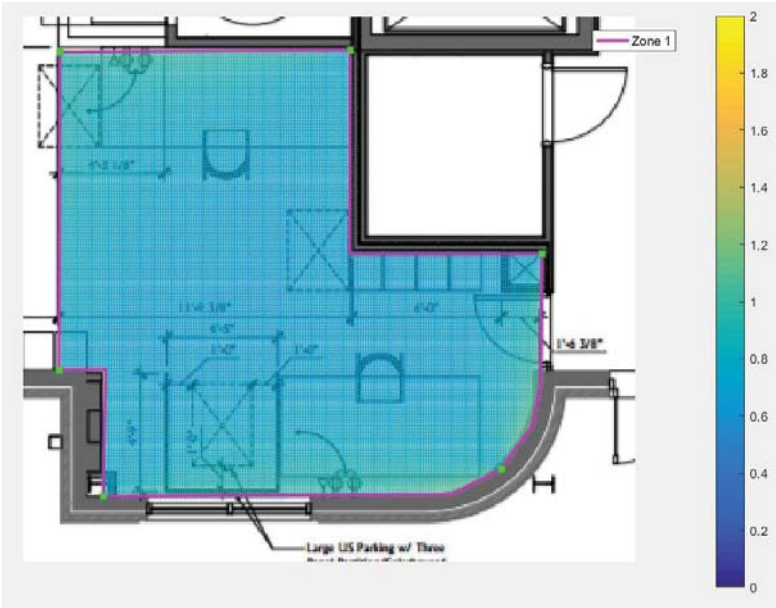

Figure 7-4 – PDOP coverage using 6 anchors

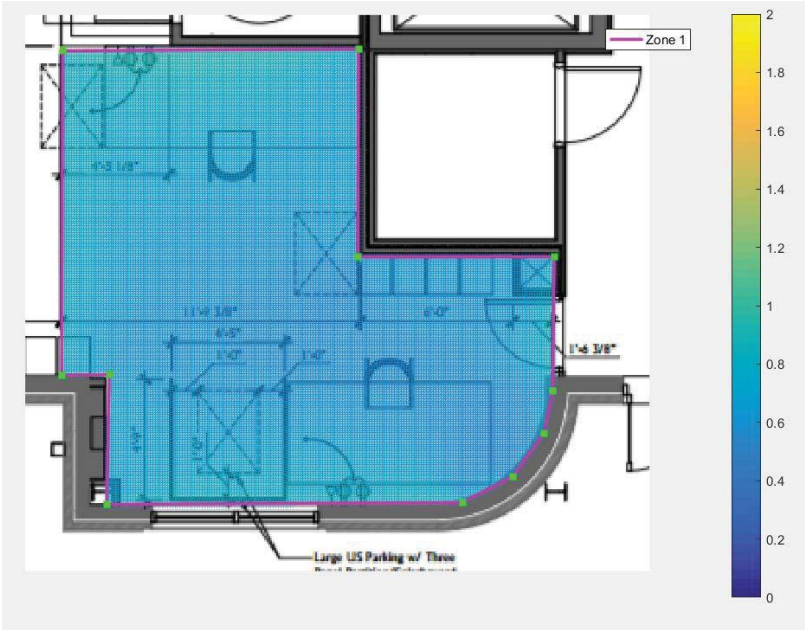

Figure 7-5 – PDOP coverage with the use of 11 anchors, creating the best PDOP coverage available with this configuration

anchor has a more substantial effect on the PDOP than the anchors added after this point. The number of anchors depends on the desired level of accuracy over your testing space and your available budget for additional anchors. The cost of each additional anchor stays constant, but the effectiveness decreases very quickly after the fifth or sixth anchor. To optimize the number of anchors best suited to your application, you should assign a cost multiplier to the number of anchors used, and an accuracy multiplier to the PDOP value achieved. This way, a total cost function can be made for the system. By changing the multipliers for your application, you can choose the best anchor setup in your specific case. For example, when cost is the most important factor, a higher anchor multiplier for a system can be used to minimize the number of anchors, optimizing the number of anchors for your specific application.

The next steps for this software application have to do with less limited anchor placement optimization and the ability to have anchors be used for multiple zones. Currently the software simply uses the user input points which make up the zone for possible anchor locations, without the ability to place anchors in other locations. This is mostly due to testing in the development of the application showing that the best PDOP values and coverage come from placing the anchors on the perimeter of the testing space. However even the ability to place anchors anywhere on the perimeter and not limit them to the user input points should provide even better PDOP coverage and lower values for a given number of anchors. Another way to improve the software is the ability to use a .

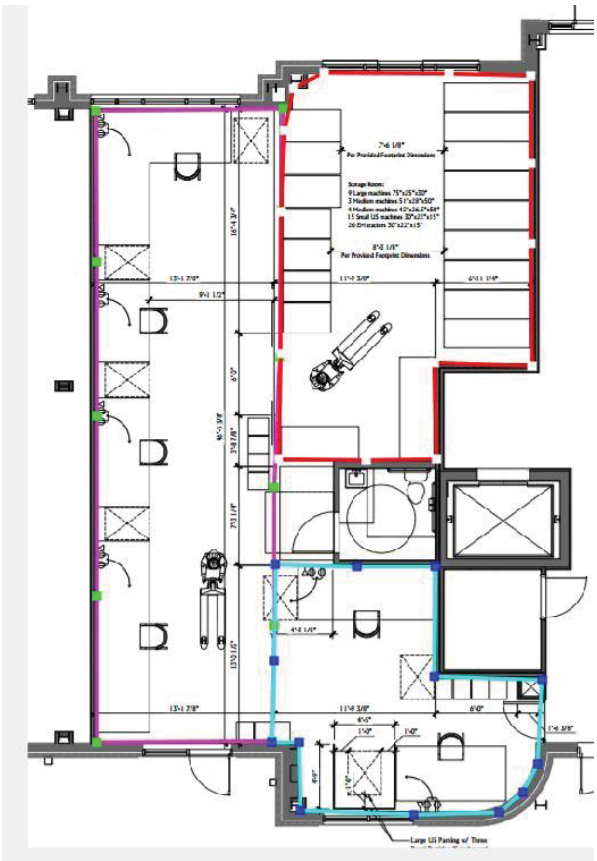

Figure 7-6 – Zone and anchor placements for the floor layout simulation. Each of the 3 zones are outlined with their corresponding anchors marked in a separate color to each other zone's anchors

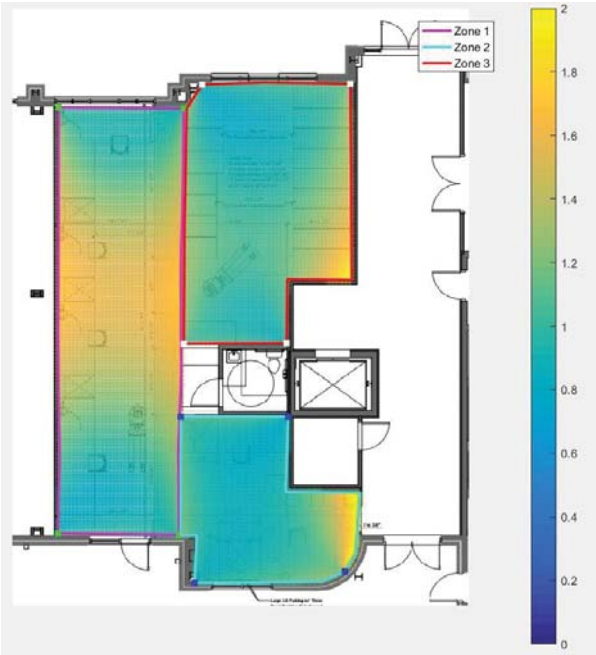

Figure 7-7 – PDOP coverage map using the minimum number of anchors per zone of the floor layout simulation

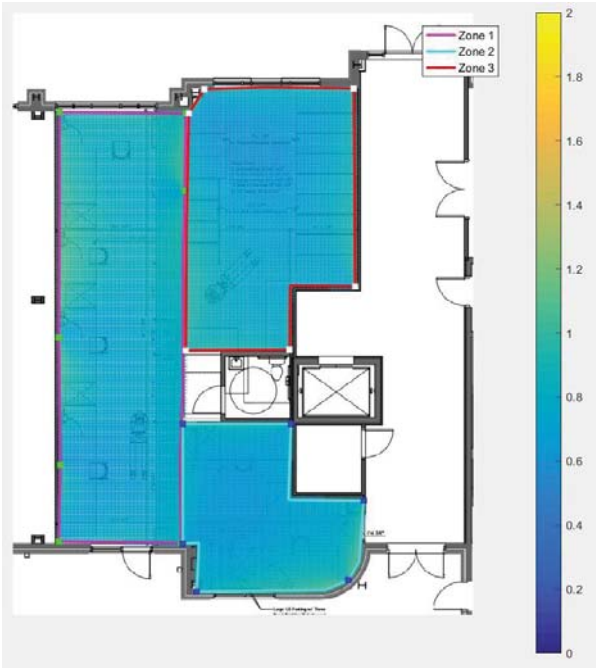

Figure 7-8 – PDOP coverage of the floor layout simulation to get a medium 95% PDOP confidence level

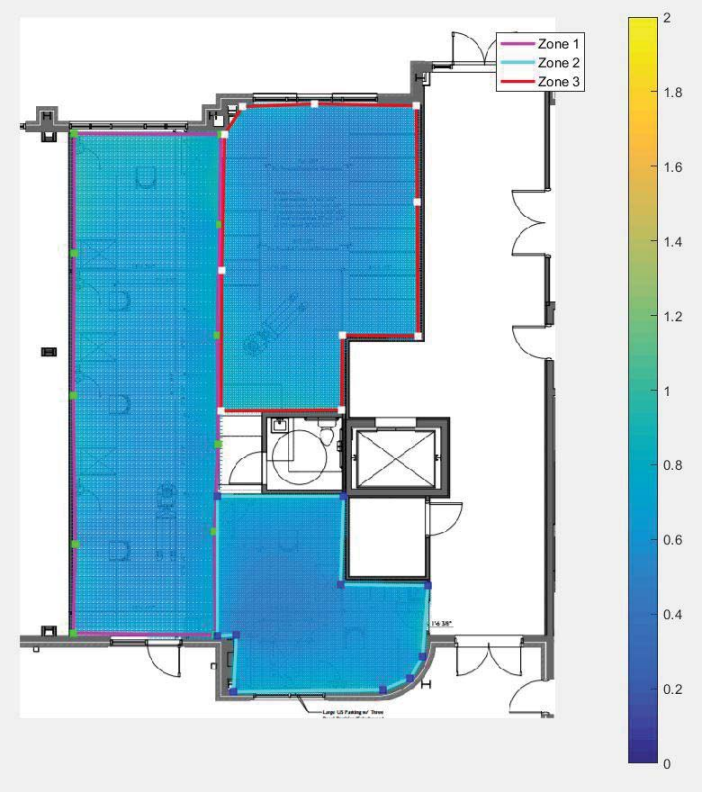

Figure 7-9 – PDOP coverage using the maximum number of anchors for each zone

Table 7-2 – Summary of the number of anchors versus the PDOP 95% confidence for each zone of the PDOP application corresponding to Figure 7-7, Figure 7-8, and Figure 7-9.

	Zone 1		Zone 2		Zone 3	
	Number of Anchors	95% confidence	Number of Anchors	95% confidence	Number of Anchors	95% confidence
High PDOP	4	1.79	4	1.61	4	1.52
Medium PDOP	7	0.98	6	0.94	6	0.93
Low PDOP	11	0.83	10	0.79	10	0.80

single anchor for multiple zones. As seen in Figure 7-8, both zones 1-2 as well as 1-3 share at least one anchor between the two zones. This ability to use one anchor would decrease the total number of anchors and create a more accurate cost function for the entire system. The most pertinent challenge to achieving this though is the difficulty of differentiating between anchors that should be combined and those that should not. An example of a pair that should not be combined is anchors that physically are not far from each other, but in the space are actually separated by a wall. This physical barrier would not change the simulation of the PDOP coverage, but in practice would create a large amount of interference and error by trying to use the anchor in the TDOA calculation.

CHAPTER EIGHT
CONCLUSIONS AND RECOMMENDATIONS

There is a plethora of commercially available tracking systems, but not many offer accuracy above 10 cm along with the ability to track multiple tags. When it comes to an asset tracking system, the ability to track numerous tags becomes crucial. The range of the system, or total volume in which the system is capable of functioning, is also necessary in the design of your positioning system.

We have been able to show that with our system we are capable of tracking as many tags as are needed, up to 10,000 tags, while maintaining an accuracy of around 5cm. With post processing and some calibration, our accuracy drastically increases, with the potential to enter accuracies in the millimeters or better. All of this is tracking a static tag, but for a number of tracking applications, most assets will be stationary for a majority of the time. For dynamic results, more testing is required with additional post processing to see if the same calibrations and offsets can be used to help increase the accuracy.

For setting up a new tracking system, it is highly recommended to first run a program to measure the PDOP of the entire space where testing is desired. This way, adjustments can be made to the anchor placements to minimize the dilution of precision over the space that is most important for accurate position calculations. This analysis will be able to show the exact positions which will result in the lowest PDOP values as well as the effects of using additional anchors in the space being tested. With this kind of analysis, a better

understanding of the testing space can be achieved in addition to being able to have a basic idea of the accuracies possible within the testing area. This is invaluable in running an analysis to determine the number of anchors to increase accuracy versus the cost per anchor. To guarantee the best accuracy out of the system, the variation in physical locations of each anchor should be maximized. As the tracking experiment illustrates, simply by lowering two anchors and increasing the variation of the Z dimension, accuracy is measurably increased over all of the channels.

When considering channel choice, reviewing the data shows that channel 7 has the highest SNR values which will result in the highest accuracy. However, both channel 4 and channel 7 show an improvement over channel 5, which exhibits the lowest SNR values in this experiment. It shows promise in the raw data, but once some post processing has been done, exhibits lower accuracy than the other channels tested. Channel 5 is especially poor over larger distances. It is the only channel that failed at the 28 meter test, not being able to collect any data in most of the configurations. Because of these factors, it is recommended to use a channel with the largest bandwidth possible for any asset tracking applications.

When looking at the best antenna for a tracking application, there are a few factors that must be considered. Strictly for performance, the DecaWave and TechMah antennas are pretty comparable. With the use of the second offset, they have almost identical performances, while with the first offset, the

DecaWave has slightly better performance on channel 4 and channel 7. However, the TechMah antenna has a measurably higher SNR value across almost every channel and distance compared to the DecaWave antenna. Another very important factor to consider when choosing an antenna is the form factor. The TechMah antenna has a much smaller profile and overall size, making it more capable at minimizing the overall size of the tags and anchors. Due to the better SNR performance and decrease in form factor, the TechMah antenna is a better choice. However, the spherical monopole antenna is another option that might be able to heavily increase the accuracy of the system because of its ability to reduce, or even fully illuminate the error introduced by phase center variation.

REFERENCES

1. Kuhn, Michael Joseph, "Development and Experimental Analysis of Wireless High Accuracy Ultra-Wideband Localization Systems for Indoor Medical Applications. " PhD diss., University of Tennessee, 2012. http://trace.tennessee.edu/utk_graddiss/1317
2. Federal Communications Commission, “The first report and order regarding ultrawideband transmission systems,” FCC 02-48, ET Docket No. 98-153, 2002.
3. C. McElroy, D. Neirynck, and M. McLaughlin, “Comparison of wireless clock synchronization algorithms for indoor location systems,” Decawave Limited
4. Elkhouly, Essam Abdelkadir, "UWB Precise Indoor Localization System Performance, Limitations and its Integration. " PhD diss., University of Tennessee, 2014. http://trace.tennessee.edu/utk_graddiss/3121
5. Smith, J. and J. Abel. "Closed-Form Least-Squares Source Location Estimation From Range-Difference Measurements". IEEE Transactions on Acoustics, Speech, and Signal Processing 35.12 (1987): 1661-1669. Web.
6. Stoica, Petre and Jian Li. "Lecture Notes - Source Localization From Range-Difference Measurements". IEEE Signal Processing Magazine 23.6 (2006): 63-66. Web.
7. Richard B. Langley (May 1999). "Dilution of Precision" (PDF). GPS World
8. Cemin Zhang, Aly E Fathy, and Mohamed Mahfouz. Performance enhancement of a sub-sampling circuit for ultra-wideband signal processing. Microwave and Wireless Components Letters, IEEE, 17(12):873{875, 2007.
9. "Redpoint Positioning – Innovators in RTLS." Redpoint Positioning. N.p., n.d. Web. 17 Jan. 2017.
10. "PulsON 440 | Time Domain." PulsON 440 | Time Domain. N.p., n.d. Web. 17 Jan. 2017.
11. "ScenSor." ScenSor Radio Comunication Products Overview | DecaWave | DecaWave. N.p., n.d. Web. 17 Jan. 2017.
12. Example Of Geometric Dilution Of Precision (GDOP) For Simple Triangulation. Three Different Situations Are Shown: A) Triangulation. B) Triangulation With Error. C) Triangulation With Error And Poor GDOP.. 2013. Web. 6 Mar. 2017.
13. ZIH Corp. "Dart Ultra Wideband UWB Technology." Zebra Technologies. ZIH Corp, n.d. Web. 13 Mar. 2017.
14. Ubisense. "Dimension4." Ubisense. Ubisense Group plc, n.d. Web. 13 Mar. 2017.
15. Symeo GmbH. "Highly-Precise Real Time Location for Indoor and Outdoor Applications." Realtime Position Detection Indoors & Outdoors - Symeo GmbH. N.p., n.d. Web. 13 Mar. 2017.
16. BeSpoon SAS. "UWB Ultra Wide Band." Bespoon. N.p., n.d. Web. 13 Mar. 2017.

17. IEEE Computer Society. “IEEE Standard for Low-Rate Wireless Networks.” IEEE Std 802.15.4™-2015
18. M. Mahfouz, C. Zhang, B. Merkl, M. Kuhn, A. Fathy, “Investigation of high accuracy indoor 3-D positioning using UWB technology,” IEEE Transactions on Microwave Theory and Techniques, 56(6), 2008, pp. 1316-1330.
19. Red Point Positioning. "RTLS Development Kit Quick Start Guide." Federal Communications Commission. Red Point Positioning, n.d. Web.
20. American Biomedical Group. "American Biomedical Group." ABGI - Asset Management and Tracking. American Biomedical Group, n.d. Web. 16 Mar. 2017.
21. American Biomedical Group. "American Biomedical Group OET Exhibits List." Federal Communications Commission. Federal Communications Commission, n.d. Web.
22. G. Heidari, WiMedia UWB : technology of choice for wireless USB and Bluetooth, 2008.

VITA

Nicholas A. Cavopol was born in Missouri but moved to Nashville before the age of one. He graduated from Martin Luther King Jr. Magnet school with honors and started his undergraduate studies at the University of Tennessee in Knoxville with a major of Electrical Engineering. After four and a half years he graduated with his degree in Electrical Engineering as well as earning two minors in Reliability and Maintainability Engineering and Material Science Engineering. To continue his academic career, he accepted an assistantship with Dr. Aly Fathy in companionship with Oak Ridge National Lab under Dr. Mike Kuhn. When presented an opportunity by Dr. Mohamed Mahfouz to join TechMah LLC to further his experience and knowledge of communication systems, and an asset tracking system more specifically, he accepted. There he finished his Masters degree with a thesis relating to the Ultra-Wide Band positioning system under Dr. Mike Kuhn. After completion of his Masters degree, he plans to join Honda Research and Development in Raymond Ohio to continue his professional career and his passion for everything automotive.